



Proximity Effects in Altermagnetic Systems

~ o ~

a bachelor thesis.

Written by Arto Steffan,
under the supervision of Prof. Dr. Jacob Wüsthoff Linder,
and corrected by Prof. Dr. Wolfgang Belzig.

Universität
Konstanz



NTNU – Trondheim
Norwegian University of
Science and Technology

Acknowledgment

— ~ —

This bachelor thesis is the results of five months of work at the NTNU Trondheim in Norway. I would like to thank my supervisor, professor doctor Jacob Linder for his guidance and support during this period, and for introducing me to an interesting branch of physics. Thanks to professor doctor Wolfgang Belzig for correcting this work.

This thesis concludes for me three years of study at the University of Constance in Germany. The way until here had many pitfalls and difficulties, and I am very grateful to you papa and maman, as well as to my brothers, Massa, Idriss and Vegar, for their encouragement and their kindness during our phone calls and visits. The chocolate and drawings you put in these packages always brought me to smile! I want to express my gratitude to my grandparents for their support, their stories and delicious meals during my visits. I am also thankful to my uncles for their great hospitality and helping me find the way in the adulthood. All the moments seeing the family felt very peaceful.

Thanks to Kai and Jakob for their friendship and interesting discussions we shared at lunch around a “Seezeitteller”. Thanks to Kim and Luca in Trondheim for our trips and your smiles. Finally, I am very grateful to you Tom, for all the times we went out in the city, built projects, watched movies, shared breakfast. I still do not understand why you need to put the butter in a dedicated container. To our deep discussions and stupid jokes. You showed me how life can be great when you use of boldness towards the ‘no balls’ situations. Your friendship is precious to me.

———— ~ —————

Contents

1	Introduction	2
2	Theoretical background	3
2.1	Bosons and fermions	3
2.2	The second quantization	5
2.2.1	Second quantization for fermions	5
2.2.2	Basis transformation	7
2.2.3	Field operators	8
2.3	Case of study: electron gas with interactions	9
3	Superconductivity	12
3.1	The non-interacting electron gas	13
3.2	Fermi-liquid: The interacting case	14
3.3	Instability due to attractive interactions	17
3.4	Attractive forces mediated by phonons	17
3.5	Construction of the effective Hamiltonian	19
3.6	On our way to the BCS-theory	21
3.7	Generalized gap equation, <i>s</i> -wave and <i>d</i> -wave superconductivity	24
3.8	Transition temperature and energy gap	28
4	Altermagnetism	30
4.1	Introduction and overview	30
4.2	Symmetries	31
4.3	Implementation of an altermagnet	33
5	Bogoliubov-de Gennes Formalism	34
5.1	Tight Binding Model	34
5.1.1	Non-interacting electrons	35
5.1.2	Superconductivity	36
5.2	A more symmetric Hamiltonian	36
5.3	Eigenvalues	38
5.4	Diagonalization	38
5.5	Physical Quantities	40
5.5.1	Superconducting Gap	40
5.5.2	Currents	41
6	Simulations and results	46
6.1	Methodology	46
6.2	Results	47
6.3	Conclusion and outlook	56
	Appendices	58
A	An unconventional superconductivity	58
A.1	Site dependent potential	58
A.2	In the vertical periodic boundary setup	59
A.2.1	BdG-transformation for a vertical Fourier transform	61
A.2.2	Pairing amplitudes	62
A.2.3	In the open boundary setup	62
A.3	Unconventional order parameters	63
A.4	Implementation of the unconventional superconductivity	64
7	Literature	65
8	Administrative documents	68

1 Introduction



Superconductivity has today a wide range of applications. We can mention a precise class of magnetometer, the superconducting quantum interference device (SQUID). Designed to measure weak fields (up to 5×10^{-18} T)[1], they are based on multiple superconducting loops involving Josephson junctions and were invented in 1963 [2]. Important imaging methods have emerged. One can mention nuclear magnetic resonance imaging (NMRI), that takes advantage of the response of the nuclear spin to an external magnetic field to provide a non-intrusive spectroscopy technique. To provide stronger fields and thus enable better imaging definition, superconducting magnets are used [3]. In fact, they allow stable and strong fields with an upper bound limit around 24 T [4], whereas conventional permanent magnets are limited around 2 T [5].

Besides, superconducting magnetic energy storage (SMES) can store energy with a capacity in an interval from one to a hundred MW of energy, and being able to discharge within a few seconds. This makes this technology interesting for the grid stabilization, providing a very responsive energy storage system [6]. SMES is based on a superconducting coil within a cryostat that stores the energy in the coil and releases it when needed. Due to the superconducting nature of the coil, an energy conversion efficiency of 95% is observed [6]. In the context of public transportation levitating trains were subject to high-scale projects. These are mostly implemented in China [7], and are planned ready for commercial use in Japan around 2027 [8].

This very promising state of matter has a main drawback, the freezing low critical temperature. Over the past century, researchers have been searching for materials that could display superconducting properties at higher temperatures [9] (Nobel prize in 1987). Reference [10] found critical temperature above the liquid nitrogen temperature. Special doping methods were proven to improve T_C [11] in 2007. In 2015 researchers found that applying a substrate to single-layer FeSe films could improve the critical temperature [12]. Multiple other studies extended the range of materials that could be in a superconductive state at higher temperatures [13], [14] and [15]. Those progresses were among other things achieved by increasing considerably the pressure, even to gigapascals in some studies [14].

Further unconventional *d*-wave superconductivity has been proven to be stable at higher temperatures than its conventional BCS-homologue. The applications we provided above need liquid helium to stay in the temperatures that allow superconductivity. *d*-wave would work with liquid nitrogen for example, which is a strong economic argument.

Superconductors were proven to exhibit different characteristics in comparison to normal conductors as Meissner and Ochsenfeld discovered in 1933 [16]. They experimented with tin Sn and lead Pb being subject to a magnetic field below a critical temperature T_C . They observed that the magnetic field lines on the surface of the superconductor were ordering in such a way, that no magnetic flux lines were able to penetrate the superconductor ($\mathbf{B} = 0$ inside). This is called the Meissner effect and presents the superconductors as perfect diamagnets.

This study is going to focus on simulating the proximity effects when the superconductor is put near another material. The material is a newly found class that settles between the ferromagnet and the antiferromagnet [17]. A proper introduction of these so-called altermagnets will be given later. For now, we want to put the theoretical basis for the superconductors.

Notation

First a few words about the notation. When having multiple indices under a symbol, we omit the comma to make the notation more readable. For example, x_{ij} is the same as $x_{i,j}$. However, when we have more complex indices such as $x_{i-1,j}$, we keep the comma between all the indices. For the summation over natural numbers we introduce the notation $\llbracket N \rrbracket = \{n \in \mathbb{N} : n \leq N\}$.

We are going to use Hilbert-space's operators. As often in physics, they will be multiplied with the wave function. This is the case for the Hamiltonian operator for example. However, the second quantization operators work differently. We will give a proper definition of these operators in the next section.

2 Theoretical background



In order to describe the superconductors we are going to introduce the second quantization formalism based on the work of John of Folk [18]. This framework allows us to picture the wave function of a system using creation and annihilation operators over energy states of the system. This simplifies a lot the notation. The mathematical foundation of this formalism lies in the Hilbert space, and requires as well its dual space. To picture the many-particles interaction we need as well to introduce the Fock space. We aim to give a practical understanding over the formal mathematical rigour. In this sense some derivations might not be as rigorous as a proper mathematical treatment could deliver.

We want to work on fermionic systems. The formalism stays the same for bosons, but the results are fundamentally different. One can mention the Pauli principle as an example, which only applies on fermions. After some definition we are going to see how to derive it with the help of the second quantization.

Please note that we aim to describe the operators with a hat: $\hat{\cdot}$. Later the expression will however involve a dense notation, such that we will drop the hat for the readability. The reader will stay informed about the nature of each symbol.

2.1 Bosons and fermions

We consider without loss of generality the following hamiltonian

$$\hat{H} = \hat{H}_0 + \hat{H}_I. \quad (1)$$

It is a very generic definition that uses a single particle operator \hat{H}_0 and the interaction operator \hat{H}_I . The single particle part sums up the kinetic and potential energy of each particle. The interaction part gives room for complex relations between the particles.

$$\hat{H}_0 = \sum_{i \in [N]} \hat{h}(x_i), \quad \hat{h}(x_i) = -\frac{\hbar^2}{2m} \nabla_i^2 + \hat{U}(x_i).$$

The potential part may depend on the particle's position \mathbf{r} or spin s . We use $x_i := (\mathbf{r}, s) \in \mathcal{X} \subseteq \mathbb{R}^3 \times \mathbb{S}$ to group this information. For example, we have for an electron: $\mathbb{S} = \{-\frac{1}{2}, \frac{1}{2}\}$.

Further we describe a quantum state that a particle can occupy with a wavefunction $\phi_\nu(x)$, which is related to a certain energy $\epsilon_\nu \in \mathbb{R}$. This energy depends on the wave vector and the spin of the particle. We define a state ν as $\nu = (\mathbf{k}, \sigma)$. The fundamental equation of quantum mechanics relates the wavefunction with the hamiltonian using the energy of the state. Using the former defined \hat{h} we have:

$$\hat{h}\phi_\nu(x) = \epsilon_\nu\phi_\nu(x).$$

The wavefunction lies in the Hilbert space \mathcal{H} . Therefore, $\phi_\nu(x)$ are eigenfunctions or -states of the Hamiltonian \hat{h} with eigenvalues ϵ_ν . Furthermore, the wavefunction should build an orthonormal basis:

$$\int_{\mathcal{X}} \phi_{\nu'}(x)\phi_\nu(x)dx = \delta_{\nu'\nu}.$$

ν and ν' are two different states. We introduced here the Kronecker delta $\delta_{\nu'\nu}$, which is one when the two indices are equal, and zero otherwise. Because the spin s is not continuous, one can understand the integral in the following way:

$$\int_{\mathcal{X}} dx = \sum_{s \in \mathbb{S}} \int_{\mathbb{R}^3} d^3r$$

where $\int_{\mathbb{R}^3} d^3r = \int_{\mathbb{R}} \int_{\mathbb{R}} \int_{\mathbb{R}} dr_1 dr_2 dr_3$. In other words we integrate over all possible states.

Now that we can picture a single particle, the next question is: how to describe the collective behaviour of a collection of such particles? This is done with a many-body wavefunction, that

sums up all possible combinations of wavefunctions in the system and should stay normalized. A combination is illustrated as the product of each possible wavefunction of the particle in a certain state. These particles can be swapped, and therefore we need to consider all the combinations. We aim to work with fermions, but give a quick insight with bosons for comparison. We admit having $N \in \mathbb{N}$ particles in the system.

Bosons

Bosons are flexible because they are not restrained by the Pauli principle. Their many-particle wavefunction is symmetric (exponent S) under swap of two particles.

$$\Phi^{(S)}(x_1, \dots, x_N) = \left(N! \prod_{\nu} (n_{\nu})! \right)^{-\frac{1}{2}} \sum_{P \in S_n} P \phi_{\nu_1}(x_1) \cdot \dots \cdot \phi_{\nu_N}(x_N).$$

This represents an eigenfunction of the non-interacting bosonic-Hamiltonian. We used n_{ν} , which represents the number of particles in the state ν . Therefore, we usually call it the occupation number of the state ν . For bosons this integer has no constraint in general. The permutation set S_n contains all the possible combinations of x_i in the state ν_j for $i, j \in \llbracket N \rrbracket$. P describes a permutation in the x_i .

For example with two particles we have x_1 and $x_2 \in \mathcal{X}$ and the later part of the expression reads $\phi_{\nu_1}(x_1) \cdot \phi_{\nu_2}(x_2) + \phi_{\nu_1}(x_2) \cdot \phi_{\nu_2}(x_1)$ and is thanks to the prefactor, normalized. We now see, the permutation aims to describe each particle (an x_i) in each possible state ν_i .

Fermions

Fermions are a bit different. Their many-particle wavefunction is antisymmetric under swap of two particles. We denote it as

$$\Phi^{(A)}(x_1, \dots, x_N) = (N!)^{-\frac{1}{2}} \sum_{P \in S_n} \text{sgn}(P) \cdot P \phi_{\nu_1}(x_1) \cdot \dots \cdot \phi_{\nu_N}(x_N),$$

which is an eigenfunction of the non-interacting fermionic-Hamiltonian. Sgn represents the signum function. Applied on a permutation P , it is one if P is even and minus one if P is odd. We already know that the Pauli principle implies that we can find up to one particle in each energy state. We therefore have $n_{\nu} \in \{0, 1\}$. The normalization factor is the same but the product over the n_{ν} is always one, we have $0! = 1$ and $\prod 1 = 1$.

At this point one might have recognized the formula of the determinant

$$\Phi^{(A)}(x_1, \dots, x_N) = (N!)^{-\frac{1}{2}} \det \begin{pmatrix} \varphi_{\nu_1}(x_1) & \cdots & \varphi_{\nu_1}(x_N) \\ \vdots & & \vdots \\ \varphi_{\nu_N}(x_1) & \cdots & \varphi_{\nu_N}(x_N) \end{pmatrix}.$$

We usually describe this expression as the Slater determinant. A determinant vanishes if two rows or columns are identical. If they are the same, we have two particles in the same state. This means that the probability of finding two fermions in the same state is zero. This is the Pauli principle. Only one or no particle may occupy each state. From this we get the constraint for n_{ν} .

However following this method may lead to a major problem. The many-particle wavefunction of fermions is defined up to a sign. For instance if we consider two particles “having” x_1 and x_2 , we have two possible states ν_1 and ν_2 . Two possible solutions are

$$\begin{aligned} \Phi^{(A_1)} &= \frac{1}{\sqrt{2}} (\varphi_{\nu_1}(x_1) \varphi_{\nu_2}(x_2) - \varphi_{\nu_1}(x_2) \varphi_{\nu_2}(x_1)) \\ \text{or } \Phi^{(A_2)} &= \frac{1}{\sqrt{2}} (\varphi_{\nu_1}(x_2) \varphi_{\nu_2}(x_1) - \varphi_{\nu_1}(x_1) \varphi_{\nu_2}(x_2)) \\ &= -\Phi^{(A_1)}. \end{aligned}$$

This sign difference may lead to computation errors. To solve this we must give a label to our states when we count them, and keep it when we come to build the Slater determinant.

These bosonic and fermionic wavefunctions are eigenstate of the Hamiltonian \hat{H}_0 and the corresponding eigenvalue E_ν is given by summing the energy of each state times its occupation number: $E_\nu = \sum_\nu \epsilon_\nu n_\nu$. The orthogonal property of the single-particle wavefunction propagates itself:

$$\int_{\mathcal{X}^N} \Phi_a^*(x_1, \dots, x_N) \Phi_b(x_1, \dots, x_N) d^N x = \delta_{ab}.$$

Therefore, we can expand any many-particle wavefunction Ψ as the linear combination of these:

$$\Psi = \sum_a f_a \Phi_a(x_1, \dots, x_N)$$

where f_a is a coefficient and a a labelling.

What we just discussed is the so-called first quantization- or wavefunction formalism. Now we intend to introduce a more compact description of our system.

2.2 The second quantization

For a better description of the many-particle system we introduce a simpler notation. The second quantization lies on three important objects. States, which are described as “kets”. We put any relevant information (e.g. quantum numbers) in the ket: $|\mathbf{k}, \sigma, \dots\rangle$. Then we need two operators that act on these states to allow evolutions in the system. The second quantization has two main operators. They can create and annihilates a state.

States

In this section we describe a state as the number of particle that occupies each single-particle state. As explained before, we need to order the state: $1 < 2 < \dots < N$. We can then describe the wavefunction as follows $|n_1, \dots, n_N\rangle$. Further the state where no particle are present is called the vacuum state, and we denote it as $|0_{\nu_1}, \dots, 0_{\nu_N}\rangle = |0\rangle$.

2.2.1 Second quantization for fermions

It is now the time to define the operators for the fermionic case.

Creation operator c_ν^\dagger

The creation operator adds a particle in the concerned state, and introduce an additional phase:

$$c_\nu^\dagger |n_1, \dots, n_\nu, \dots\rangle = (-1)^{\sum_{\mu < \nu} n_\mu} (1 - n_\nu) |n_1, \dots, n_\nu + 1, \dots\rangle.$$

We intentionally discarded the hat on the c as said before. We notice the $(1 - n_\nu)$ term, which avoids creating a particle in an already occupied state. This is the way we express the Pauli principle. Further we can construct a state by applying this operator one after another on the vacuum state. To avoid the minus one adding a negative sign, we start from the end, and add the particle backwards in the order of the state:

$$|n_1, \dots, n_N\rangle = (c_1^\dagger)^{n_1} \dots (c_N^\dagger)^{n_N} |0\rangle.$$

Annihilation operator c_ν

Likewise, the annihilation operator destroys a particle in the corresponding state. The operator reads

$$c_\nu |n_1, \dots, n_\nu, \dots\rangle = (-1)^{\sum_{\mu < \nu} n_\mu} (n_\nu) |n_1, \dots, n_\nu - 1, \dots\rangle.$$

We can easily recognize, that due to the n_ν -term, destroying a particle that does not exist gives zero, so it is only possible to annihilate existing particles. Now that we can bring the particles into new states, we can introduce some rules the operators yield.

The anticommutator of two operators reads $[A, B]_+$ or $\{A, B\} := AB + BA$ and is an operator as well. We are going to stick with $[A, B]_+$ since it is more consistent with the commutator notation $[A, B]_-$ (or simply $[A, B]$).

The following results are obtained by separating the $\nu = \mu$ from the $\nu \neq \mu$. We must also say that the dagger \dagger should be understood as the complex transpose of the operator: $(AB)^\dagger = B^\dagger A^\dagger$.

$$[c_\nu, c_\mu]_+ = 0 \quad (2)$$

$$[c_\nu^\dagger, c_\mu^\dagger]_+ = 0 \quad (3)$$

$$[c_\nu^\dagger, c_\mu]_+ = \delta_{\mu, \nu} \quad (4)$$

Fermionic operators “anticommute”. We can combine the creation and annihilation operators to count the number of particles in a state:

$$c_\nu^\dagger c_\nu |n_1, \dots, n_\nu, \dots\rangle = n_\nu |n_1, \dots, n_\nu, \dots\rangle.$$

From this we can define the number operator $\hat{n}_\nu := c_\nu^\dagger c_\nu$ which we can combine in the total number operator:

$$\hat{N} = \sum_\nu \hat{n}_\nu, \quad \text{where logically } N = \sum_\nu n_\nu.$$

If we apply the total number operator on the system wavefunction, we obtain the total number of particles. We keep the hat on the operator to avoid the confusion with the actual number n_ν of particles.

Second quantization description of the single- and two- particle operators

The next step is to translate the Hamiltonian in our formalism. First we introduce two basis element $|\Phi_\alpha\rangle$ and $|\Phi_\beta\rangle$, which can be many-particles eigenstate of the system. We can also call them Slater determinants. Then we introduce the probability of the configuration $|\Phi_\alpha\rangle$ to scatter into the $|\Phi_\beta\rangle$ due to the action of an operator A (either momentum, potential, interactions,...). This is described by the matrix element $\langle\Phi_\alpha|A|\Phi_\beta\rangle$ which involves the single particle states $|\alpha_1\rangle, \dots, |\alpha_N\rangle$ of $|\Phi_\alpha\rangle$ and $|\beta_1\rangle, \dots, |\beta_N\rangle$ of $|\Phi_\beta\rangle$.

$$\langle\Phi_\alpha|A|\Phi_\beta\rangle = \sum_{ij} C_{ij} \langle\alpha_i|A|\beta_j\rangle$$

involving some constants C_{ij} . This describes the overlap of the two configurations, after that we modified $|\Phi_\beta\rangle$ with A . On the right-hand side (r.h.s) we introduced the bracket scalar product notation. The bra $\langle\alpha|$ lives in the dual space of the Hilbert space. One reads it as the complex transpose of $|\alpha\rangle$. The bracket scalar product will be defined in the next paragraphs.

We recall the single particle Hamiltonian we introduced earlier. Its second quantization representation reads

$$\hat{H}_0 = \sum_{i \in [N]} \hat{h}(x_i) \rightsquigarrow \sum_{\alpha\beta} \langle\alpha|\hat{h}|\beta\rangle c_\alpha^\dagger c_\beta, \quad (5)$$

where α and β are single-particle states of the system. $c_\alpha^\dagger c_\beta$ tries to transfer a fermion from the state $|\beta\rangle$ to the state $|\alpha\rangle$. However, this transition can be restricted by physical laws. This is the role of the matrix element. It returns zero, if the operation does not bring $|\alpha\rangle$ into $|\beta\rangle$.

The equivalent expression in the wavefunction formalism is

$$\langle\alpha|\hat{h}|\beta\rangle = \int \varphi_\alpha^*(x) \hat{h}(x) \varphi_\beta(x) dx, \quad (6)$$

where x still represents the position and the spin of the particle. \hat{h} is a single particle operator, it means it acts on one particle at a time. Two states are going to be changed. $|\alpha\rangle$ loses a particle and $|\beta\rangle$ gains one. We say for instance, that the configuration before the scattering

is $|\Phi\rangle$ and after the scattering is $|\Phi'\rangle$. This means, if our two Slater determinant $|\Phi\rangle$ and $|\Phi'\rangle$ differs in more than two states, there are some scattering processes which give zero overlap.

In other words, we allow only two states to be modified. Otherwise, the single-particle states differ and due to their orthogonal properties, we get a zero.

Similarly, for the two-particle operator we have

$$\hat{H}_I = \frac{1}{2} \sum_{i \neq j \in \llbracket N \rrbracket} \hat{v}(x_i, x_j) \rightsquigarrow \frac{1}{2} \sum_{\alpha, \beta, \gamma, \delta} \langle \alpha \beta | \hat{v} | \gamma \delta \rangle c_\alpha^\dagger c_\beta^\dagger c_\gamma c_\delta, \quad (7)$$

involving a more nested overlap of the four states α, β, γ and δ :

$$\langle \alpha \beta | \hat{v} | \gamma \delta \rangle = \int \int \varphi_\alpha^*(x) \varphi_\beta^*(x') \hat{v}(x, x') \varphi_\gamma(x) \varphi_\delta(x') dx dx'. \quad (8)$$

This expression modifies four states, so that the overlap of two Slater determinant vanishes, if the determinant differs in at least four states. We kept the hats to be consistent with the definition of \hat{H}_0 . The l.h.s of the equation is the matrix element $\langle \Phi_\alpha | \hat{v} | \Phi_\beta \rangle$ of the operator \hat{v} , which involves two basis state $|\Phi_\alpha\rangle$ and $|\Phi_\beta\rangle$.

What we defined here, is the bridge between the first and the second quantization. In later expressions with proper states we could compute each formalism separately, and notice that both lead to the same result. It is important to note that both Eq. 6 and 8 build a scalar.

It exists as well a second quantization for bosons, but this is not the aim of this thesis. For additional information, please refer to [18].

2.2.2 Basis transformation

Until now, we considered the wavefunction in a restricted basis $\{\varphi_\alpha(x)\}$. A single-particle wavefunction is defined as the overlap between a single-particle ket $|\alpha\rangle$ and an eigenstate $|x\rangle$:

$$\phi(x) = \langle x | \alpha \rangle.$$

Let us now define a new, more general operator that creates a state $|\alpha\rangle = a_\alpha |0\rangle$ for fermions. (This works as well for bosons). We assume that we have another basis $\{|\tilde{\alpha}\rangle\}$. We now want to show, that the new operator a_α can be expressed as a linear combination of the other operator $a_{\tilde{\alpha}}$. This will be a useful tool, allowing us to jump from one basis to another. We first notice the following identity relation:

$$\mathbb{I} = \sum_{\alpha} |\alpha\rangle \langle \alpha| = \sum_{\tilde{\alpha}} |\tilde{\alpha}\rangle \langle \tilde{\alpha}|,$$

this allows us to write

$$a_\alpha^\dagger |0\rangle = |\alpha\rangle = \sum_{\tilde{\alpha}} \mathcal{I} |\alpha\rangle = \sum_{\tilde{\alpha}} |\tilde{\alpha}\rangle \underbrace{\langle \tilde{\alpha} | \alpha \rangle}_{\text{scalar}} = \sum_{\tilde{\alpha}} \langle \tilde{\alpha} | \alpha \rangle |\tilde{\alpha}\rangle.$$

Please note that we write $|\tilde{\alpha}\rangle \langle \tilde{\alpha} | \alpha \rangle = |\tilde{\alpha}\rangle \langle \tilde{\alpha} | \alpha \rangle$. Inverting the indices leads to the same result, which yields to the transformation rules:

$$\begin{aligned} a_\alpha^\dagger &= \sum_{\tilde{\alpha}} \langle \tilde{\alpha} | \alpha \rangle a_{\tilde{\alpha}}^\dagger \\ a_\alpha &= \sum_{\tilde{\alpha}} \langle \alpha | \tilde{\alpha} \rangle a_{\tilde{\alpha}}. \end{aligned}$$

Furthermore, we can use these relations to express a wavefunction in the basis of another wavefunction. We have:

$$\phi_\alpha(x) = \langle x | \alpha \rangle = \langle x | \left(\sum_{\tilde{\alpha}} \langle \tilde{\alpha} | \alpha \rangle |\tilde{\alpha}\rangle \right) = \sum_{\tilde{\alpha}} \langle \tilde{\alpha} | \alpha \rangle \langle x | \tilde{\alpha} \rangle = \sum_{\tilde{\alpha}} \langle \tilde{\alpha} | \alpha \rangle \varphi_{\tilde{\alpha}}(x).$$

Inverting α and $\tilde{\alpha}$ works as well: $\varphi_{\tilde{\alpha}}(x) = \sum_{\alpha} \langle \alpha | \tilde{\alpha} \rangle \phi_\alpha(x)$.

Additionally, we can show that the basis transformation is unitary. This is an important feature because we can simplify the calculation by changing the basis, and the result would remain the same, if we use unitary transformations. Such transformations play a major role later in the thesis. We can save the $\langle \tilde{\alpha} | \alpha \rangle$ in a matrix element $D_{\tilde{\alpha}\alpha}$, and prove that the matrix D is unitary. Here we need $\langle \gamma | \beta \rangle = (\langle \beta | \gamma \rangle)^*$.

$$\begin{aligned} \langle \tilde{\alpha} | \tilde{\beta} \rangle &= \sum_{\gamma} \langle \tilde{\alpha} | \gamma \rangle \langle \gamma | \beta \rangle = \sum_{\gamma} \langle \tilde{\alpha} | \gamma \rangle (\langle \beta | \gamma \rangle)^* \\ &= \sum_{\gamma} D_{\alpha\gamma} D_{\beta\gamma}^* = \sum_{\gamma} D_{\alpha\gamma} D_{\gamma\beta}^\dagger = (DD^\dagger)_{\alpha\beta}, \end{aligned}$$

where $\langle \tilde{\alpha} | \tilde{\beta} \rangle = \delta_{\tilde{\alpha}\tilde{\beta}}$ such that $DD^\dagger = \mathbb{I}$. The matrix D is therefore unitary.

The last important step is to show that the basis transformation keeps the anti-, commutation relations. Let us for the sake of readability use the notation $[A, B]_\xi = AB + \xi BA$ where $\xi = -1$ for bosons and $\xi = +1$ for fermions. We have for example, using $[a_\alpha, a_{\alpha'}^\dagger]_\xi = \delta_{\alpha\alpha'}$

$$[a_{\tilde{\alpha}}, a_{\tilde{\alpha}'}^\dagger]_\xi = \sum_{\alpha\alpha'} \langle \tilde{\alpha} | \alpha \rangle \langle \alpha' | \tilde{\alpha}' \rangle [a_\alpha, a_{\alpha'}^\dagger]_\xi = \langle \tilde{\alpha} | \tilde{\alpha}' \rangle = \delta_{\tilde{\alpha}\tilde{\alpha}'}.$$

The first step follows after splitting the commutator in two parts, insert the transformation and recombine the new commutator. The last step involves the orthonormality of the basis. In the same way one can prove $[a_{\tilde{\alpha}}, a_{\tilde{\alpha}'}] = [a_{\tilde{\alpha}}^\dagger, a_{\tilde{\alpha}'}^\dagger] = 0$.

2.2.3 Field operators

Later in this thesis we are going to use field operators to describe an order parameter of a superconductive system. These are creation and annihilation operators that are defined in the $|x\rangle$ spin-space basis regarding another basis $\{|\alpha\rangle\}$. We here give the state as an argument and not as an index any more. Despite the notation, the following operators must not be confused with a wavefunction.

$$\hat{\psi}^\dagger(x) = \sum_{\alpha} \langle \alpha | x \rangle a_{\alpha}^\dagger = \sum_{\alpha} \varphi_{\alpha}^*(x) a_{\alpha}^\dagger, \quad (9)$$

$$\hat{\psi}(x) = \sum_{\alpha} \langle \alpha | x \rangle a_{\alpha} = \sum_{\alpha} \varphi_{\alpha}(x) a_{\alpha}, \quad (10)$$

involving fermionic or bosonic operators a . We can then annihilate and create a particle at a spin-space location x . Because the a operators are involved, the commutations properties should be respected. Using the result we had for $[a_\alpha, a_{\alpha'}]_\xi$, $[a_\alpha, a_{\alpha'}^\dagger]_\xi$ and $[a_\alpha^\dagger, a_{\alpha'}^\dagger]_\xi$ where $\xi = -$ for the bosons and $+$ for the fermions. We find the following commutation relations:

$$\begin{aligned} \left[\hat{\psi}(x), \hat{\psi}(x') \right]_\xi &= \left[\hat{\psi}(x)^\dagger, \hat{\psi}^\dagger(x') \right]_\xi = 0 \\ \left[\hat{\psi}(x), \hat{\psi}^\dagger(x') \right]_\xi &= \delta(x - x') \end{aligned}$$

In the last expression we obtain a $\langle x | x' \rangle$ which can not be normalized the $\{|x\rangle\}$ -basis. Instead of a Kronecker delta $\delta_{xx'}$, we get a delta distribution $\delta(x - x')$. This can be justified because the wavefunction is normalized and can be “seen” as well, as a distribution. The goal is now to describe the Hamiltonian using this fields operators. Therefore, we rebuild these operators in the Hamiltonian using a $\{|x\rangle\}$ basis:

$$\begin{aligned} \hat{H}_0 &= \int \hat{\psi}^\dagger(x) \hat{h}(x) \hat{\psi}(x) dx, \\ \hat{H}_I &= \frac{1}{2} \int \int \hat{\psi}^\dagger(x) \hat{\psi}^\dagger(x') \hat{v}(x, x') \hat{\psi}(x') \hat{\psi}(x) dx' dx. \end{aligned}$$

This paragraph closes the discussion of the second quantization. We introduced the creation and annihilation operators and showed how to build a second quantized version of the Hamiltonian. The goal is now to apply this formalism on a system of electrons that is going to be relevant in a later part of this work.

2.3 Case of study: electron gas with interactions

As we are later going to study, the electrons are allowed to interact with each other. The most simple interacting system involving electrons is the electron-gas. During these processes, virtual photons mediate interactions between electrons. We are going to use the formalism we introduced, to find a second quantization representation of the interacting Hamiltonian.

The system we are studying is a cube of side length L with volume $\Omega = L^3$ containing N electrons. Further we consider a periodic boundary condition for an arbitrary position vector $\mathbf{r} = (x, y, z)$:

$$(L, y, z) = (0, y, z), \quad (x, L, z) = (x, 0, z), \quad (x, y, L) = (x, y, 0).$$

We use the general form of the Hamiltonian introduced in the beginning under the Eq. 1. We consider a Coulomb potential and a kinetic energy term.

$$\hat{H}_0 = \hat{T} + \hat{U} = - \sum_{i \in \llbracket N \rrbracket} \frac{\hbar^2}{2m} \nabla_i^2 + \sum_{i \in \llbracket N \rrbracket} \hat{u}(x_i), \quad (11)$$

$$\hat{H}_I = \hat{V} = \sum_{i \neq j \in \llbracket N \rrbracket} \hat{v}(x_i, x_j), \quad (12)$$

where the pairwise potential is just a Coulomb potential $\hat{v}(x_i, x_j) = \frac{e^2}{4\pi\epsilon_0|x_i - x_j|} = v(|x_i - x_j|)$. We aim to describe the Hamiltonian in the momentum space, which is more convenient for the second quantization. Therefore, we first need to find an expression for the wave vector \mathbf{k} . We describe a state $\alpha = (\mathbf{k}, \sigma)$ at a spin-space coordinate $x = (\mathbf{r}, s)$. First we take a plane wave solution of the Schrödinger equation:

$$\psi_{\mathbf{k}}(\mathbf{r}) = \frac{1}{\sqrt{\Omega}} e^{i\mathbf{k} \cdot \mathbf{r}} \chi_{\sigma}(s)$$

The periodicity of the system allows us to write for each dimension $\psi(x=0) = \psi(x=L)$. Using these boundary conditions we obtain $1 = e^{ik_x L}$ in all directions. The result reflects itself in the wave vector \mathbf{k} , which becomes quantized:

$$\mathbf{k} = \frac{2\pi}{L} (n_x, n_y, n_z), \quad n_i \in \mathbb{Z}.$$

As we saw earlier, the eigenfunctions build a complete basis:

$$\begin{aligned} \int \psi_{\alpha'}^*(x) \psi_{\alpha}(x) dx &= \int \sum_s \psi_{\alpha'}^*(x) \psi_{\alpha}(x) d^3 r \\ &= \frac{1}{\Omega} \int e^{i\mathbf{r} \cdot (\mathbf{k} - \mathbf{k}')} \underbrace{\sum_s \delta_{s\sigma} \delta_{s\sigma'}}_{\delta_{\sigma\sigma'}} d^3 r \\ &= \delta_{\mathbf{k}\mathbf{k}'} \delta_{\sigma\sigma'} = \delta_{\alpha\alpha'}. \end{aligned}$$

The integral over the exponential function diverges if $\mathbf{k} \neq \mathbf{k}'$, so we use the case $\mathbf{k} = \mathbf{k}'$ and set the integral to zero otherwise. The kinetic energy operator is a single-particle operator. We have according to Eq. 5:

$$T = \sum_{\alpha\alpha'} \langle \alpha | \frac{\hat{\mathbf{p}}^2}{2m} | \alpha' \rangle c_{\alpha}^{\dagger} c_{\alpha'},$$

with $\hat{\mathbf{p}}$ the impulse operator in all space directions: $\hat{\mathbf{p}} = -i\hbar\nabla$. To compute this expression we use its first quantized form (see Eq. 6) involving the $\delta_{\sigma\sigma'}$ trick we introduced in the derivation of the complete basis. We also use $\mathbf{k}' = \mathbf{k}$ and hide the $\frac{1}{\Omega}$ is the $\delta_{\mathbf{k}\mathbf{k}'}$. The result reads

$$T = \sum_{\alpha, \alpha'} \delta_{\alpha\alpha'} \frac{\hbar \mathbf{k}^2}{2m} c_{\alpha'}^{\dagger} c_{\alpha} = \sum_{\alpha} \underbrace{\frac{\hbar \mathbf{k}^2}{2m}}_{=: \epsilon_{\mathbf{k}}} c_{\alpha}^{\dagger} c_{\alpha}. \quad (13)$$

We recognize the occupation number operator $\hat{n}_{\alpha} = c_{\alpha}^{\dagger} c_{\alpha}$ and the energy of the state $\epsilon_{\mathbf{k}}$. This variable plays a central role later. We obtain a quite meaningful result: The non-interacting

energy part of the system is the product of the energy of a state with the number of particle within that state, summed over all states. The single-particle operator engage a \hat{u} -term as well. This can be used by a single-particle potential such as an external electric field in the case of the electrons. We will ignore this term.

For the interaction potential we have a two-particles operator. This is described by Eq. 7 and requires Eq. 8 to be solved:

$$\hat{V} = \frac{1}{2} \sum_{\alpha\beta\gamma\delta} \langle \alpha\beta | \hat{v} | \gamma\delta \rangle c_{\alpha}^{\dagger} c_{\beta}^{\dagger} c_{\gamma} c_{\delta}.$$

We can first work on the matrix element using $v(\mathbf{r}, \mathbf{r}') = v(\mathbf{r} - \mathbf{r}')$:

$$\langle \alpha\beta | \hat{v} | \gamma\delta \rangle = \frac{1}{\Omega^2} \delta_{\sigma_{\alpha}\sigma_{\gamma}} \delta_{\sigma_{\beta}\sigma_{\delta}} \int \int e^{i\mathbf{r}(\mathbf{k}_{\gamma}-\mathbf{k}_{\alpha})} e^{i\mathbf{r}'(\mathbf{k}_{\delta}-\mathbf{k}_{\beta})} v(\mathbf{r} - \mathbf{r}') d\mathbf{r}' d\mathbf{r}.$$

After making a substitution $\mathbf{R} = \mathbf{r} - \mathbf{r}'$, adding and subtracting a $(\mathbf{k}_{\gamma} - \mathbf{k}_{\alpha})\mathbf{r}'$, we obtain:

$$\langle \alpha\beta | \hat{v} | \gamma\delta \rangle = \frac{1}{\Omega^2} \delta_{\sigma_{\alpha}\sigma_{\gamma}} \delta_{\sigma_{\beta}\sigma_{\delta}} \underbrace{\int e^{-i\mathbf{R}(\mathbf{k}_{\alpha}-\mathbf{k}_{\delta})} v(\mathbf{R}) d\mathbf{R}}_{v_{\mathbf{k}_{\delta}-\mathbf{k}_{\alpha}}} \underbrace{\int e^{i\mathbf{r}'(\mathbf{k}_{\gamma}-\mathbf{k}_{\beta}+\mathbf{k}_{\delta}-\mathbf{k}_{\alpha})} d\mathbf{r}'}_{=\delta_{\mathbf{k}_{\gamma}-\mathbf{k}_{\beta}+\mathbf{k}_{\delta}, \mathbf{k}_{\alpha}}}.$$

Here we see that the first underbraced term is the Fourier transform of a Coulomb potential v , and the second term is a Kronecker delta. From this we derive a cumbersome equation

$$\hat{V} = \frac{1}{2\Omega} \sum_{\substack{\mathbf{k}_{\alpha}\mathbf{k}_{\beta}\mathbf{k}_{\gamma}\mathbf{k}_{\delta} \\ \sigma_{\alpha}\sigma_{\beta}\sigma_{\gamma}\sigma_{\delta}}} \delta_{\sigma_{\alpha}\sigma_{\gamma}} \delta_{\sigma_{\beta}\sigma_{\delta}} \delta_{\sigma_{\alpha}\sigma_{\gamma}} \delta_{\sigma_{\beta}\sigma_{\delta}} \delta_{\mathbf{k}_{\alpha}, \mathbf{k}_{\gamma}-\mathbf{k}_{\beta}+\mathbf{k}_{\delta}} v_{\mathbf{k}_{\alpha}-\mathbf{k}_{\delta}} c_{\mathbf{k}_{\alpha}\sigma_{\alpha}}^{\dagger} c_{\mathbf{k}_{\beta}\sigma_{\beta}}^{\dagger} c_{\mathbf{k}_{\gamma}\sigma_{\gamma}} c_{\mathbf{k}_{\delta}\sigma_{\delta}}.$$

We can sum over the \mathbf{k}_{α} , rename $\sigma_{\alpha} \rightarrow \sigma$ and $\sigma_{\beta} \rightarrow \sigma'$ and sum up over σ_{γ} and σ_{δ} to simplify the Kronecker deltas.

$$\hat{V} = \frac{1}{2\Omega} \sum \sigma \sigma' \sum_{\mathbf{k}_{\beta}\mathbf{k}_{\gamma}\mathbf{k}_{\delta}} v_{\mathbf{k}_{\gamma}-\mathbf{k}_{\beta}} c_{\mathbf{k}_{\delta}+\mathbf{k}_{\gamma}-\mathbf{k}_{\beta}, \sigma}^{\dagger} c_{\mathbf{k}_{\beta}, \sigma'}^{\dagger} c_{\mathbf{k}_{\gamma}\sigma'} c_{\mathbf{k}_{\delta}\sigma'},$$

where using $\mathbf{k}_{\alpha} = \mathbf{k}_{\gamma} - \mathbf{k}_{\beta} + \mathbf{k}_{\delta}$ from the Kronecker delta we get $v_{\mathbf{k}_{\alpha}-\mathbf{k}_{\delta}} = v_{\mathbf{k}_{\gamma}-\mathbf{k}_{\beta}+\mathbf{k}_{\delta}-\mathbf{k}_{\delta}}$. Then we can introduce the following variable transformations:

$$\mathbf{k}_{\delta} \rightarrow \mathbf{k}, \quad \mathbf{k}_{\gamma} \rightarrow \mathbf{k}', \quad \mathbf{k}_{\beta} \rightarrow \mathbf{k}' - \mathbf{q},$$

which yields:

$$\begin{aligned} \mathbf{k}_{\delta} + \mathbf{k}_{\gamma} - \mathbf{k}_{\beta} &= \mathbf{k} + \mathbf{q}, \\ \mathbf{k}_{\gamma} - \mathbf{k}_{\beta} &= -\mathbf{q}, \end{aligned}$$

and we finally get our second quantized interaction operator:

$$\hat{V} = \frac{1}{2\Omega} \sum_{\mathbf{q}} v_{\mathbf{q}} \sum_{\substack{\mathbf{k} \\ \mathbf{k}'\sigma'}} c_{\mathbf{k}+\mathbf{q}, \sigma}^{\dagger} c_{\mathbf{k}'-\mathbf{q}, \sigma'}^{\dagger} c_{\mathbf{k}'\sigma'} c_{\mathbf{k}\sigma}.$$

This describes an electron transferring a momentum \mathbf{q} to another electron. The formula tells that we first destroy both electrons as they are before the interaction. Then we create two in the new states, where one lost some momentum that has been transferred the other electron. Here the v -term modulates the strength of the process. The Coulomb force is known to decline with the inverse of the distance $\mathbf{r} - \mathbf{r}'$ between the electrons, but do not depend on their respective positions \mathbf{r} and \mathbf{r}' . This exchange is therefore invariant under translations. The following Feynman-diagram is a good illustration of this process.

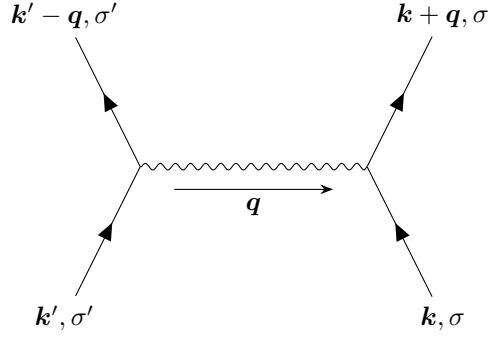


Figure 2: Feynman-diagram of the interaction of two electrons modulated by a photon of momentum \mathbf{q} . The leftmost starts in the state (\mathbf{k}', σ') and gives a momentum \mathbf{q} to the rightmost electron. The time is represented on the horizontal axis and the space on the vertical one.

This closes the introduction theory on the second quantization. We saw how we can express integrals of wave functions over the spin-space space as bracket scalar products. We introduce two operators that create and annihilate particles in a certain state. Using this formalism we were able to compute the Hamiltonian of the system in the momentum space. We found that the non-interacting-part relies on the energy of each state times their occupation number. In the last part we showed that an interaction between two electrons can be described as a momentum transfer between them, which is modulated by the Fourier transform of the Coulomb potential.

The goal of this thesis is to study how the superconductivity behaves in the proximity of an altermagnet. Over the next chapter we are going to explain how a superconductive state works. The altermagnet will be presented in a later part of this work.

3 Superconductivity



Along with the derivation of the superconductivity, we are going to follow closely the work of Fossheim and Sudbø [19] from chapter 1 to 4. Superconductivity can be illustrated as a phase transition of a metal when its temperature lies under a crystal temperature T_C . In the superconductive state the material becomes a perfect diamagnet and its resistivity vanishes. If we apply a magnetic field on superconductive metal, we will observe some shielding currents that arise on its surface. They are labelled as Meissner currents. We have as well an internal magnetic field, that cancels exactly the one that is applied outside. The magnetic susceptibility in the body is then $\chi = -1$.

A second property that found multiple technical use cases is the friction-less flow of a current in the metal. The current can flow for a very long time without losing energy. In the first chapter of [19] Fossheim and Sudbø even calculated a significant decay of this current that exceeds the age of the universe. The superconductive state is also described as a Meissner state.

Suppose that we now heat the material at the critical temperature T_C , some fluctuation effects appear and break the superconductive state. We usually distinguish type I and type II superconductors. The type I superconductors lose abruptly their magnetization over T_C . Type II have a mix of ordinary and superconductive properties at intermediate temperatures. In this mixed states the magnetization slowly decreases while heating the metal, until we can not measure any Meissner state any more over T_C . Above an intermediate field strength, we observe as well some vortices and flux lines that pierce the material.

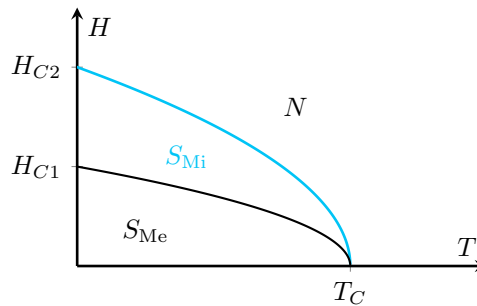


Figure 3: The phase diagram of a superconductive material regarding the temperature and the external applied magnetic field strength. Type I superconductor can only be in the Meissner state S_{Me} or in the normal state N . Type II superconductor additionally have mixed state S_{Mi} between the two. The critical values depend on the material. Increasing the field strength lowers the critical temperature. The diagram is inspired by [19].

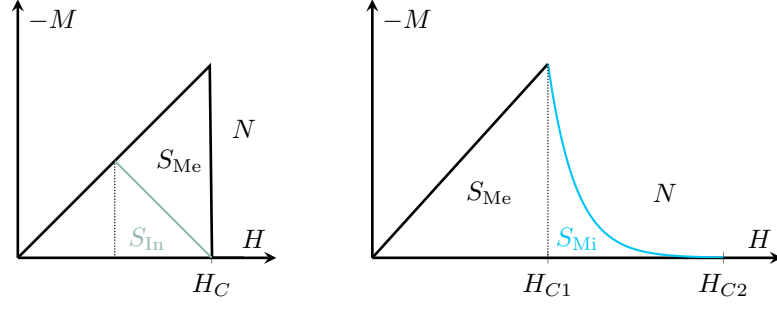


Figure 4: The left plot shows how the magnetization of a type I grows with the external field strength to cancel the applied field inside the material. Above the critical field strength H_C the material becomes a normal metal and the field flows through it. If the material has a non-zero demagnetization factor, the field starts to penetrate the body at an intermediate field strength, leading to an intermediate (not mixed!) state S_{In} . The field penetrates in form of flux lines, along the normal to the surface. On the other hand we have a figure that after showing the cancellation of the field inside the body, highlights the presence of a mixed state in a type II superconductor. The field penetrates the material in the form of vortices, and finally let all the external field stream in the material. The picture is inspired by [19].

During the suppression of the superconductive state more and more magnetic field is permitted inside the material. Assuming that some particles are responsible for the superconductivity, the field will penetrate more easily where we observe a lower density of these particles.

The Meissner state is a thermodynamic state. This means that we can completely identify it with a set of variable that we are going to derive. We can show that the free energy of the superconductive state is lower than the normal state. This results in a lower entropy compared to the normal state ([19] chap. 1.6). For readability reason we set the reduced Planck constant $\hbar = 1$ in the following. Further we include the chemical potential in the energy of the state, such that now $\epsilon_k - \mu \rightarrow \epsilon_k$, which was originally defined at Eq. 13.

The Hamiltonian of the system is described by the solid state physics. We consider the energy of the electrons and the ions in a lattice and the interaction between them resulting in the following, very generic expression of the Hamiltonian:

$$H = H_{e-e} + H_{e-ion} + H_{ion-ion}.$$

Each term consist of a kinetic and potential energy term. For a more mathematical approach we consider a system of N electrons and L ions and define:

$$\begin{aligned} H_{e-e} &= \sum_{i \in \llbracket N \rrbracket} \frac{p_i^2}{2m} + \sum_{ij \in \llbracket N \rrbracket} V_{\text{Coulomb}}^{e-e}(\mathbf{r}_i - \mathbf{r}_j), \\ H_{ion-ion} &= \sum_{i \in \llbracket M \rrbracket} \frac{p_i^2}{2M} + \sum_{ij \in \llbracket L \rrbracket} V_{\text{Coulomb}}^{\text{ion-ion}}(\mathbf{R}_i - \mathbf{R}_j), \\ H_{e-ion} &= \sum_{i \in \llbracket N \rrbracket, j \in \llbracket L \rrbracket} V_{\text{Coulomb}}^{e-ion}(\mathbf{r}_i - \mathbf{R}_j). \end{aligned}$$

We have m and M as the mass of the electron and the ion. \mathbf{r} and \mathbf{R} are the position of the electron and the ion. The ion-ion potential freezes the ions into the lattice. First, we are going to introduce some concepts by describing a non-interacting electron and then improve the model by including the interactions. Usually, the potential of a lattice is periodic. If so, according to the Bloch theorem, the wave function of a particle moving in the system is a plane wave modulated by a periodic function. Eigenstates of the corresponding Hamiltonian are called Bloch states.

3.1 The non-interacting electron gas

In this case of study the Hamiltonian only includes a kinetic term

$$H = \sum_{\mathbf{k}, \sigma} \epsilon_{\mathbf{k}} c_{\mathbf{k}\sigma}^\dagger c_{\mathbf{k}\sigma}. \quad (14)$$

We assume that there exists a ground state $|0\rangle$, where the system is filled up with a certain amount of electrons until the Fermi-energy ϵ_F is reached. Associated with this energy, we find a wave vector \mathbf{k}_F , the Fermi-momentum. The set of energy up to ϵ_F is called the Fermi-sea, as an analogy to the level zero of the topographic maps. Put into a mathematical form, the Fermi-sea is defined as:

$$\hat{n}_{\mathbf{k},\sigma}|0\rangle = \Theta(\epsilon_F - \epsilon_{\mathbf{k}})|0\rangle. \quad (15)$$

We introduced here a very useful tool called the Heaviside step function, which is defined as:

$$\Theta(x) = \begin{cases} 1, & x > 0 \\ 0, & x < 0 \end{cases}, \quad \Theta(-x) = 1 - \Theta(x). \quad (16)$$

This means that we find no particles that have an energy higher than the Fermi-energy ($\mathbf{k} > \mathbf{k}_F$).

Now we want to study how the electron can scatter in different states. The function that we are using is called the propagator, and gives the probability to find the particle in the state $|\mathbf{k}', \sigma\rangle$ at a time t' , knowing it at $|\mathbf{k}, \sigma\rangle$ and t . An important fact is that without interaction, the particle should not scatter in another state, due to energy conservation. Therefore,

$$G_0(\mathbf{k}, \mathbf{k}', t' - t) = G_0(\mathbf{k}, t' - t)\delta_{\mathbf{k}, \mathbf{k}'},$$

which is zero if the wave-vectors between the two time points differs. We observe that only the pastime $t' - t$ is relevant. This is due to the time independence of the Hamiltonian. We are going to use the representation in the frequency space, using a Fourier-transformation.

$$G_0(\mathbf{k}, \omega) = \int_{\mathbb{R}} e^{i\omega t} G_0(\mathbf{k}, t) dt = \frac{1}{\omega - \epsilon_{\mathbf{k}} + i\delta_{\mathbf{k}}}, \quad (17)$$

where $\delta_{\mathbf{k}} = \delta \cdot \text{sgn}(\epsilon_{\mathbf{k}} - \epsilon_F)$ involving a very small, non-zero number δ . We observe that this analytical function has a pole given by:

$$\begin{aligned} \omega - \epsilon_{\mathbf{k}} + i\delta_{\mathbf{k}} &= 0 \\ \iff \omega &= \epsilon_{\mathbf{k}} - i\delta_{\mathbf{k}}, \end{aligned}$$

where we denote i as the imaginary unit to avoid confusion with the index i . The variable $\epsilon_{\mathbf{k}}$ gives the so-called spectrum or dispersion relation of the excitations. Please remember that we set $\hbar = 1$. The imaginary part serves as a damping term and is inversely proportional to the lifetime of the particle. As a result of the absence of scattering, δ is a small number due to the infinitely long lifetime of the electrons.

Further the propagator yields important information on the system, when considering the integration over its different arguments. First we take the imaginary part of the propagator, called the single particle spectral weight $A(\mathbf{k}, \omega)$.

$$\begin{aligned} A(\mathbf{k}, \omega) &= -\frac{1}{\pi} \text{Im} [G_0(\mathbf{k}, \omega)] = \frac{1}{\pi} \frac{\delta_{\mathbf{k}}}{(\omega - \epsilon_{\mathbf{k}})^2 + \delta_{\mathbf{k}}} \\ &= \delta(\omega - \epsilon_{\mathbf{k}}) \end{aligned} \quad (18)$$

which informs us about possible available state which may be occupied. We can find a form for the momentum distribution $n(\mathbf{k})$:

$$n(\mathbf{k}) = \int A(\mathbf{k}, \omega) d\omega, \quad (19)$$

and for the density of state:

$$D(\omega) = \int A(\mathbf{k}, \omega) d^3k, \quad \text{or for discontinuous state } \sum_{\mathbf{k}} A(\mathbf{k}, \omega). \quad (20)$$

These equations picture the non-interacting electron gas. Now that we put the ground corners, we can make the model more advanced.

3.2 Fermi-liquid: the interacting case

Now that we have described the non-interacting system, let us make the model more precise by introducing the interactions. In an earlier section we saw how

$$H = \sum_{\mathbf{k}\sigma} \epsilon_{\mathbf{k}} c_{\mathbf{k},\sigma}^\dagger c_{\mathbf{k},\sigma} + \sum_{\mathbf{k}\sigma\mathbf{k}'\sigma'} V_{\mathbf{k}\mathbf{k}',\mathbf{q}} c_{\mathbf{k}-\mathbf{q},\sigma}^\dagger c_{\mathbf{k}+\mathbf{q},\sigma'}^\dagger c_{\mathbf{k},\sigma} c_{\mathbf{k}',\sigma'} \quad (21)$$

represents the pairwise interaction of multiple electrons and their respective energy.

To extend the model we now want to introduce two new quantities, the propagator G and the one-particle irreducible self-energy Σ . The propagator $G : \mathbb{R}^3 \times \mathbb{R} \mapsto \mathbb{C}$ gives the probability amplitude of finding a particle in the state $|\mathbf{k}, \sigma\rangle$ at a time t . On the other hand for $\Sigma_R, \Sigma_I \in \mathbb{R}$ and $\Sigma \in \mathbb{C}$, we define the complex self energy $\Sigma = \Sigma_R + i\Sigma_I$. This variable contains the lifetime of the particle in this state, and the shift of the particle's energy due to the interaction with the surroundings. The framework defines the non-interacting energy of the particle as $\epsilon_{\mathbf{k}}$. When put in an interacting system, the spectrum shifts and becomes $\tilde{\epsilon}_{\mathbf{k}} = \epsilon_{\mathbf{k}} + \Sigma_R$. Due to the interactions, the particle then has a much smaller lifetime. Σ_I is inversely proportional to the particle's lifetime $\tau_{\mathbf{k}}$. As said, Σ_I is very small in the non-interacting case. These two quantities are linked through the Dyson equation, which reads

$$(G(\mathbf{k}, \omega))^{-1} = (G_0(\mathbf{k}, \omega))^{-1} - \Sigma(\mathbf{k}, \omega). \quad (22)$$

One can use a Fourier-transformation to switch from the time representation to the frequency representation ω . Reordering the equation and using the result from Eq. 17 we obtain

$$G(\mathbf{k}, \omega) = \frac{1}{\omega - \epsilon_{\mathbf{k}} - \Sigma}.$$

This function has a pole at $\omega = \epsilon_{\mathbf{k}} + \Sigma_R + i\Sigma_I$, where in the none interacting case $\omega = \epsilon_{\mathbf{k}} + i\delta_{\mathbf{k}}$. This expression makes sense, the particle spectrum is now shifted due to its finite lifetime, as a result of the interaction. The pole yields to an expression for the spectrum

$$\omega - \epsilon_{\mathbf{k}} - (\Sigma_R(\mathbf{k}, \omega) + i\Sigma_I(\mathbf{k}, \omega)) = 0. \quad (23)$$

In complex analysis, the order of a pole is given as n , if $f(z)$ is meromorphic and has a pole at z_0 where

$$(z - z_0)^n f(z)$$

is also meromorphic in the neighbourhood of z_0 . In our case we are interested in the 0-th order of the pole and first ignore the imaginary part of the pole. What we get is an expression for the energy shift:

$$\omega = \epsilon_{\mathbf{k}} + \Sigma_R(\mathbf{k}, \epsilon_{\mathbf{k}}) = \tilde{\epsilon}_{\mathbf{k}}.$$

If we take into account a tiny imaginary part of Σ we obtain a shifted pole. Performing a Taylor expansion of Σ_R in the neighbourhood of $\omega = \tilde{\epsilon}_{\mathbf{k}}$ will help us for the simplifications done towards a better understanding.

$$\Sigma_R(\mathbf{k}, \omega) = \Sigma_R(\mathbf{k}, \tilde{\epsilon}_{\mathbf{k}}) + (\omega - \tilde{\epsilon}_{\mathbf{k}}) \left. \frac{\partial \Sigma_R}{\partial \omega} \right|_{\omega=\tilde{\epsilon}_{\mathbf{k}}} + \mathcal{O}(\omega^2)$$

We aim to compute to the first order in Σ_I such that we evaluate it at $\omega = \tilde{\epsilon}_{\mathbf{k}}$. Starting from Eq. 23, and after inserting the Taylor expansion for Σ_R , we obtain

$$\begin{aligned} \omega - \underbrace{(\epsilon_{\mathbf{k}} + \Sigma_R(\mathbf{k}, \tilde{\epsilon}_{\mathbf{k}}))}_{=\tilde{\epsilon}_{\mathbf{k}}} - (\omega - \tilde{\epsilon}_{\mathbf{k}}) \left. \frac{\partial \Sigma_R}{\partial \omega} \right|_{\omega=\tilde{\epsilon}_{\mathbf{k}}} - i\Sigma_I(\mathbf{k}, \tilde{\epsilon}_{\mathbf{k}}) &= 0 \\ \iff (\omega - \tilde{\epsilon}_{\mathbf{k}}) \left(1 - \left. \frac{\partial \Sigma_R}{\partial \omega} \right|_{\omega=\tilde{\epsilon}_{\mathbf{k}}} \right) - i\Sigma_I(\mathbf{k}, \tilde{\epsilon}_{\mathbf{k}}) &= 0. \end{aligned} \quad (24)$$

We define the residue of the propagator as


$$z_{\mathbf{k}} = \frac{1}{1 - \left. \frac{\partial \Sigma}{\partial \omega} \right|_{\omega=\tilde{\epsilon}_{\mathbf{k}}}}, \quad (25)$$

which we can insert in the inverse lifetime of the electron occupying the state $|\mathbf{k}, \sigma\rangle$:

$$\frac{1}{\tau_{\mathbf{k}}} = -z_{\mathbf{k}} \Sigma_I(\mathbf{k}, \tilde{\epsilon}_{\mathbf{k}}).$$

This justifies the statement $\Sigma_I \propto 1/\tau_{\mathbf{k}}$. This residue is a decreasing function of the energy, which means that its influence is more important for low energies. An interpretation could be that the slow moving electrons have less time to interact with their fast homologues, which results in a longer lifetime.

We recall once again the difference of the propagators to conclude this section:

Free electron		Interacting electron
$G_0(\mathbf{k}, \omega) = \frac{1}{\omega - \epsilon_{\mathbf{k}} + i\delta_{\mathbf{k}}}$		$G(\mathbf{k}, \omega) = \frac{z_{\mathbf{k}}}{\omega - \tilde{\epsilon}_{\mathbf{k}} + i\frac{1}{\tau_{\mathbf{k}}}}$

Interacting electrons represent a degraded version of the free-electron case, characterized by a quasiparticle weight $z_{\mathbf{k}} < 1$.

Quasi-particles

The main question we have now is: What does the residue look like on the Fermi surface? Consider a low energy electron, close to the Fermi-surface and after an interaction happened. It turns out, that if there is a $z_{\mathbf{k}_F} > 0$, we find a precise low energy single particle excitation. This excitation is very close to the exact eigenfunction of a non-interacting Hamiltonian. We call this state akin to the free electron, a quasi-particle.

This is it, a Fermi-liquid is a system of interacting electrons and quasi-particles. These quasi-particles are not exact eigenstates of the non-interacting Hamiltonian: We can not consider them as an electron-like excitation in the non-interacting context. In fact, the interactions allow to scatter some states in and out of the Bloch-State. However, in a Fermi-Liquid, they are well-defined enough to be interpreted as electron-akin excitation of the interacting system.

The above expression for the momentum distribution $n(\mathbf{k})$ at Eq. 19 can be plotted, and we recognize a gap of $z_{\mathbf{k}_F} < 1$. This property of the Fermi liquid is a central difference with the non-interacting system. Back then the momentum distribution had a discontinuity from one to zero when crossing the Fermi surface (Eq. 15).

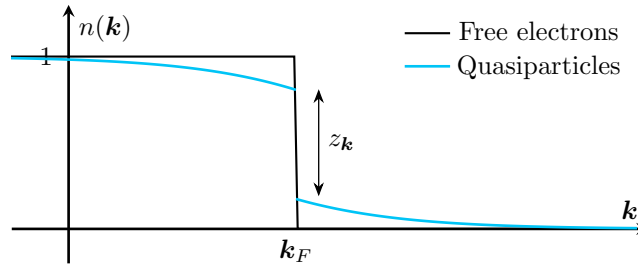


Figure 5: The momentum distribution in a Fermi liquid for free electrons and quasi-particles. The quasi-particles have a smaller gap, allowing to have energies beyond the Fermi surface. This gap has exactly the magnitude of the quasiparticle's weight defined in Eq. 25. Inspired by [19].

An important feature to mention, that is the key understanding of the Fermi-liquid, is the one-to-one correspondence of quantum numbers between the interacting and non-interacting electrons. This revealed itself to be correct for metals. This means we can start with simple Hamiltonian like Eq. 14 and add new particles by introducing some perturbations. The obtained quasi-particles are a result of the excitation of the non-interacting system. We then

observe this one-to-one correspondence.

The last question one can ask is: Why does this approximation work so well in the most case? The answer lies in the reference system we choose to perturb around. Keeping in mind the Pauli principle, we notice that the added particles are restricted in their scattering. This is so strong, that it almost cancels out the “switching-on” of the interactions. It is a good decision to perturb around the free system. In the free case we are limited in the number of particle in the ground state (Pauli principle). Therefore, [19] points out that thermodynamic quantities change smoothly when we incorporate the interactions in the system.

We want to emphasize one last time that the Fermi-liquid formalism work because of the momentum restrictions due to the Pauli exclusion principle.

Repulsive interactions

In condensed matter physics the dominant effect is the repulsive interactions between the electrons due to the Coulomb potential. We already described it in the Hamiltonian H_{e-e} using some pairwise interactions in Eq. 21. Therefore, the goal is now to find an expression for the Coulomb potential in momentum space.

As we can see in Eq. 21 the system is described in the momentum-space. For this reason we need to consider the Fourier-transform of the real space potential. We start with the Coulomb potential which is predominant in the solid state physics. However, the integral is going to diverge for $r \rightarrow 0$. To solve this problem We introduce the Yakuwa potential which exponentially modulates the Coulomb potential:

$$V_\lambda(r) = \frac{1}{4\pi\epsilon_0} \frac{e^2}{r} e^{-r\lambda}, \quad (26)$$

The motivation for introducing the exponential factor is so that the Fourier transform can be more easily performed. Letting $\lambda \rightarrow 0$ in the result, we obtain after [20]:

$$V_{\mathbf{k},\mathbf{k}',\mathbf{q}} = V_{\text{el}}(\mathbf{q}) := \frac{1}{4\pi\epsilon_0} \frac{2\pi e^2}{\mathbf{q}^2}, \quad (27)$$

with \mathbf{q} the momentum transfer during the interaction. We see that in the same way Coulomb potential in its real space form does not depend on the respective positions but only on the distance, this expression is independent of the initial states. The Fermi-liquid remains stable to the repulsive processes, because the accessed energy level are all avoid the surface.

However, as we are going to see in the next section, attractive interactions also take place due to an exchange of phonons between two electrons. This will be an additional step towards the description of the Meissner state.

3.3 Instability due to attractive interactions

We are going to show how the attractive interactions destabilize the Fermi-liquid. This is done by proving that new ground states open. Leon Cooper introduced a very specific context of attraction, that has a strong influence on the stability. Taking this example we are going to make clear that attractive interactions can in some cases exceed the Coulomb force, resulting in unexpected new eigenstates.

Let's assume we have an inert Fermi sea, where the electrons are considered non-interactive. Adding electrons requires to place them above the sea. The exotic context is due to the interactions. They can only interact if they are within a small frequency cover ω_0 over the Fermi surface, one on each side, facing them through the complete surface. If this is not the case the interaction vanishes.

Fossheim and Sudbø derived a method in [19] from p.67 to 69. They conclude with the fact that allowing such interaction leads to a total energy of the interacting system E smaller than $2\epsilon_F$. This means that the attraction of the electrons shift them in a state that lies under the Fermi sea. Further they showed that if the Fermi sea vanishes (one could take electrons out of the system), then this attractive pairing disappears. The same is observed as we approach the

classical limit. By forming a pair the electrons effectively acts as a boson in some ways. These pairs are named Cooper pairs by the eponymous physicist. The Pauli principle does not rule their energies any more.

We now understand why attractive processes create instabilities in the liquid. An energy gap opens below the energy surface, reflecting the energy needed to break the new formed Cooper pairs. The shell ω_0 is the maximum frequency delivering the “adhesive” that allows the electron to pair. Now that we showed the influence of attractive interactions, we seek some candidate processes that are attractive.

3.4 Attractive forces mediated by phonons

As known from condensed matter physics, the lattice can have some internal oscillations called phonons resulting from the spring coupling between the ions. Now we can imagine that due to the Coulomb interactions, an electron can shift the ions producing a phonon. If this phonon travels and influences another electron on its way, we result in an effective electron-electron interaction thanks to the phonon. A similar case would be the exchange of a photon between two electrons. We are going to show how this exchange can lead to an attractive interaction.

In a dense lattice the ions move much slower around their equilibrium positions than the light electrons who pass by. The electrons move the charges of the ions, inducing in a small dipole moment. A second electron that also passes in the surrounding is going to feel the dipole moment, and will be attracted. Then the ion shifts back in its new equilibrium position, and the dipole moment vanishes long after the first electron passed.

Moreover, due to the Coulomb interactions, the electrons aim to put as much distance as they can between them, in a minimal amount of time. Therefore, we can say that the \mathbf{k} -quantum number should be opposite between the two electron. If we target to put these concepts in a mathematical form, we use our previous Hamiltonian, and add an electron-phonon interaction term.

$$H = \sum_{\mathbf{k},\sigma} \epsilon_{\mathbf{k}} c_{\mathbf{k},\sigma}^\dagger c_{\mathbf{k},\sigma} + \sum_{\mathbf{k},\sigma,\mathbf{k}',\sigma'} V_{\mathbf{k}\mathbf{k}',\mathbf{q}} c_{\mathbf{k}-\mathbf{q},\sigma}^\dagger c_{\mathbf{k}+\mathbf{q},\sigma'}^\dagger c_{\mathbf{k},\sigma} c_{\mathbf{k}',\sigma'} + V_{e\text{-phonon}}$$

where $V_{e\text{-phonon}}$ usually depends on the sum picturing the phonons-modes λ . These modes are similar to the oscillations modes we have in a CO_2 -molecule for example. The expression that forms the phonon-depend potential in momentum space reads

$$V_{e\text{-phonon}} = \sum_{\mathbf{k},\mathbf{q},\sigma} M_{\mathbf{q}} (a_{-\mathbf{q}}^\dagger + a_{\mathbf{q}}) c_{\mathbf{k}+\mathbf{q},\sigma}^\dagger c_{\mathbf{k},\sigma}. \quad (28)$$

$M_{\mathbf{q}} (a_{-\mathbf{q}}^\dagger + a_{\mathbf{q}})$ is a matrix element of the coupling between the electron and the phonon. The $a_{\mathbf{q}}$ and $a_{\mathbf{q}}^\dagger$ are annihilation and creation operators of a phonon with wave vector \mathbf{q} .

Let us now take a step aside and recall the quantum oscillator. Its eigenstates are considered as bosonic. This is achieved by showing that the ladder operators verify the commutation relation $[a, a^\dagger] = 1$. On the other side, the phonons are modelled with springs between the ions. For this reason they behave in the same manner as the quantum oscillator: By extension phonons act like bosons. For this reason they verify:

$$[a_{\mathbf{q}}, a_{\mathbf{q}'}^\dagger] = \delta_{\mathbf{q},\mathbf{q}'}$$

Their number is however not conserved in a solid. The matrix element M is a function of the eigenfrequency of the phonon $\omega_{\mathbf{q},\lambda}$ and the Fourier transform \tilde{V} of the electrostatic potential $V_\lambda(\mathbf{q})$ between the electron and the phonon of mode λ , if included.

$$M_{\mathbf{q},\lambda} = i(\mathbf{q} \cdot \boldsymbol{\xi}_\lambda) \sqrt{\frac{\hbar}{2M\omega_{\mathbf{q},\lambda}}} \tilde{V}_\lambda(\mathbf{q}).$$

We do not provide here a detailed calculation of $M_{\mathbf{q},\lambda}$. This pairing is much weaker than the electron-photon interaction. Another important fact is that for $\mathbf{q} \rightarrow 0$ the matrix element M vanishes. M is proportional to \mathbf{q} which illustrates how the electron-phonon interaction happens between a point charge and a dipole.

The goal is now to implicitly express the phonon exchange with an effective electron-electron process. If we consider two diagrams, one aiming to describe the absorption of a phonon and one the emission of a phonon, we can combine them to get a new effective interaction like the photon exchange case.

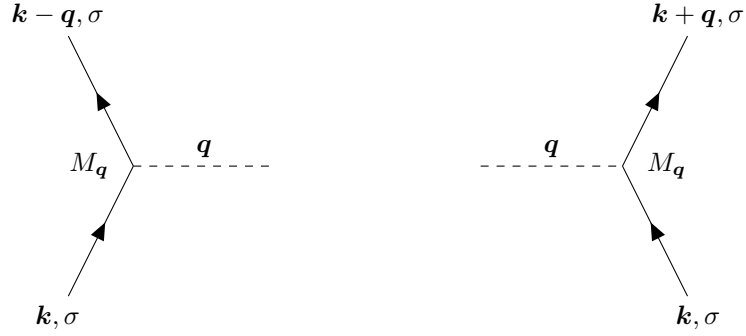


Figure 6: The emission (left) and absorption (right) diagram of a phonon of wave vector \mathbf{q} by an electron. The matrix element $M_{\mathbf{q}}$ gives the probability amplitude of emitting or absorbing the phonon. This plays a role in the Fermi golden rule, when it comes to give the transition rate of the scattering of the electron in its new state.

If we represent this interaction by linking both \mathbf{q} -edges, i.e. the emitted phonon is absorbed by another electron, the energy of phonon is simply defined as

$$H_{\text{phonon}} = \sum_{\mathbf{q}} \omega_{\mathbf{q}} a_{\mathbf{q}}^{\dagger} a_{\mathbf{q}}.$$

We can write a propagator which describes the dashed line in a connected context similarly to the photon case described in Fig. 2.

$$D_0(\mathbf{q}, \omega) = \frac{2\omega_{\mathbf{q}}}{\omega^2 - \omega_{\mathbf{q}}^2 + i\eta},$$

involving a very small quantity η . From this we obtain an expression for the phonon-mediated interaction of two electrons. This is performed using $V_{\text{eff}}^{(ph)}(\mathbf{q}, \omega) = \text{Re}(|M_{\mathbf{q}}|^2 D_0(\mathbf{q}, \omega))$ and discarding the second order η term which is very small. We get:

$$V_{\text{eff}}^{(ph)}(\mathbf{q}, \omega) = \frac{2|M_{\mathbf{q}}|^2 \omega_{\mathbf{q}}}{\omega^2 - \omega_{\mathbf{q}}^2}, \quad (29)$$

with \mathbf{q} the momentum transfer. We can now use a more complete potential in the Hamiltonian involving both the electrostatic (Eq. 27) and effective phonon-mediated interactions (Eq. 29):

$$V_{\text{eff}}(\mathbf{q}, \omega) = V_{\text{el}}(\mathbf{q}) + V_{\text{eff}}^{(ph)}(\mathbf{q}, \omega) = \frac{1}{4\pi\epsilon_0} \frac{2\pi e^2}{\mathbf{q}^2} + \frac{2|M_{\mathbf{q}}|^2 \omega_{\mathbf{q}}}{\omega^2 - \omega_{\mathbf{q}}^2}. \quad (30)$$

Here we have reached a very important point. This new potential can be in some case negative, which means it results in an attractive interaction between the electrons. In other words, in some cases the phonon exchange can be attractive and even overcome the strong repulsive Coulomb potential.

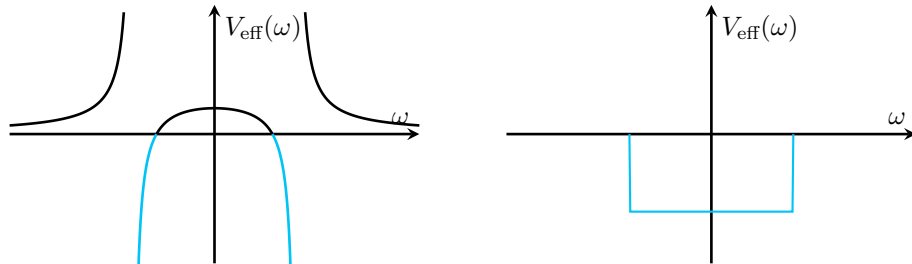


Figure 7: Left the course of the phonon-mediated effective potential V_{eff} defined in Eq. 30. For some values of ω the potential is attractive. On the right is a simplified version of the potential that revealed itself to be very accurate with the experiments. Inspired by [19].

3.5 Construction of the effective Hamiltonian

We want to restrict ourselves in the case where the effective Hamiltonian is attractive. This happens in a small shell around the Fermi-surface. If we want to maximize the phase space for the scattering, the state before and after the scattering have to be in this shell. A good idea is to consider that the two electrons have opposite wave vectors. The following figure illustrates this process.

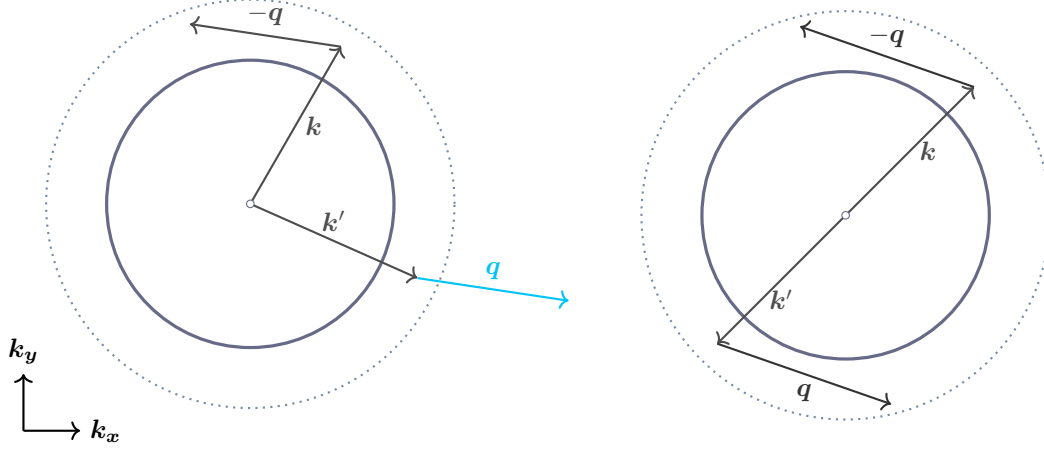


Figure 8: The scattering process of two electrons with opposite wave vectors \mathbf{k} and \mathbf{k}' . We have a momentum transfer \mathbf{q} between them. The thick line illustrates the Fermi surface and the dotted one the thin shell. As we see, if the electrons have opposite wave vectors, and the \mathbf{k} electron scatters into the shell, then the \mathbf{k}' electron scatters in the shell as well. This is not always the case if the wave vectors do not agree, as we can see on the left figure. The right figure points out the maximization process. With opposite wave vectors, we get the largest possibility spectrum for the scattering. Inspired by [19].

Further the attraction is a short range effect, so if we want to consider it, we must think that the electrons are very close to each other. This requires the electrons to have opposite spins due to the Pauli principle. Latter we are going to introduce the tight binding formalism. In this context we want the electrons to be on the same lattice site to be able to form a pair. This shell approximation turns out to be a good model.

Now we allow us to rename some variables:

$$\mathbf{k} + \mathbf{q} \longrightarrow \mathbf{k}, \quad \mathbf{k} \longrightarrow \mathbf{k}'.$$

The Hamiltonian that follows from these transformations is called the BCS-reduced Hamiltonian and first found by Bardeen, Cooper and Schrieffer in 1957 [21].

$$H = \sum_{\mathbf{k}, \sigma} \epsilon_{\mathbf{k}} c_{\mathbf{k}, \sigma}^{\dagger} c_{\mathbf{k}, \sigma} + \sum_{\mathbf{k}, \mathbf{k}', \sigma} V_{\mathbf{k} \mathbf{k}'} c_{\mathbf{k}, \sigma}^{\dagger} c_{-\mathbf{k}, \bar{\sigma}}^{\dagger} c_{-\mathbf{k}', \bar{\sigma}} c_{\mathbf{k}', \sigma}, \quad (31)$$

where $\bar{\sigma}$ is the opposite spin of σ . The two rightmost operators destroy the electron with opposite wave vectors and spin before the interaction and creates two new with opposite wave vectors, including the loss/gain of momentum, and opposite spin after the interaction. To convince oneself, we can just look at the expression before the variable transformation. The potential $V_{\mathbf{k} \mathbf{k}'}$ that modulates the strength of this pairing is now a matrix element that acts if the wave vectors are close to the Fermi-surface. The electrons have to move in opposite directions with opposite spins. Due to the retardation processes we introduced earlier, there remains a distortion in the lattice long after the electrons passed. Due to the inducing dipole moment, the other electron is attracted towards the distortion. As we also saw, the Coulomb repulsion causes a collinear displacement, close to the distortion that its homologue produced. This phenomenon is called the Cooper-pairing and is a coupling that happens in momentum space.

The reader might want to see a picture of what is happening in the real space. To achieve a representation two simple statements are enough. First, the Coulomb force aims to maximize

the distance between the electrons in minimal time. This is achieved by moving them collinearly in opposite directions. Second, due to the retardation process, it is energetically more favourable for the electron to move along the distortion of the lattice. The result is illustrated in Fig. 9.

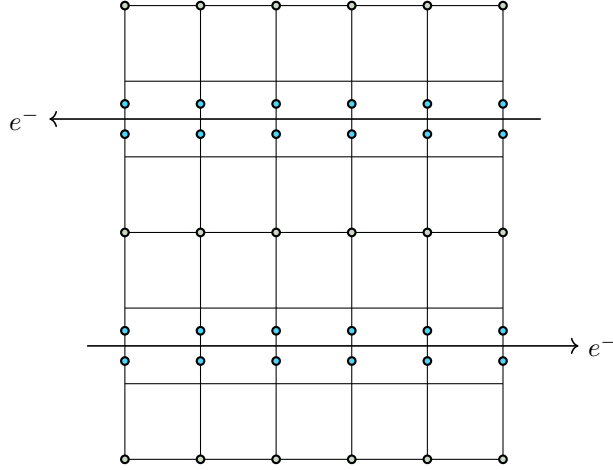


Figure 9: A lattice of ions, where two electrons propagate with opposite directions. Inspired by [19].

Here the moved ions in blue are shifting back to their equilibrium position long after the passage of the second electron. However, it is important to remember, that when the second electron passes, it experiences almost the same distortion everywhere. An interesting fact is that these interactions are the source of the superconductivity, but also the main origin of resistivity in clean materials.

3.6 On our way to the BCS-theory

After this introduction on the phonon coupling between the electrons in the momentum space, or Cooper-pairing, we aim to describe the energy of the superconductor in a mean-field approach. The goal of it is to reduce the description involving neighbours, to an on-site representation in the mean field of the other sites. Therefore, we are going to describe a one-body problem which is easier to compute. As known, mean-fields approaches require self-consistent equations to be comprehensive.

The first step is to introduce the following expectation values:

$$b_{\mathbf{k}} = \langle c_{-\mathbf{k}\downarrow} c_{\mathbf{k}\uparrow} \rangle \quad (32)$$

$$b_{\mathbf{k}}^{\dagger} = \langle c_{\mathbf{k}\uparrow}^{\dagger} c_{-\mathbf{k}\downarrow}^{\dagger} \rangle \quad (33)$$

which lead to a new expression for the c operators:

$$c_{-\mathbf{k}\downarrow} c_{\mathbf{k}\uparrow} = b_{\mathbf{k}} + \underbrace{c_{-\mathbf{k}\downarrow} c_{\mathbf{k}\uparrow} - b_{\mathbf{k}}}_{\delta_{b_{\mathbf{k}}}}, \quad (34)$$

where we can see the $\delta_{b_{\mathbf{k}}}$ as a deviation, or fluctuation term. If we introduce it back into the BCS-reduced Hamiltonian of Eq. 31, we can write

$$H = \sum_{\mathbf{k}\sigma} \epsilon_{\mathbf{k}} c_{\mathbf{k}\sigma}^{\dagger} c_{\mathbf{k}\sigma} + \sum_{\mathbf{k}, \mathbf{k}'} V_{\mathbf{k}\mathbf{k}'} (b_{\mathbf{k}}^{\dagger} + \delta_{b_{\mathbf{k}}}) (b_{\mathbf{k}} + \delta_{b_{\mathbf{k}}}).$$

We can compute the product of the two terms in parentheses and forget the terms in $\mathcal{O}(\delta_{b_{\mathbf{k}}}^2)$, because the fluctuation are small. We then obtain the following expression

$$H = \sum_{\mathbf{k}\sigma} \epsilon_{\mathbf{k}} c_{\mathbf{k}\sigma}^{\dagger} c_{\mathbf{k}\sigma} + \sum_{\mathbf{k}, \mathbf{k}'} V_{\mathbf{k}\mathbf{k}'} \left(b_{\mathbf{k}}^{\dagger} c_{-\mathbf{k}'\downarrow} c_{\mathbf{k}'\uparrow} + b_{\mathbf{k}'}^{\dagger} c_{\mathbf{k}\uparrow}^{\dagger} c_{-\mathbf{k}\downarrow}^{\dagger} - b_{\mathbf{k}}^{\dagger} b_{\mathbf{k}'} \right).$$

The next step is to define the superconducting gap parameter Δ , which is a key thermodynamic variable to the description of the Cooper-pairs:

$$\Delta_{\mathbf{k}} := - \sum_{\mathbf{k}'} V_{\mathbf{k}\mathbf{k}'} b_{\mathbf{k}}^\dagger, \quad (35)$$

$$\Delta_{\mathbf{k}}^\dagger := - \sum_{\mathbf{k}'} V_{\mathbf{k}\mathbf{k}'} b_{\mathbf{k}'}^\dagger. \quad (36)$$

This brings our Hamiltonian in another form:

$$H = \sum_{\mathbf{k}\sigma} \epsilon_{\mathbf{k}} c_{\mathbf{k}\sigma}^\dagger c_{\mathbf{k}\sigma} - \sum_{\mathbf{k}} \left(\Delta_{\mathbf{k}}^\dagger c_{-\mathbf{k}'\downarrow} c_{\mathbf{k}'\uparrow} + \Delta_{\mathbf{k}} c_{\mathbf{k}\uparrow}^\dagger c_{-\mathbf{k}\downarrow}^\dagger - b_{\mathbf{k}}^\dagger \Delta_{\mathbf{k}}^\dagger \right). \quad (37)$$

We took the liberty to split the sum, rename the \mathbf{k}' to \mathbf{k} and recombine the sum. We notice that this form involves a lot of creation and annihilation terms, and this is not rather uncommon for an effective non-interacting electron gas. Furthermore, we remember that we aim a one particle description in the mean field of its neighbours. This complexity will lead to some difficulties to express the quasi-particle spectrum. A good solution is to rotate the basis of the c operators, to land in a basis that diagonalizes the Hamiltonian and therefore minimizes the number of operators.

The transformation involves two new fermionic operators η and γ that therefore respect Eq. 2 to 4 and reads in a matrix form:

$$\begin{pmatrix} c_{\mathbf{k}\uparrow} \\ c_{-\mathbf{k}\downarrow}^\dagger \end{pmatrix} = \begin{pmatrix} \cos(\theta) & -\sin(\theta) \\ \sin(\theta) & \cos(\theta) \end{pmatrix} \begin{pmatrix} \eta_{\mathbf{k}} \\ \gamma_{\mathbf{k}} \end{pmatrix}, \quad (38)$$

along with the conjugate transpose of each component of the l.h.s vector, as well in a matrix-vector form:

$$\begin{pmatrix} c_{\mathbf{k}\uparrow}^\dagger \\ c_{-\mathbf{k}\downarrow} \end{pmatrix} = \begin{pmatrix} \cos(\theta) & -\sin(\theta) \\ \sin(\theta) & \cos(\theta) \end{pmatrix} \begin{pmatrix} \eta_{\mathbf{k}}^\dagger \\ \gamma_{\mathbf{k}}^\dagger \end{pmatrix}. \quad (39)$$

We can reintroduce these into the Hamiltonian of Eq. 37. Some multiplications involve $\cos(\theta)^2 - \sin(\theta)^2 = \cos(2\theta)$ and $\cos(\theta)^2 + \sin(\theta)^2 = 1$. Further due to the anticommutations we have $\eta\gamma^\dagger = -\gamma^\dagger\eta$ and so on for $\gamma\eta^\dagger = -\eta^\dagger\gamma$. We obtain the following expression

$$\begin{aligned} H = & \sum_{\mathbf{k}} \epsilon_{\mathbf{k}} + \Delta_{\mathbf{k}} b_{\mathbf{k}}^\dagger \\ & + \sum_{\mathbf{k}} \left[\epsilon_{\mathbf{k}} \cos(2\theta) - \cos(\theta) \sin(\theta) \left(\Delta_{\mathbf{k}}^\dagger + \Delta_{\mathbf{k}} \right) \right] \eta_{\mathbf{k}}^\dagger \eta_{\mathbf{k}} \\ & - \sum_{\mathbf{k}} \left[\epsilon_{\mathbf{k}} \cos(2\theta) - \sin(\theta) \cos(\theta) \left(\Delta_{\mathbf{k}}^\dagger + \Delta_{\mathbf{k}} \right) \right] \gamma_{\mathbf{k}}^\dagger \eta_{\mathbf{k}} \\ & - \sum_{\mathbf{k}} \left[\Delta_{\mathbf{k}} \cos(\theta)^2 - \Delta_{\mathbf{k}}^\dagger \sin(\theta)^2 + 2\epsilon_{\mathbf{k}} \cos(\theta) \sin(\theta) \right] \eta_{\mathbf{k}}^\dagger \gamma_{\mathbf{k}} \\ & - \sum_{\mathbf{k}} \left[\Delta_{\mathbf{k}} \cos(\theta)^2 - \Delta_{\mathbf{k}}^\dagger \sin(\theta)^2 + 2\epsilon_{\mathbf{k}} \cos(\theta) \sin(\theta) \right] \gamma_{\mathbf{k}}^\dagger \eta_{\mathbf{k}}. \end{aligned} \quad (40)$$

The goal is to diagonalize the Hamiltonian in the (γ, η) basis. Therefore, we have to choose θ , such that the terms with $\gamma^\dagger\eta$ and $\eta^\dagger\gamma$ vanish. A difficulty that we may encounter along with this idea is that Δ is an order parameter and own a complex phase fluctuation. In other words one can write $\Delta = |\Delta|e^{i\tau}$ where τ has some fluctuations, but we are going to ignore them.

We can set

$$\Delta_{\mathbf{k}} = \Delta_{\mathbf{k}}^\dagger \quad \text{and} \quad \tan(2\theta) = -\frac{\Delta_{\mathbf{k}}}{\epsilon_{\mathbf{k}}}$$

and introduce two new variables called the coherence factors:

$$v_{\mathbf{k}}^2 := \sin(\theta)^2 = \frac{1}{2} \left(1 - \frac{\epsilon_{\mathbf{k}}}{E_{\mathbf{k}}} \right), \quad (41)$$

$$u_{\mathbf{k}}^2 := \cos(\theta)^2 = \frac{1}{2} \left(1 + \frac{\epsilon_{\mathbf{k}}}{E_{\mathbf{k}}} \right), \quad (42)$$

along with a new energy $E_{\mathbf{k}} = \sqrt{\epsilon_{\mathbf{k}}^2 + |\Delta_{\mathbf{k}}|^2}$. These factors play an important role in NMR as well as in the ultrasound propagation in superconductors. Cooper and Schrieffer made some correct predictions in an advanced many-body system. This is labelled as one of the greatest achievements in condensed matter physics in the 20th century [19]. They are going as well to play a central role in the simulations later.

We obtain a Hamiltonian that looks very similar to a free fermion quasiparticle gas:

$$H = \underbrace{\sum_{\mathbf{k}} (\epsilon_{\mathbf{k}} + \Delta_{\mathbf{k}} b_{\mathbf{k}}^\dagger)}_{=: H_0 \text{ constant mean-field term}} + \underbrace{\sum_{\mathbf{k}} E_{\mathbf{k}} (\eta_{\mathbf{k}}^\dagger \eta_{\mathbf{k}} - \gamma_{\mathbf{k}}^\dagger \gamma_{\mathbf{k}})}_{\text{Spinless fermion system with two types of fermions of energies } E_{\mathbf{k}} \text{ and } -E_{\mathbf{k}}}. \quad (43)$$

This expression forgets the interactions to describe two types of particles in a mean field. As [19] described it in chapter 3, p.83-84, one can note that we do not have any spins involved. This is due to the fact that we describe the quasiparticles as a linear combination of electrons and holes with opposite spins (see Eq. 38). The two relevant degrees of freedom are distinct linear combinations of particle-hole pairs with spin-singlet components. However, the resulting quasiparticles are not spin-singlets, as they carry a non-zero spin. The degrees of freedom are therefore preserved.

The energy $E_{\mathbf{k}}$ present a gap in the energy of the quasiparticles when looking at the Fermi surface $\epsilon_{\mathbf{k}} = 0$ (we remember that μ is present in $\epsilon_{\mathbf{k}}$). This is due to the fact that the expectation values we introduced in 32 and 33 do not vanish. The gap is a result of the Cooper-pairing. These expectation values are the order parameters of the Meissner state and shouldn't be confused with the superconducting gap Δ . They can however be zero both at the same time.

This free particle context is a good opportunity to introduce the grand canonical ensemble of the Hamiltonian. Even if we could give the direct result, deriving this ensemble involves a lot of important steps, so for the seek of completeness, we are going to go step to step through it.

We define the particle number operator $N = \sum_{\mathbf{k}} (n_{\eta\mathbf{k}} + n_{\gamma\mathbf{k}})$, that counts the quasiparticles of both class. Further the possible states \mathbf{k} are in a “continuous” set $\mathfrak{K} = \{\mathbf{k}_1, \mathbf{k}_2, \dots\}$. The set $\{n_{\mathbf{k}}\}$ gathers the different occupation numbers of all the states \mathbf{k} under one configuration. The configurations are stored in an ensemble \mathcal{C} . Further we consider fermions, so the occupation numbers of the particle type η or γ in state \mathbf{k} are labelled $n_{\eta\mathbf{k}}$ and $n_{\gamma\mathbf{k}}$ and equals either 0 or 1.

$$\begin{aligned} Z_G &= \text{Tr} \left(e^{-\beta(H)} \right) \\ &= \sum_{\{n_{\mathbf{k}}\} \in \mathcal{C}} e^{-\beta H_0} \langle \{n_{\mathbf{k}}\} | \exp \left(\sum_{\mathbf{k}'} -\beta E_{\mathbf{k}'} \eta_{\mathbf{k}'}^\dagger \eta_{\mathbf{k}'} + \beta E_{\mathbf{k}'} \gamma_{\mathbf{k}'}^\dagger \gamma_{\mathbf{k}'} \right) | \{n_{\mathbf{k}}\} \rangle \\ &= \sum_{\{n_{\eta\mathbf{k}}\}} \sum_{\{n_{\gamma\mathbf{k}}\}} e^{-\beta H_0} \exp \left(\sum_{\mathbf{k}} -\beta [E_{\mathbf{k}} \eta_{\mathbf{k}}^\dagger \eta_{\mathbf{k}}] + \beta [E_{\mathbf{k}} \gamma_{\mathbf{k}}^\dagger \gamma_{\mathbf{k}}] \right) \\ &= e^{-\beta H_0} \sum_{\substack{n_{\eta\mathbf{k}_1}, \\ n_{\eta\mathbf{k}_2}, \dots}} \sum_{\substack{n_{\gamma\mathbf{k}_1}, \\ n_{\gamma\mathbf{k}_2}, \dots}} \exp \left(\sum_{\mathbf{k}} -\beta [E_{\mathbf{k}} n_{\eta\mathbf{k}}] + \beta [E_{\mathbf{k}} n_{\gamma\mathbf{k}}] \right) \\ &= e^{-\beta H_0} \sum_{\substack{n_{\eta\mathbf{k}_1}, \\ n_{\eta\mathbf{k}_2}, \dots}} \prod_{\mathbf{k}} \exp(-\beta [E_{\mathbf{k}} n_{\eta\mathbf{k}}]) \sum_{\substack{n_{\gamma\mathbf{k}_1}, \\ n_{\gamma\mathbf{k}_2}, \dots}} \prod_{\mathbf{k}} \exp(\beta [E_{\mathbf{k}} n_{\gamma\mathbf{k}}]) \\ &= e^{-\beta H_0} \sum_{n_{\eta\mathbf{k}_1}} \exp(-\beta [E_{\mathbf{k}_1} n_{\eta\mathbf{k}_1}]) \sum_{n_{\eta\mathbf{k}_2}} \exp(-\beta [E_{\mathbf{k}_2} n_{\eta\mathbf{k}_2}]) \dots \\ &\quad \sum_{n_{\gamma\mathbf{k}_1}} \exp(\beta [E_{\mathbf{k}_1} n_{\gamma\mathbf{k}_1}]) \sum_{n_{\gamma\mathbf{k}_2}} \exp(\beta [E_{\mathbf{k}_2} n_{\gamma\mathbf{k}_2}]) \dots \\ &= e^{-\beta H_0} \prod_{\mathbf{k}} (1 + e^{-\beta E_{\mathbf{k}}}) (1 + e^{\beta E_{\mathbf{k}}}) \end{aligned}$$

This partition function becomes useful if we want to derive the free energy of the system. It will help us to solve the self-consistent equation for the gap.

According to [22] p.99 the free energy can be derived from the partition function as:

$$F = -\frac{1}{\beta} \ln(Z_G) = H_0 - \frac{1}{\beta} \sum_{\mathbf{k}} + \ln(1 + e^{-\beta E_{\mathbf{k}}}) \ln(1 + e^{\beta E_{\mathbf{k}}}).$$

Following [19] we obtain in the limit of low temperatures ($\beta \rightarrow \infty$):

$$\begin{aligned} F &= H_0 + \sum_{\mathbf{k}} E_{\mathbf{k}} \theta(-E_{\mathbf{k}}) + E_{\mathbf{k}} \theta(E_{\mathbf{k}}) \\ &= H_0 + \sum_{\mathbf{k}} E_{\mathbf{k}} - E_{\mathbf{k}} \theta(E_{\mathbf{k}}) + E_{\mathbf{k}} \theta(E_{\mathbf{k}}) \\ &= \sum_{\mathbf{k}} \epsilon_{\mathbf{k}} + \Delta_{\mathbf{k}} b_{\mathbf{k}}^{\dagger} E_{\mathbf{k}}, \end{aligned}$$

where we used the properties from the Heaviside step-function described in 16. The minimization of the free energy F should self-consistently determine the gap $\Delta_{\mathbf{k}}$. This is a statement that depends neither on the momentum space structure, nor on the attraction of the potential [19]. $E_{\mathbf{k}}$ has an implicit $\Delta_{\mathbf{k}}$ -dependence. We compute the derivation $\frac{\partial F}{\partial \Delta_{\mathbf{k}}}$ and search the argument of the zero-position. Deriving one \mathbf{k} from the sum is enough. We demand the following to be satisfied:

$$\frac{\partial F}{\partial \Delta_{\mathbf{k}}} = 0, \quad \frac{\partial F}{\partial \Delta_{\mathbf{k}}^{\dagger}} = 0. \quad (44)$$

This leads to

$$b_{\mathbf{k}}^{\dagger} = \Delta_{\mathbf{k}} \underbrace{\frac{\tanh(\beta E_{\mathbf{k}}/2)}{E_{\mathbf{k}}}}_{\chi(\mathbf{k})},$$

defining $\chi(\mathbf{k})$ as the pair-susceptibility, and gives how capable the system is to create Cooper-pairs [19]. If we allow us to relabel $\mathbf{k} \rightarrow \mathbf{k}'$, then multiply on both sides with $-\sum_{\mathbf{k}} V_{\mathbf{k}\mathbf{k}'}$ and introduce Eq. 36, we obtain the self-consistent equation for the gap. This is usually designated as the BCS gap equation.

$$\Delta_{\mathbf{k}} = - \sum_{\mathbf{k}'} V_{\mathbf{k}\mathbf{k}'} \Delta_{\mathbf{k}'} \frac{\tanh(\beta E_{\mathbf{k}'}/2)}{E_{\mathbf{k}'}}. \quad (45)$$

Fossheim and Sudbø [19] emphasize that this equation is not limited to phonon mediated interaction, as long we do not specify the potential. Further Cooper-pairs can condensate, because in the pair, the spin of the electrons adds up to zero. The pair is not ruled any more by the Pauli principle and can take part into the superconducting condensate. Even if the formation temperature of Cooper-pairs is higher than the critical temperature T_C , these mean field approach makes these temperatures agree.

As we introduced earlier the gap has a complex phase fluctuation. This phase is hard to vary in good metals because the number of carrier electrons is high. On the other side in poor metals, the fluctuations that break the pair are more easily reached, i.e. at a lower temperature than in good metal. Superconductivity is therefore more stable in metals of good value.

In this section we saw how to reduce the many-body Hamiltonian to a single-body problem in the means field of its neighbours. The system that follows from this is a non-interacting gas of electrons and holes. This involves the introduction of the superconducting gap parameter that we can thank to the statistical mechanics formalism express in a self-consistent way.

3.7 Generalized gap equation, *s*-wave and *d*-wave superconductivity

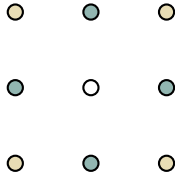
As we introduced in an earlier section, the formalism follows from the attractive phonon exchange but can be generalized. The superconductivity is the result of the pairing of the electrons into Cooper-pairs. These pairs shift into a condensate and take part to a coherent matter-wave. Making a link to the coherent light wave, superconductivity can be seen as the *analogos* of lasers like Fossheim and Sudbø highlight it in [19].

To achieve such generalization we let the formalism be open to other kind of interactions and do not restrict it to the thin shell around the Fermi-surface. The potential matrix-element can therefore take a more complex form than introduced in Eq. 30.

We recall that the electrons move into a lattice. We can assume that this crystal owns some symmetries that are reflected in its crystallographic (complete) basis $\{g_\eta(\mathbf{k})\}$. Similar to the Bloch state, we could imagine that the symmetries emphasize some physical quantities. Assuming this, we propose a form for the potential that takes advantage of the basis.

$$V_{\mathbf{k}\mathbf{k}'} = \sum_{\eta} \lambda_{\eta} g_{\eta}(\mathbf{k}) g_{\eta}(\mathbf{k}')$$

η is also often labelled as the channel [19]. Assuming we have a square lattice,



with interaction strength $U/2$ on site, for nearest neighbours $2V$ and $4W$ for second-nearest neighbours. We can for each site describe their position with a shift vector to the central site. Using

$$f(k, k') = \cos(k) \cos(k') + \sin(k) \sin(k'),$$

Fourier transforming these displacements leads to the following:

$$V_{\mathbf{k}\mathbf{k}'} = U + 2V (f(k_x, k'_x) + f(k_y, k'_y)) \\ + 4W (f(k_x, k'_x) \cdot f(k_y, k'_y))$$

We can then introduce the basis-functions $\{g_\eta(\mathbf{k})\}$ we talked about a few paragraphs ago.

$$\begin{aligned} g_1(\mathbf{k}) &= \frac{1}{2\pi} \\ g_2(\mathbf{k}) &= \frac{1}{2\pi} (\cos(k_x) + \cos(k_y)) && (s\text{-wave}) \\ g_3(\mathbf{k}) &= \frac{1}{2\pi} \cos(k_x) \cos(k_y) \\ g_4(\mathbf{k}) &= \frac{1}{2\pi} (\cos(k_x) - \cos(k_y)) && (d\text{-wave}) \\ g_5(\mathbf{k}) &= \frac{1}{2\pi} \sin(k_x) \sin(k_y) \end{aligned}$$

from which involves the following lambdas $\lambda_1 = 2U\pi^2$, $\lambda_2 = \lambda_4 = 4V\pi^2$, $\lambda_3 = \lambda_5 = 4W\pi^2$, and for greater η we set $\lambda_{\eta \geq 6} = 0$.

For $\eta \in \{1, 2\}$, the corresponding g is the identity under all symmetries of C_{v4} and for $\eta \in \{3, 4, 5\}$ we observe a change of sign under $\pi/2$ rotations. The same behaviour is found in the spherical harmonics for the respective quantum numbers $l = 0$ and $l = 2$. From this we can deduce the use of the terms *s-wave* and *d-wave*. *s-wave* is isotropic in the momentum space whereas the *d-wave* has a different contour for its part with positive phase

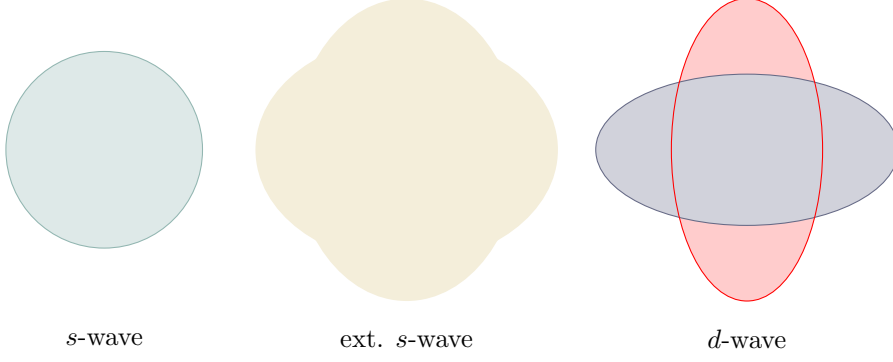


Figure 10: Different gap contours in the momentum space. The s -wave is isotropic and extended s -wave has a more complex surface (see appendix A.3). The d -wave has a splitting for its part with positive and negative phase. We observe a degeneracy where the two parts overlap.

Further we can reintroduce the BCS gap equation 45 and obtain a lattice-dependent form for the gap:

$$\begin{aligned}
 \Delta_{\mathbf{k}} &= - \sum_{\mathbf{k}'} V_{\mathbf{k}\mathbf{k}'} \Delta_{\mathbf{k}'} \chi(E_{\mathbf{k}}) \\
 &= - \sum_{\eta \in \llbracket 5 \rrbracket} \lambda_{\eta} g_{\eta}(\mathbf{k}) \underbrace{\sum_{\mathbf{k}'} g_{\eta}(\mathbf{k}') \Delta_{\mathbf{k}'} \chi(E_{\mathbf{k}'})}_{=:\Delta_{\eta}/\lambda_{\eta}} \\
 &= \sum_{\eta \in \llbracket 5 \rrbracket} \Delta_{\eta} g_{\eta}(\mathbf{k}).
 \end{aligned} \tag{46}$$

This is a nice form to have as Fossheim and Sudbø [19] point out p.92. The gap is a linear combination of the physical quantities $g_{\eta}(\mathbf{k})$. The newly introduced Δ_{η} are independent of the wave vector \mathbf{k} but are function of the temperature. We can express these in the basis of another η' ($\lambda_{\eta \geq 6} = 0$):

$$\begin{aligned}
 \Delta_{\eta} &= \sum_{\eta' \in \llbracket 5 \rrbracket} \Delta_{\eta'} \mathcal{M}_{\eta, \eta'} \\
 \mathcal{M}_{\eta, \eta'} &= - \lambda_{\eta} \sum_{\mathbf{k}} g_{\eta}(\mathbf{k}) g_{\eta'}(\mathbf{k}) \chi(E_{\mathbf{k}}).
 \end{aligned}$$

These are numerical cumbersome to compute, but taking $U > 0$, $V < 0$ and $W = 0$ in the square lattice we obtain no attraction in the λ_1 -channel but attraction in the s - and d -wave channels. This tells us a lot like [19] analysed it. First the gap is highly associated to the Fourier transform of the wave function of the Cooper-pairs. Further the gap accommodate itself “to be zero in the channel where the wave function is non-zero for zero separation between the electrons” [19] p.92. The s - and d -wave channels are preferred in order to avoid the on-site Coulomb repulsion (i.e. the Coulomb force between the two members of the pair). This can be put in comparison with the special case of the phonon pairing. In the latest the electrons used retardation processes to cancel out the repulsion. They avoided themselves in time. Here the avoidance takes place in space.

The manifestation of the retardation effects are actually a direct consequence of restricting ourselves to a thin shell around the Fermi-surface. Logically if we have a Cooper pair formation that does not follow this restriction, the whole Brillouin zone should be taken into account to compute the gap.

Further we can express the Fourier transform of the gap as $\Delta(\mathbf{r}) = \sum_{\mathbf{k}} \Delta_{\mathbf{k}} e^{i\mathbf{k}\mathbf{r}}$ which leads $\Delta(0) = \sum_{\mathbf{k}} \Delta_{\mathbf{k}}$. However, a repulsive interaction is obtained for $\Delta(\mathbf{0}) \neq 0$, so we need to find $\Delta_{\mathbf{k}}$ s whose sum satisfies this. This can be done using the s -wave and d -wave channels, i.e. $\Delta_{\mathbf{k}} = \Delta_0(T) g_2(\mathbf{k})$ and $\Delta_{\mathbf{k}} = \Delta_0(T) g_4(\mathbf{k})$. We already motivated superconductivity and its difficulty to maintain due to the phase fluctuations above the (freezing) critical temperature T_C . However, superconductivity involving d -wave channels is believed [19] p.92 to be found in materials with high T_C . $\Delta_{\mathbf{k}} = \Delta_0(T) g_4(\mathbf{k})$ is therefore a good case of study.

Density of Meissner states

We imagine some fluctuation described by $g(\mathbf{k})$ that only depend on $E_{\mathbf{k}} = \sqrt{\epsilon_{\mathbf{k}}^2 + \Delta_{\mathbf{k}}^2}$. Further we assume Δ being \mathbf{k} - independent for now. We can introduce the normal density of states.

$$D_n(\epsilon) = \frac{1}{N} \sum_{\mathbf{k}} \delta(\epsilon - \epsilon_{\mathbf{k}})$$

with N the number of Fourier modes. This is the same as the number of lattice sites for us [19] p.93.

$$\sum_{\mathbf{k}} g(\mathbf{k}) = \int D_n(\epsilon) g(\sqrt{\epsilon^2 - \Delta^2}) d\epsilon$$

as well as a variable transformation $E = \sqrt{\epsilon^2 + \Delta^2}$ which leads to

$$dE = \frac{\epsilon}{\sqrt{\epsilon^2 + \Delta^2}} d\epsilon \iff d\epsilon = \frac{E}{\epsilon} dE,$$

$$\sum_{\mathbf{k}} g(\mathbf{k}) = \int D_n(\epsilon) g(E) \frac{E}{\epsilon} dE.$$

Further we have $\frac{\partial \epsilon}{\partial E} = \frac{E}{\sqrt{E^2 - \Delta^2}} = \frac{E}{\epsilon}$ so that

$$\sum_{\mathbf{k}} g(\mathbf{k}) = \int g(E) \underbrace{D_n(\epsilon) \frac{\partial \epsilon}{\partial E}}_{D_s(E)} dE.$$

Then we use a common method in solid state physics to simplify the expression. We assume that $D_n(\epsilon)$ is slowly varying so that $D_n(\epsilon) \approx D_n(0)$ where ϵ is measured relative to the Fermi surface. Hopefully we do not have any sharpness around the Fermi-surface [19] p.93. We can therefore exclude the Van Hove singularities close to the Fermi-surface.

$$\begin{aligned} \frac{D_s(E)}{D_n(0)} \frac{E}{\sqrt{E^2 - \Delta^2}} &= \frac{E}{\sqrt{E^2 - \Delta^2}} \frac{D_n(\epsilon)}{D_n(0)} \\ &= \frac{E}{\sqrt{E^2 - \Delta^2}} \Theta(E - |\Delta|) \end{aligned}$$

We use the Heaviside step-function because the last term is either one or zero. This is our final expression for the density of the Meissner state when the gap is \mathbf{k} -independent. For the \mathbf{k} dependence of the gap we can use the spectral weight introduced in Eq. 18. In analogy to the propagator or Green function introduced through the Dyson equation at Eq. 22 for the electrons, we can define one for the superconducting condensate that involves time-dependent fermionic operators.

$$G(\mathbf{k}, t; \sigma) = -i \langle 0 | c_{\mathbf{k}\sigma}(t) c_{\mathbf{k}\sigma}^\dagger(0) | 0 \rangle$$

involving the BCS superconducting ground state $|0\rangle$ which is an eigenstate of the Hamiltonian of Eq. 43. As before we can consider the Fourier transform of the propagator $G(\mathbf{k}, \omega; \sigma)$

$$G(\mathbf{k}, \omega; \sigma) = \frac{1}{2\pi} \int e^{i\omega t} G(\mathbf{k}, \omega; \sigma) dt.$$

We recall that Cooper pairs are made of two electrons with opposite spin. We can first take a look at the density of state of the pair-member with $\sigma = \uparrow$. However, we here are only considering spin singlet pairing, so proving that the spectral weight A is spin independent should show that computing it for $\sigma = \uparrow$ is enough as Fossheim and Sudbø argued in [19] p.94.

So without loss of generality we set $\sigma = \uparrow$ and reintroduce the rotation of the basis of the c operators we performed in Eqs.38 and 39.

$$\begin{aligned} G(\mathbf{k}, t; \uparrow) &= -i \langle 0 | \left(\cos(\theta) \eta_{\mathbf{k}}^\dagger(t) - \sin(\theta) \gamma_{\mathbf{k}}^\dagger(t) \right) \\ &\quad \cdot \left(\cos(\theta) \eta_{\mathbf{k}}(0) - \sin(\theta) \gamma_{\mathbf{k}}(0) \right) | 0 \rangle \end{aligned}$$

The goal of these rotated operators was to diagonalize the hamiltonian. It follows

$$\langle 0 | \eta_{\mathbf{k}}^\dagger \gamma_{\mathbf{k}}^\dagger | 0 \rangle = 0 = \langle 0 | \eta_{\mathbf{k}} \gamma_{\mathbf{k}} | 0 \rangle$$

and therefore

$$\begin{aligned} G(\mathbf{k}, t; \uparrow) &= -i \cos(\theta)^2 \langle 0 | \eta_{\mathbf{k}}^\dagger(t) \eta_{\mathbf{k}}(0) | 0 \rangle \\ &\quad - i \sin(\theta)^2 \langle 0 | \eta_{\mathbf{k}}^\dagger(t) \eta_{\mathbf{k}}(0) | 0 \rangle. \end{aligned} \quad (47)$$

We can nicely split the propagator in the sum of free η - and γ -particles in the superconducting state. Employing to coherence factors of Eqs.42 and 41 in the Fourier transform of we obtain

$$G(\mathbf{k}, \omega; \uparrow) = \frac{u_{\mathbf{k}}^2}{\omega - E_{\mathbf{k}} + i\delta_{\mathbf{k}}} + \frac{v_{\mathbf{k}}^2}{\omega + E_{\mathbf{k}} - i\delta_{\mathbf{k}}}.$$

From this we achieve an expression for the spectral weight:

$$A(\mathbf{k}, \omega; \uparrow) = u_{\mathbf{k}}^2 \delta(\omega - E_{\mathbf{k}}) + v_{\mathbf{k}}^2 \delta(\omega + E_{\mathbf{k}}).$$

This value is spin independent and using the arguments we've just given in such a case, we find

$$\begin{aligned} D_s(\omega) &= \frac{1}{N} \sum_{\mathbf{k}} A(\mathbf{k}, \omega) \\ &= \frac{1}{N} \sum_{\mathbf{k}} (u_{\mathbf{k}}^2 \delta(\omega - E_{\mathbf{k}}) + v_{\mathbf{k}}^2 \delta(\omega + E_{\mathbf{k}})). \end{aligned}$$

The density of state of the superconductive condensate D_s is also spin independent since we are considering spin-singlet pairings. This formula should be used when computing simulations of the superconducting state.

3.8 Transition temperature and energy gap

The goal of this discussion will be to derive a universal ratio between Δ and the crystal temperature. In the last section we already introduced some expressions for $\Delta_{\mathbf{k}}(T)$ and $V_{\mathbf{k}\mathbf{k}'}$. Let us consider the simplest case where the potential stays constant $V_{\mathbf{k}\mathbf{k}'} = V$.

The phonon modulated interaction has a cover $\omega_0 = \omega_D$, that is the Debye frequency. Inserting this back to the BCS gap equation 45, we see that the gap loses its \mathbf{k} -dependence and results as the identity when applying the symmetries ruling the crystal:

$$1 = V \sum_{\mathbf{k}'} \frac{\tanh(\beta E_{\mathbf{k}'})}{2E_{\mathbf{k}'}}.$$

This equation can be easily solved for $T = T_C$ or $T = 0$.

Considering T approaching T_C from bellow, we can assume that the gap vanishes. We replace the \mathbf{k} -sum by an integral over the normal density of state $D_n(\epsilon)$. Due to the shell the sum occurs in a tiny volume around the Fermi-Surface, so that $D_n(\epsilon)$ is evaluated close to the surface. We assume that in this neighbourhood D_n varies slowly, such that avoid some van Hove singularities we simply approximate $D_n(\epsilon) \rightarrow D_n(0)$. We choose zero because ϵ is counted relative to the surface in our early thoughts. When introducing $\lambda = V D_n(0)$ we obtain:

$$\begin{aligned} 1 &= \lambda \int_0^{\omega_D} \frac{\tanh(\beta\epsilon/2)}{\epsilon} d\epsilon \\ &= \lambda \ln \left(\frac{2e^\gamma \beta \omega_D}{\pi} \right). \end{aligned}$$

Using $\gamma := \lim_{m \rightarrow \infty} \left(\sum_{l \in [m]} 1/l - \ln(m) \right)$ the Euler-Mascheroni constant. More details are provided in [19] p.88-89. We obtain

$$k_B T_C \approx 1.13 \cdot \omega_D e^{-1/\lambda}$$

For $T \rightarrow 0$ the gap equation takes a simpler form to solve:

$$1 = V \sum_{\mathbf{k}'} \frac{1}{2E_{\mathbf{k}'}} = \lambda \int_0^{\omega_D} \frac{1}{\sqrt{\epsilon^2 + \Delta^2}} d\epsilon$$

and leads to

$$\Delta(T = 0) = 2\omega_D e^{-1/\lambda}$$

according to the same source. We see how these expressions are closely dependent on λ . Moreover, we can interpret the essential singularity at $\lambda \rightarrow 0$ as following: The attractive processes are singular perturbations of the non-interacting electron gas. m is very demanding to solve even for simple metals and is a function of multiple small details of the system. We aim here to acquire qualitative knowledge. Let us now bring the ratio

$$\frac{2\Delta(T = 0)}{k_B T_C} = \frac{2\pi}{e^\gamma} \approx 3.52$$

which is a universal ratio and does not depend any more on the properties of the material. Knowing the critical temperature one can know the gap at 0K.

In this long section we have derived how the Cooper pairs raise from the coupling of two electrons of opposite spin and momentum. Using a mean field approach and a rotation of the basis we were able to reduce the many-body Hamiltonian to a single-body problem. This allowed use to derive a self-consistent solution for the energy gap that the coupling of the electrons left behind. Then we have seen how the gap can be expressed in a basis of the crystallographic symmetries. Finally, we derived an expression for the density of the Meissner state.

Now that we have a better understanding of the superconductivity, we can move on to the next section where we will present a method to self consistently solve the gap. This will be done by diagonalizing the Hamiltonian and read the superconductivity from the eigenvalues and -vectors. To do so we need to discretize the system, by introducing the tight binding model.

4 Altermagnetism



4.1 Introduction and overview

The reader might already be familiar with ferromagnets and all the regular magnetic models. Taking into account the spin and wave vector of each particle in a site, one can derive some symmetries under transform operations. For example a ferromagnet is symmetric under time-reversal and spin-rotation. In the example of the antiferromagnetism, we have two sub-lattice with opposite spins. In such systems the spin compensate each other resulting in a null magnetization. The system is symmetric under spin-flip and translation and was theorized in 1948 by Louis Néel as the Néel antiferromagnets [23]. Allowing more complexity one could imagine multiple ions in a unit cell linked by symmetries such as rotation and screw operations. Half of the ions in the cell own an opposite spin from the other half. The spectra compensate each other resulting in a zero net magnetization. Moreover, these mediums keep the same electron spectra under such transformations, making them the same as Néel's antiferromagnets. These material are labelled as zero q antiferromagnets. This section summarizes the historical work of [24].

Altermagnets implement two or more sub-lattice which are not related between each other by translation or inversion. The symmetry that actually links these sublattices is a rotation, along with a spin-polarisation in the momentum space linked with a rotation as well [17]. In general, rotation does not conserve the electrons spectra. We actually observe a band splitting of the spectra with respect to the spins. There is an alternating sign in the spin-splitted momenta, as well as an alternating spin of the polarization in real space, which leads to the name altermagnetism [25]. This class of material was discovered in 2019 [26].

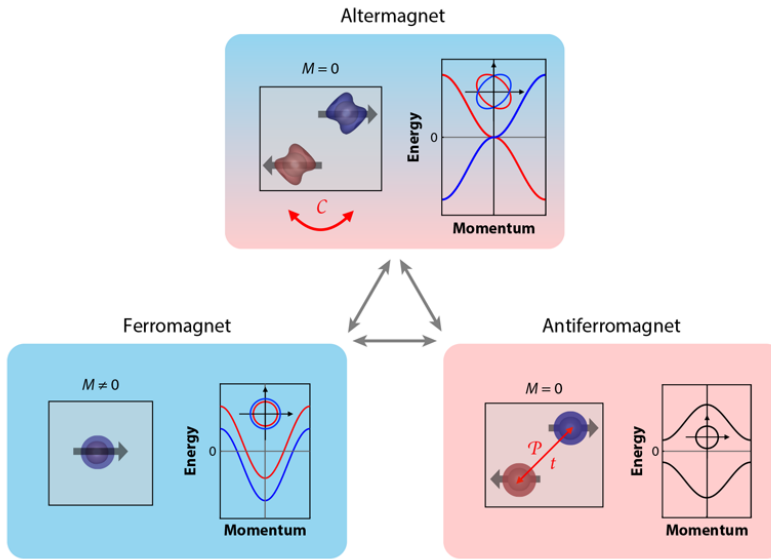


Figure 11: The altermagnet shares similar properties with the antiferromagnets like two sub-lattices of opposite spin, resulting in a zero net magnetization. Whereas the antiferromagnet's sublattices are linked by a translation t and a space inversion \mathcal{P} , in the altermagnet one can link each sublattice with a rotation, here labelled as \mathcal{C} . We observe as well an alternating sign in the energy spectra of both altermagnet's sublattices. Figure taken from [17][27].

These properties put the altermagnet in between the conventional dichotomy of ferromagnets and antiferromagnet. In fact the altermagnet compensates its magnetical moments taking advantage of the two sublattices, like the antiferromagnet does. On the other hand, it shares similar properties with the ferromagnets, such as anomalous Hall effect, spin current [28], magneto-electric effect [29], tunnelling magnetoresistance [30] among other [25].

A few materials seem to exhibit these properties. 1D material won't work because of lack of rotation possibilities. A diverse list of two and three-dimensional materials were listed by [17]

such as semimetals with a Cr_2O monolayer [31], a variety of insulators like perovskite oxide LaMnO_3 [32] CaCrO_3 [33], ferrite Fe_2O_3 [25], or organic insulators $\kappa\text{-Cl}$ [34]. We find as well the chalcogenide MnTe semiconductor [25].

On the sake of practical application, researchers have found (an exhaustive list is provided in [24]) that domain like tunnelling magnetoresistance (TMR) are limited under the properties of the material. For instance the actual use of ferromagnets limits the frequency to the gigahertz range [24]. This has to deal with the ferromagnetic resonance that connects the magnetization with electromagnetic waves. The altermagnets could be used in the terahertz range. Mentioning that TMR is a key component of the magnetic random access memory (MRAM) [35][36], the reader can easily estimate the performance improvement such upgrade could deliver in a computer.

After this introduction on altermagnets, we intend to find a way to implement these into our system. In a more formal way, we can distinguish two types of altermagnet. In the first type, the altermagnet's lattice site have different distance to the neighbours depending on the linking axis and the spin of the particle in the site. This is illustrated in Fig. 12 (a). On the other hand, we can consider a unit cell being unsymmetrical in its ion position. We consider a square lattice were each unit cell has a non-magnetic ion and two magnetic ions with opposite spin. Please consider the second schema (b).

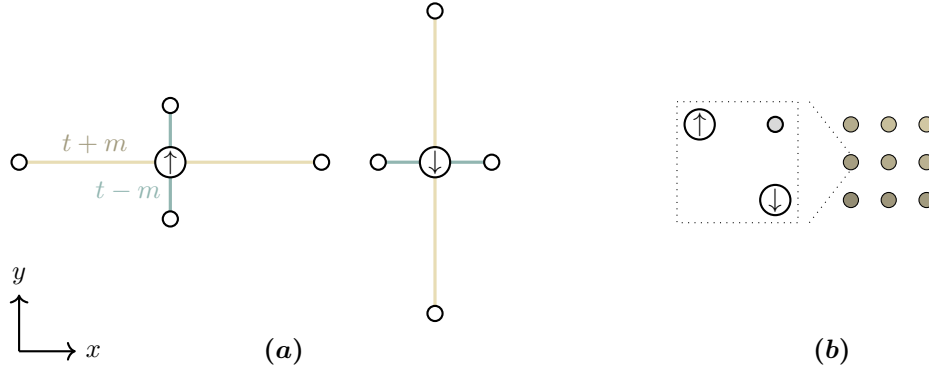


Figure 12: Altermagnet of type 1 and 2.

4.2 Symmetries

After giving an introduction on the geometric background of altermagnet we can now focus on the symmetries of the material. In this section we are going to focus on two simple transformation. The inversion P and the spin flip (time reversal) T which are broadly discussed in the literature [17][25].

$$\begin{aligned} P : \mathbf{r} &\mapsto -\mathbf{r} & \mathbb{R}^3 &\rightarrow \mathbb{R}^3, \\ T : t &\mapsto -t \hat{=} \sigma \mapsto -\sigma & \mathbb{R} &\rightarrow \mathbb{R}. \end{aligned}$$

We can first assume that the energy ϵ of the particle (or band structure) depends on the spin σ and the wave vector \mathbf{k} . Using $\mathbf{p} = d\mathbf{r}/dt$ and the de Broglie hypothesis $\mathbf{p} = \hbar\mathbf{k}$ [37] leads to:

$$\begin{aligned} P(\epsilon(\mathbf{k}, \sigma)) &= \epsilon(-\mathbf{k}, \sigma) \\ T(\epsilon(\mathbf{k}, \sigma)) &= \epsilon(-\mathbf{k}, -\sigma) \end{aligned}$$

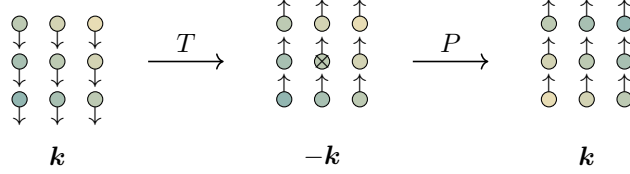
We observe the PT operation $P \circ T$. If the system is PT symmetric one should get $\epsilon(\mathbf{k}, \sigma) = P \circ T(\epsilon(\mathbf{k}, \sigma))$. Assuming it's the case we can write

$$\epsilon(\mathbf{k}, \sigma) = P \circ T(\epsilon(\mathbf{k}, \sigma)) = \epsilon(\mathbf{k}, \downarrow)$$

and therefore the PT -symmetric systems are spin-degenerated. We have the same energy for a given momentum at two opposite spins. Reciprocally this means that the existence of $\epsilon(\mathbf{k}, \sigma)$ is followed by an observation of $\epsilon(\mathbf{k}, -\sigma)$.

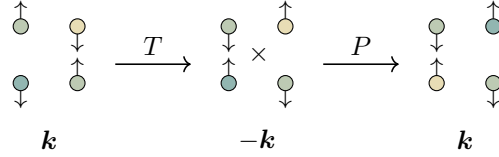
A few examples

To illustrate these symmetries we can consider a few examples. We can imagine having a small lattice section for the sake of readability. First we choose a ferromagnetic lattice, where we apply the space inversion in the middle where the black cross is. The arrows represent the spin and the overall sign of the wave vector \mathbf{k} is given under each state. Moreover, we use the shading to keep track of the real space location of the site. This representation is in the real space.

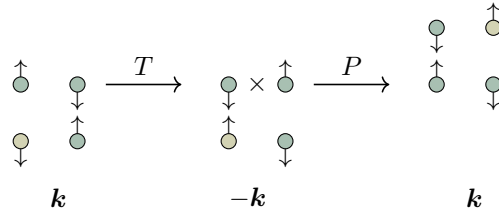


The relevant variables for the symmetry in the spectrum are the spin projection and the momentum. We see however that the spin are flipped before and after the PT -operation. Letting the spin points downwards again will require to use an additional operation. Therefore, the ferromagnet is not PT -symmetric, and we observe no spin degeneracy as the equation shows it.

The antiferromagnet has a spin switch in every direction. Here, when choosing a point to apply our operations to, we see that neither a lattice point nor a point in the middle on two sites lead to a PT symmetry. As we see the spins points in different directions.



However, if we apply the inversion in the in-between, we observe something different.



At this point, we apply the P transformation around makes the antiferromagnets having a PT symmetry. We see that the lattice site have moved but only the spin and the wave vector takes part to the band ϵ . We therefore have a degeneracy in the energy spectrum. Finding at least one point where the PT symmetry works makes the system PT symmetric.

If we now take a look at an altermagnets pictured in Fig. 12, we have two different models to test. In the first one **(a)** the effect of the time reversal T makes the hopping change $m \rightarrow -m$. Then we find no point to invert the system around so that this first model doesn't have a PT symmetry. For the second one **(b)** we can first invert all spin but afterwards inverting the space doesn't bring back the system in the original configuration. In fact neither applying the P after T on the lattice point nor on the space in-between leads to the lattice we began with. In both cases the degeneracy is lifted, we have dissimilar energies for the different spin-orientation. This is the reason for the band splitting we discussed in the introducing paragraph.

Brief mention of spin-orbit coupling

We refer as spin-orbit coupling (SOC) the interaction between the spin of the electron and the orbital motion. When SOC is discarded we observe a rotation symmetry around the spins. A rotation R can turn the spin back after the application of T resulting in a RT symmetry. $RT(\epsilon(\mathbf{k}, \sigma)) = \epsilon(-\mathbf{k}, \sigma)$ must equal $\epsilon(\mathbf{k}, \sigma)$.

If we now consider a collinear magnet without SOC, we have a RT but no PT symmetry. Under such circumstances the spin-splitting must be symmetric under $\epsilon(-\mathbf{k}, \sigma) = \epsilon(\mathbf{k}, \sigma)$ which describes an even band structure. Such systems are called inversion symmetric altermagnets.

4.3 Implementation of an altermagnet

After introducing the basic properties of an altermagnet, we now aim to describe this system with the already introduced formalism. We are going to consider the first model involving a spin-dependent hopping. The Hamiltonian is given by [38] as:

$$H_{AM} = - \sum_{\langle i,j \rangle \sigma \sigma'} (\mathbf{m}_{ij} \cdot \boldsymbol{\sigma})_{\sigma \sigma'} c_{i\sigma}^\dagger c_{j\sigma'}$$

involving $\boldsymbol{\sigma} = (\sigma_1, \sigma_2, \sigma_3)^T$ the Pauli matrices. \mathbf{m}_{ij} is the actual spin dependent hopping term. If the connection line between the two sites i and j lies on the \mathbf{e}_x axis, we have $\mathbf{m}_{ij} = m(0, 0, 1)$ and $\mathbf{m}_{ji} = m(0, 0, -1)$ along \mathbf{e}_y . m is the desired hopping amplitude, and \mathbf{m}_{ij} scales and masks the Pauli matrices. σ_3 puts m on the diagonal, and takes care of the sign switch. Now having the normal metal t-hopping and this term leads to the $t \pm m$ we described in Fig. 12 (a).

Since the BdG formalism uses fermionic operators, we again need to bring the matrix in a way that reflects the fermionic properties with regard to the \tilde{c} operator. We can remake use of Eq. 54:

$$H_{AM} = - \sum_{\langle ij \rangle \sigma \sigma'} (\mathbf{m}_{ij} \cdot \boldsymbol{\sigma})_{\sigma \sigma'} \frac{1}{2} \left(c_{i\sigma}^\dagger c_{j\sigma'} - c_{i\sigma'} c_{j\sigma}^\dagger \right).$$

For the last summand we split the sum, exchanged the labelling of the states i and j and recombined the sums. However, due to the matrix element in the front that we want to factorize with, we can't exchange the labellings of σ and σ' . Bringing this Hamiltonian in the Nambu formalism we obtain by defining $(\mathbf{m}_{ij} \cdot \boldsymbol{\sigma})_{\sigma \sigma'} = \mathcal{M}_{\sigma \sigma'}$ the following Hamiltonian:

$$H_{ij}^{(AM)} = \frac{1}{2} \begin{pmatrix} -\mathcal{M} & \mathcal{O} \\ \mathcal{O} & \mathcal{M}^T \end{pmatrix}, \quad \text{where} \quad \mathcal{M} = \begin{pmatrix} \mathcal{M}_{\uparrow\uparrow} & \mathcal{M}_{\uparrow\downarrow} \\ \mathcal{M}_{\downarrow\uparrow} & \mathcal{M}_{\downarrow\downarrow} \end{pmatrix}.$$

Making use of this matrix in an altermagnetic lattice point, we can generate the according eigenvectors and -values. We can then study how the physical quantities behave in this material.

5 Bogoliubov-de Gennes Formalism



The Bogoliubov-de Gennes transformation allows us to express the Hamiltonian in a diagonal way. This allows us to define our quantities by looking at the eigenvectors of the Hamiltonian. The resulting matrix lies in a huge space and is very sparse. This section follows closely the derivation of J. A. Ouassou in [39]. Some details of this derivation are also found in [40].

To give an example, it will allow us to rewrite our Hamiltonian as following

$$H = E_0 - \frac{1}{2} \tilde{c}^\dagger \tilde{H} \tilde{c}, \quad (48)$$

involving $\tilde{c} = (\hat{c}_1, \dots, \hat{c}_N)$, where each \hat{c}_i is a vector containing the creation and annihilation operators of a lattice site i : $\hat{c}_i = (c_{i\uparrow}, c_{i\downarrow}, c_{i\uparrow}^\dagger, c_{i\downarrow}^\dagger)$.

As we see, we just describe each site with the four possible c -operators. This means for each lattice site, we have a 4×4 -submatrix that reflects the possible combinations of creation and annihilation operators of both spins. For the readability we are going to drop the comma between the site and spin indices.

For example, if one has (without loss of generality) a chemical potential at the site i , then the Hamiltonian is described in the following way:

$$H_{\mu i} = - \sum_{\sigma} \mu_i c_{i\sigma}^\dagger c_{i\sigma}.$$

If we want to describe it in terms of \hat{c}_i we have:

$$H_{\mu, i} = \begin{pmatrix} c_{i\uparrow}^\dagger \\ c_{i\downarrow}^\dagger \\ c_{i\uparrow} \\ c_{i\downarrow} \end{pmatrix} \cdot \mu_i \begin{pmatrix} 1 & 0 & 0 & 0 \\ 0 & 1 & 0 & 0 \\ 0 & 0 & 0 & 0 \\ 0 & 0 & 0 & 0 \end{pmatrix} \begin{pmatrix} c_{i\uparrow} \\ c_{i\downarrow} \\ c_{i\uparrow}^\dagger \\ c_{i\downarrow}^\dagger \end{pmatrix}$$

Please note that in later discussions we will see the matrix must exhibit a certain symmetry to respect the fermionic relations and have real eigenvalues. This was just an example.

Depending on the interaction we wish to describe, we can figure out what combination of operators we want and design the 4×4 matrix accordingly. To achieve a full description of the system we can consider the interaction between two site i, j as a 4×4 matrix involving the \hat{c}_i^\dagger and c_j operators. Then we can build a huge matrix \tilde{H} based on 4×4 matrices at \tilde{H}_{ij} . The vectors we multiply this matrix with are just the \hat{c}_i^\dagger and c_j operators stack above one and other forming the above-introduced \tilde{c} vector. As a result, one gets the first formula introduced in this section at Eq. 48. We can then compute the eigenvalues and -vectors to express the quantities we're interested in. This is what we call the Bogoliubov-de Gennes transformation.

Now that the motivation is clear, we need to bring our Hamiltonian in a form that involves the fermionic operators $c_{i\sigma}$ and $c_{i\sigma}^\dagger$.

5.1 Tight Binding Model

Our goal is now to fix our particles on lattice sites and describe their interactions. We are therefore going to translate our wave function formalism in an on-site plus nearest neighbour description.

For the generalities, we assume we have the Hamiltonian in the second quantization formalism:

$$H = \sum_{\sigma\sigma'} \int \phi_\sigma^\dagger(\mathbf{r}) H_{\sigma\sigma'}(\mathbf{r}) \psi_{\sigma'}(\mathbf{r}) d^3r \\ + \sum_{\sigma\sigma'} \int \int \phi_\sigma^\dagger(\mathbf{r}) \phi_{\sigma'}^\dagger(\mathbf{r}') V_{\sigma\sigma'}(\mathbf{r}, \mathbf{r}') \phi_{\sigma'}(\mathbf{r}') \phi_\sigma(\mathbf{r}) d^3r' d^3r.$$

We introduce a basis of so called Wannier orbitals $w(\mathbf{r} - \mathbf{R}_i)$ with \mathbf{R}_i an atom location. There are a multiple way to define these orbitals [41], but the most simple ones [42] is enough here. These describe where the electrons evolve around the atoms and should be large in the neighbourhood of \mathbf{R}_i and vanishes when the distance tends to infinity. They are therefore called “localized”. The orbital can build a complete basis and verify the orthonormality condition:

$$\int w^*(\mathbf{r} - \mathbf{R}_i)w(\mathbf{r} - \mathbf{R}_j)d^3r = \delta_{ij}.$$

From this property we can define some field operators in this basis, based on creation and annihilation operators acting on a lattice site i :

$$\phi_\sigma(\mathbf{r}) := \sum_i w(\mathbf{r} - \mathbf{R}_i)c_{i\sigma}, \quad \phi_\sigma^\dagger(\mathbf{r}) := \sum_i w^*(\mathbf{r} - \mathbf{R}_i)c_{i\sigma}^\dagger \quad (49)$$

which is not a continuous description any more. Inserting these operators back into our above Hamiltonian and using the orthonormality allows us to have an on site/nearest neighbour description of the Hamiltonian. Taking for instance the first part of the Hamiltonian, we have:

$$\begin{aligned} H &= \sum_{\sigma\sigma'} \int \psi_\sigma^\dagger(\mathbf{r})H_{\sigma\sigma'}(\mathbf{r})\psi_{\sigma'}(\mathbf{r})d^3r \\ &= \sum_{ij\sigma\sigma'} c_{i\sigma}^\dagger c_{j\sigma'} \int w^*(\mathbf{r} - \mathbf{R}_i)H_{\sigma\sigma'}(\mathbf{r})w(\mathbf{r} - \mathbf{R}_j)d^3r \\ &:= \sum_{i\sigma\sigma'} \epsilon_i^{\sigma\sigma'} c_{i\sigma}^\dagger c_{i\sigma} - \sum_{\langle ij \rangle \sigma\sigma'} t_{ij}^{\sigma\sigma'} c_{i\sigma}^\dagger c_{j\sigma'} + .. \end{aligned}$$

In the last line we include a local energy term ϵ and the so-called hopping term t_{ij} , which is the interaction with the nearest neighbour sites j of i . For a more precise description one could consider more neighbours. The spin dependent term can be used to describe spin orbit coupling or spin-flip processes.

We now aim to define the useful processes for this thesis using this formalism.

5.1.1 Non-interacting electrons

The two main components of the non-interacting system Hamiltonian H_N are the chemical potential μ_i which is specific to each site and the hopping term t_{ij} . The chemical potential is modulated by the number of particles on the site i and the hopping term gives the amplitudes of moving an electron from site i to j . We assume it as spin-independent here.

$$H_N = - \sum_{i\sigma} \mu_i c_{i\sigma}^\dagger c_{i\sigma} - \sum_{\langle ij \rangle \sigma} t_{ij} c_{i\sigma}^\dagger c_{j\sigma}, \quad (50)$$

where $\langle ij \rangle$ is a commonly used notation to sum over i and its nearest neighbours j , skipping $i = j$. We label it the normal Hamiltonian.

The hopping amplitude can be computed from the overlap of the orbitals under a kinetic operator $-\nabla^2/(2m)$, which explains the meaning of the term “hopping”:

$$\begin{aligned} t_{ij} &= - \int w^*(\mathbf{r} - \mathbf{R}_i) \frac{\nabla^2}{2m} w(\mathbf{r} - \mathbf{R}_j) d^3r \\ &= + \frac{1}{2m} \int (\nabla w(\mathbf{r} - \mathbf{R}_i))^* (\nabla w(\mathbf{r} - \mathbf{R}_j)) d^3r. \end{aligned}$$

We used a partial integration considering the boundary conditions of the Wannier orbitals $w(\pm\infty) = 0$. Therefore, one part of the partial integration vanishes, and we integrate/differentiate the integrands in the other integral, leading to two ∇ s. Further we see that $t_{ij} = t_{ji}^*$ by swapping the two integrands.

5.1.2 Superconductivity

A previous study of ours on the superconductivity have led us to the following Hamiltonian:

$$H_S = - \int U(\mathbf{r}) \psi_{\downarrow}^{\dagger}(\mathbf{r}) \psi_{\uparrow}^{\dagger}(\mathbf{r}) \psi_{\uparrow}(\mathbf{r}) \psi_{\downarrow}(\mathbf{r}) d^3r \quad (51)$$

on which we can apply a mean field approximation $\Delta(\mathbf{r}) = U(\mathbf{r}) \langle \psi_{\uparrow}(\mathbf{r}) \psi_{\downarrow}(\mathbf{r}) \rangle$. This yields to a common BCS-Hamiltonian for regular superconductors.

$$H_S = - \int \left(\Delta(\mathbf{r}) \psi_{\downarrow}^{\dagger}(\mathbf{r}) \psi_{\uparrow}^{\dagger}(\mathbf{r}) + \Delta(\mathbf{r})^* \psi_{\uparrow}(\mathbf{r}) \psi_{\downarrow}(\mathbf{r}) \right) d^3r.$$

We see that the second integrand is just the complex conjugate of the first one. To spare some place, we are going to focus ourselves on the first one and denoted its homologue with *h.c.* “hermitian conjugate”. We insert Eq. 49 in our last expression and obtain:

$$\begin{aligned} H_S &= - \sum_{ij} c_{i\downarrow}^{\dagger} c_{i\uparrow}^{\dagger} \int \Delta(\mathbf{r}) w^*(\mathbf{r} - \mathbf{R}_i) w^*(\mathbf{r} - \mathbf{R}_j) d^3r + \text{h.c.} \\ &:= - \sum_{ij} \Delta_{ij} c_{i\downarrow}^{\dagger} c_{i\uparrow}^{\dagger} + \text{h.c.} \end{aligned}$$

Let us introduce the coherence length of the Cooper pairs. Its is inversely proportional to the gap Δ and gives the extent of the correlation of the operators $c_{i\uparrow}$ and $c_{j\downarrow}$. $\Delta(\mathbf{r})$ is an order parameter and doesn't vary much in the coherence length, which is much bigger than the atomic length. Therefore, we can say that the orbitals vary faster than the gap [Jabir2021]. Moreover, these orbitals are picked in the neighbourhood of the atomic location \mathbf{R}_i and \mathbf{R}_j . Achieving the integral we get $\Delta_{ij} = \Delta_i \delta_{ij}$. We can from then reintroduce the h.c. and we get:

$$H_S = - \sum_i \Delta_i c_{i\downarrow}^{\dagger} c_{i\uparrow}^{\dagger} + \Delta_i^* c_{i\uparrow} c_{i\downarrow}. \quad (52)$$

We are missing the mean field term E_0 :

$$E_0 = \int U \langle \psi_{\downarrow}^{\dagger} \psi_{\uparrow}^{\dagger} \rangle \langle \psi_{\uparrow} \psi_{\downarrow} \rangle d^3r = \int U \frac{\Delta^*}{U} \frac{\Delta}{U} d^3r = \int \frac{|\Delta|^2}{U} d^3r.$$

After applying the tight binding formalism we get:

$$E_0 = \sum_i \frac{|\Delta_i|^2}{U},$$

which is a term we can add to the Hamiltonian in Eq. 51. Form these equations we have the final Hamiltonian for the superconducting system:

$$H = E_0 + H_N + H_S.$$

5.2 A more symmetric Hamiltonian

As we introduced it while motivating the Bogoliubov-de Gennes formalism, we aspire to describe each state as a vector-matrix-vector product of

$$\hat{c}_i = \left(c_{i\uparrow}, c_{i\downarrow}, c_{i\uparrow}^{\dagger}, c_{i\downarrow}^{\dagger} \right).$$

However, using the form we have in the superconducting (Eq. 51) and normal (Eq. 50) Hamiltonian will later not act as a fermionic operator upon the transformation we are about to do. We need to rewrite the Hamiltonian in a more symmetric way to later respect the anticommutation relations.

The chemical potential

It can be expressed using the anticommutation relations of the fermionic operators $[c_{i\sigma}^\dagger, c_{i\sigma}]_+ = 1$:

$$\sum_{i\sigma} \mu_i c_{i\sigma}^\dagger c_{i\sigma} = \frac{1}{2} \sum_{i\sigma} \mu_i (c_{i\sigma}^\dagger c_{i\sigma} - c_{i\sigma} c_{i\sigma}^\dagger + 1) \quad (53)$$

The trick we used is quite straight forward but not obvious. Taking two different states α and γ we have:

$$c_\alpha^\dagger c_\gamma = \frac{1}{2} c_\alpha^\dagger c_\gamma + \frac{1}{2} c_\alpha^\dagger c_\gamma = \frac{1}{2} c_\alpha^\dagger c_\gamma + \underbrace{\frac{1}{2} c_\alpha^\dagger c_\gamma + \frac{1}{2} c_\gamma c_\alpha^\dagger - \frac{1}{2} c_\gamma c_\alpha^\dagger}_{\frac{1}{2} [c_\alpha^\dagger, c_\gamma]_+ = \frac{1}{2} \delta_{\alpha\gamma}}. \quad (54)$$

The hopping term

We can express this term in the same way:

$$\sum_{\langle ij \rangle \sigma} t_{ij} c_{i\sigma}^\dagger c_{j\sigma} = \frac{1}{2} \sum_{\langle ij \rangle \sigma} t_{ij} (c_{i\sigma}^\dagger c_{j\sigma} - c_{j\sigma} c_{i\sigma}^\dagger).$$

This has to be done so that the γ operators respect the fermionic anticommutation relations. The same method is involved for the chemical potential term. We can also take the liberty to reorder the indices and use the fact that $t_{ij} = t_{ji}^*$:

$$\sum_{\langle ij \rangle \sigma} t_{ij} c_{i\sigma}^\dagger c_{j\sigma} = \frac{1}{2} \sum_{\langle ij \rangle \sigma} t_{ij} c_{i\sigma}^\dagger c_{j\sigma} - t_{ij} c_{i\sigma} c_{j\sigma}^\dagger = \frac{1}{2} \sum_{\langle ij \rangle \sigma} t_{ij} c_{i\sigma}^\dagger c_{j\sigma} - t_{ij}^* c_{i\sigma} c_{j\sigma}^\dagger. \quad (55)$$

The superconducting term

This term takes the following form:

$$\sum_i \Delta_i c_{i\downarrow}^\dagger c_{i\uparrow}^\dagger + \Delta_i^* c_{i\uparrow} c_{i\downarrow} = \frac{1}{2} \sum_i \Delta_i (c_{i\downarrow}^\dagger c_{i\uparrow}^\dagger - c_{i\uparrow}^\dagger c_{i\downarrow}^\dagger) + \Delta_i^* (c_{i\uparrow} c_{i\downarrow} - c_{i\downarrow} c_{i\uparrow}). \quad (56)$$

We then finish this section by using Eqs. 53, 55 and 56 in the Hamiltonian and obtain the following form:

$$\begin{aligned} H = E_0 & - \frac{1}{2} \sum_{i\sigma} \mu_i (c_{i\sigma}^\dagger c_{i\sigma} - c_{i\sigma} c_{i\sigma}^\dagger) \\ & - \frac{1}{2} \sum_{\langle ij \rangle \sigma} t_{ij} c_{i\sigma}^\dagger c_{j\sigma} - t_{ji}^* c_{i\sigma} c_{j\sigma}^\dagger \\ & - \frac{1}{2} \sum_i \Delta_i (c_{i\downarrow}^\dagger c_{i\uparrow}^\dagger - c_{i\uparrow}^\dagger c_{i\downarrow}^\dagger) + \Delta_i^* (c_{i\uparrow} c_{i\downarrow} - c_{i\downarrow} c_{i\uparrow}). \end{aligned} \quad (57)$$

The constant term $\frac{1}{2} \sum_{i\sigma} \mu_i$ of the normal Hamiltonian summed up into E_0 . We can now rewrite the Hamiltonian in a more compact way:

$$H = E_0 - \frac{1}{2} \sum_{i,j} \hat{c}_i^\dagger \hat{H}_{ij} \hat{c}_j \quad (58)$$

where the on site matrix reads

$$\hat{H}_{ij} = \begin{pmatrix} \mu_i \mathbb{I}_2 \delta_{ij} + t_{ij} & -i\sigma_2 \Delta_i \delta_{ij} \\ i\sigma_2 \Delta_i^* \delta_{ij} & -\mu_i \mathbb{I}_2 \delta_{ij} - t_{ij}^* \end{pmatrix} = \begin{pmatrix} H_{ij} & \Delta_{ij} \\ \Delta_{ij}^\dagger & -H_{ij}^* \end{pmatrix} \quad (59)$$

where we use \mathbb{I}_n as an n -dimensional identity matrix. We haven't explicitly removed the t_{ij} if we are not considering nearest neighbours. At this point it's interesting to note that if we wish to build some periodic boundary conditions, it might be the case that a site on a side is neighbour with a site on the other side.

We can further compress our \hat{c}_i operator by introducing

$$\check{c} = (\hat{c}_1, \dots, \hat{c}_N)$$

along with the system Hamiltonian-matrix \check{H}_{ij} that orders the \hat{H}_{ij} matrices together. Please note that \check{H}_{ij} corresponds to an entry of \hat{H}_{ij} . The later maps two sites i, j to a 4×4 matrix while the second concatenate all the matrices. In \check{H}_{ij} taking the entries $a = 4(i - 1) + 1$ to $4(i - 1) + 4$ and $b = 4(j - 1) + 1$ to $4(j - 1) + 4$ corresponds to \hat{H}_{ab} if a is the site i and b the site j . This allows us to rewrite the Hamiltonian 58 as:

$$H = E_0 - \frac{1}{2}\check{c}^\dagger \check{H} \check{c}. \quad (60)$$

5.3 Eigenvalues

We now have a look at the following eigenvalue problem, which later helps from the diagonalization of the Hamiltonian:

$$\check{H}\check{\chi}_n = E_n\check{\chi}_n, \quad (61)$$

n runs over the number of the eigenvalue and $\check{\chi}_n$ is the corresponding eigenvector. We can decompose the $\check{\chi}_n$ term to reflect each lattice site: $\check{\chi}_n = (\hat{\chi}_{n1}, \dots, \hat{\chi}_{nN})$. This means χ_{ni} refers to a 4×4 block, i.e. the on the sub-matrix we had earlier talked about. Therefore, this χ_{ni} contains four values, grouped in two vectors of length two, one for each spin: $\chi_{n,i} = (u_{ni}, v_{ni})$. Further $u_{ni} = (u_{ni\uparrow}, u_{ni\downarrow})$ couples to the two first components $(c_{i\uparrow}, c_{i\downarrow})$ we had in \hat{c} and similarly $v_{ni} = (v_{ni\uparrow}, v_{ni\downarrow})$ to the two last components $(c_{i\uparrow}^\dagger, c_{i\downarrow}^\dagger)$ of the four operator \hat{c} . These values represent the coherence factors we defined in Eqs. 41 and 42.

We can simplify the eigenvalue problem by only taking a look at a site i . We then sum up over i :

$$\sum_{j \in \llbracket N \rrbracket} \hat{H}_{ij} \hat{\chi}_{nj} = E_n \hat{\chi}_{ni}.$$

To generalize, we can sum over the rows of \check{H}_{ij} with the components of $\check{\chi}_n$. We remember that \check{H}_{ij} represent a complex scalar and \hat{H}_{ij} is a 4×4 matrix with complex entries. So it follows by reintroducing Eq. 59 the following set of equations:

$$\left\{ \begin{array}{l} \sum_{j \in \llbracket N \rrbracket} H_{ij} u_{nj} + \Delta v_{nj} = E_n u_{nj} \\ \sum_{j \in \llbracket N \rrbracket} \Delta^\dagger u_{nj} - H_{ij}^* v_{nj} = E_n v_{nj} \end{array} \right. \xrightarrow{(1)} \left\{ \begin{array}{l} \sum_j H_{ij} u_{nj} + \Delta v_{nj} = E_n u_{nj} \\ \sum_j H_{ij} v_{nj}^* + \Delta^\dagger u_{nj}^* = -E_n v_{nj}^* \end{array} \right. \quad (62)$$

Where in (1) we took the conjugate of the second equation and used $\Delta^\dagger = -\Delta^*$. This is an important result, because it shows that if $\check{\chi}_n = (u_{n1}, v_{n1}, u_{n2}, v_{n2}, \dots)$ is an eigenvector with eigenvalue E_n , then so should be $(v_{n1}^*, u_{n1}^*, v_{n2}^*, u_{n2}^*, \dots)$ with the eigenvalue $-E_n$.

This leads to a symmetry in the energy spectrum of $H = E_0 \pm \frac{1}{2}\check{c}^\dagger \check{H} \check{c}$. A flexibility which allows us to choose the version of H with the positive sign, which is more commonly used.

5.4 Diagonalization

Our goal is now to express the Hamiltonian relative to its energy eigenvalues, which is more particle to work with. As we have seen in the last section, eigenvectors χ_n allows us to compute the energies.

First, we define a matrix from all the eigenstates $\check{X} = [\check{\chi}_{\pm 1}, \dots, \check{\chi}_{\pm 2N}]$. We then introduce a matrix $\check{D} = \text{diag}(E_{\pm 1}, \dots, E_{\pm 2N})$ with the eigenvalues sorted on the diagonal. The order in which the eigenvectors appear is not important but $\check{\chi}_i$ should be on the same column index as E_i not to lose track of which eigenvector is linked with which eigenvalue. Then, assuming that the Hamiltonian can be diagonalized, we can write it as:

$$\check{H} = \check{X} \check{D} \check{X}^{-1} = \check{X} \check{D} \check{X}^\dagger \quad (63)$$

The eigenvalues correspond to the energies of the system, this means they should be real because they correspond to a physical quantity. The above expression is equivalent to saying that

\check{H} is hermitian. Hermitian matrices are known to have real eigenvalues and can be represented with a unitary matrix \check{X} [43]. We can then transform the Hamiltonian with $\check{c} := \check{X}\gamma$:

$$\begin{aligned} H &= E_0 + \frac{1}{2}\check{c}^\dagger \check{H} \check{c} = E_0 + \frac{1}{2}\gamma^\dagger \check{X}^\dagger \check{H} \check{X} \gamma \\ &= E_0 + \frac{1}{2}\gamma^\dagger \underbrace{\check{X}^\dagger \check{X}}_{=\mathbb{I}} \check{D} \underbrace{\check{X}^{-1} \check{X}}_{=\mathbb{I}} \gamma \\ &= E_0 + \frac{1}{2}\gamma^\dagger \check{D} \gamma \\ &= E_0 + \frac{1}{2} \sum_{n \in \mathcal{N}} E_n \gamma_n^\dagger \gamma_n, \end{aligned}$$

where $\mathcal{N} = \{\pm n : n \in \llbracket N \rrbracket\}$. Rearranging the transformation of \check{c} , we get $\gamma = \check{X}^\dagger \check{c}$. Now that we made the structure of the involved variables clear in the last section, we find the expression of the γ which is $2N$ -dimensional. A component of γ is:

$$\begin{aligned} \gamma_n &= \sum_i \left(u_{ni\uparrow}^* c_{i\uparrow} + v_{ni\uparrow}^* c_{i\uparrow}^\dagger + u_{ni\downarrow}^* c_{i\downarrow} + v_{ni\downarrow}^* c_{i\downarrow}^\dagger \right) \\ &= \sum_{i\sigma} \left(u_{ni\sigma}^* c_{i\sigma} + v_{ni\sigma}^* c_{i\sigma}^\dagger \right), \end{aligned}$$

and due to the symmetry we saw earlier,

$$\gamma_{-n} = \sum_{i\sigma} \left(v_{ni\sigma} c_{i\sigma} + u_{ni\sigma} c_{i\sigma}^\dagger \right)$$

for $n \in \llbracket N \rrbracket$. We now take a look at the conjugate transpose of γ_{-n} . Because scalar are dimension 1×1 we have $(uc^\dagger)^\dagger = (c^\dagger)^\dagger u^\dagger = cu^* = u^*c$ and it follows:

$$\gamma_{-n}^\dagger = \sum_{i\sigma} \left(v_{ni\sigma}^* c_{i\sigma}^\dagger + u_{ni\sigma}^* c_{i\sigma} \right) = \gamma_n.$$

Using this we can link each γ_i to the corresponding eigenvalue E_i : γ_n to the corresponding eigenvalue E_n and γ_{-n} to the corresponding eigenvalue $E_{-n} = -E_n$. We recall that we had $2N$ degrees of freedom $c_{i\sigma}$ due to the two possible spins, but after the transformation we get $4N$ degrees into \hat{c}_i nevertheless. But because our energies E_n and E_{-n} are related to each other, we can keep only the positive $2N$ eigenvalues and this maintain the total number of degree of freedom.

We can now apply this statement into the expression. First we can split the sum over the $n \in \mathcal{N}$ in two parts: $\mathcal{N}_+ = \{n \in \mathcal{N} : n > 0\}$ and $\mathcal{N}_- = \{n \in \mathcal{N} : n < 0\}$.

$$\begin{aligned} H &= E_0 + \frac{1}{2} \sum_{n \in \mathcal{N}_+} E_n \gamma_n^\dagger \gamma_n + \frac{1}{2} \sum_{n \in \mathcal{N}_-} E_n \gamma_n^\dagger \gamma_n \\ &= E_0 + \frac{1}{2} \sum_{n \in \mathcal{N}_+} E_n \gamma_n^\dagger \gamma_n + \frac{1}{2} \sum_{n \in \mathcal{N}_+} E_{-n} \gamma_{-n}^\dagger \gamma_{-n} \\ &= E_0 + \frac{1}{2} \sum_{n \in \mathcal{N}_+} E_n \gamma_n^\dagger \gamma_n - \frac{1}{2} \sum_{n \in \mathcal{N}_+} E_n \gamma_{-n}^\dagger \gamma_{-n} \\ &= E_0 + \frac{1}{2} \sum_{n \in \mathcal{N}_+} E_n \gamma_n^\dagger \gamma_n - \frac{1}{2} \sum_{n \in \mathcal{N}_+} E_n \gamma_n \gamma_n^\dagger \\ &= E_0 + \frac{1}{2} \sum_{n \in \mathcal{N}_+} E_n (\gamma_n^\dagger \gamma_n - \gamma_n \gamma_n^\dagger). \end{aligned}$$

We used the energy symmetry $E_{-n} = -E_n$, $\gamma_{-n}^\dagger = \gamma_n$, as well as $\gamma_{-n} = \gamma_n^\dagger$.

Using this knowledge, we can express a final formula for the Hamiltonian by using the anticommutation properties of the fermionic γ -operators: $[\gamma_n^\dagger, \gamma_n]_+ = 1$, so using the trick 54 and bringing the $\frac{1}{2}$ prefactor in the sum:

$$H = E_0 - \sum_{n \in \llbracket N \rrbracket} E_n \left(\gamma_n^\dagger \gamma_n - \frac{1}{2} \right). \quad (64)$$

This is the final form of the Hamiltonian in the Bogoliubov-de Gennes formalism. As a user one should build the Hamiltonian and compute its eigenvalues,-vector and use them to compute some physical quantities.

5.5 Physical Quantities

5.5.1 Superconducting Gap

We already covered how the superconducting gap Δ is a relevant property of the Meissner state. We now aim to use the mean field theory in order to find the gap. This requires a self-consistent equation, which we can be derived from the Hamiltonian.

The gap was defined as $\Delta(\mathbf{r}) := U(\mathbf{r})\langle\psi_\uparrow(\mathbf{r})\psi_\downarrow(\mathbf{r})\rangle$. Back to the tight binding formalism, the gap now depends on the lattice site i and reads $\Delta_i = U_i\langle c_{i\uparrow}c_{i\downarrow}\rangle$, and we can express $c_{i\sigma}$ in terms of the γ -operators:

$$\begin{aligned}
 c_{i\sigma} &= \sum_{n \in \mathcal{N}} u_{ni\sigma} \gamma_n \\
 &= \sum_{n \in \mathcal{N}_+} u_{ni\sigma} \gamma_n + u_{-n,i\sigma} \gamma_{-n} \quad (65) \\
 &= \sum_{n \in \mathcal{N}_+} u_{ni\sigma} \gamma_n + v_{ni\sigma}^* \gamma_n^\dagger
 \end{aligned}
 \quad \begin{array}{c} \circ \\ | \\ \circ \end{array}
 \quad
 \begin{aligned}
 c_{i\sigma}^\dagger &= \sum_{n \in \mathcal{N}_+} (u_{ni\sigma} \gamma_n)^\dagger + (v_{ni\sigma}^* \gamma_n^\dagger)^\dagger \\
 &= \sum_{n \in \mathcal{N}_+} \gamma_n^\dagger u_{ni\sigma}^\dagger + \gamma_n (v_{ni\sigma}^*)^\dagger \quad (66) \\
 &= \sum_{n \in \mathcal{N}_+} u_{ni\sigma}^* \gamma_n^\dagger + v_{ni\sigma} \gamma_n
 \end{aligned}$$

where we used the symmetry of the eigenvectors. We can now compute expectation value involved in the gap by taking the thermal average and the quantum expectation value:

$$\begin{aligned}
 \langle c_{i\uparrow}c_{i\downarrow} \rangle &= \sum_{n,m \in \mathcal{N}_+} \langle (u_{ni\uparrow} \gamma_n + v_{ni\uparrow}^* \gamma_n^\dagger) (u_{mi\downarrow} \gamma_m + v_{mi\downarrow}^* \gamma_m^\dagger) \rangle \\
 &= \sum_{n,m \in \mathcal{N}_+} \langle (u_{ni\uparrow} u_{mi\downarrow} \gamma_n \gamma_m + u_{ni\uparrow} v_{mi\downarrow}^* \gamma_n \gamma_m^\dagger + v_{ni\uparrow}^* u_{mi\downarrow} \gamma_n^\dagger \gamma_m + v_{ni\uparrow}^* v_{mi\downarrow}^* \gamma_n^\dagger \gamma_m^\dagger) \rangle \\
 &\stackrel{(*)}{=} \sum_{n \in \mathcal{N}_+} \langle u_{ni\uparrow} v_{ni\downarrow}^* \gamma_n \gamma_n^\dagger \rangle + \langle v_{ni\uparrow}^* u_{ni\downarrow} \gamma_n^\dagger \gamma_n \rangle \quad (67) \\
 &= \sum_{n \in \mathcal{N}_+} u_{ni\uparrow} v_{ni\downarrow}^* \langle \gamma_n \gamma_n^\dagger \rangle + v_{ni\uparrow}^* u_{ni\downarrow} \langle \gamma_n^\dagger \gamma_n \rangle \\
 &= \sum_{n \in \mathcal{N}_+} u_{ni\uparrow} v_{ni\downarrow}^* (1 - f(E_n)) + v_{ni\uparrow}^* u_{ni\downarrow} f(E_n)
 \end{aligned}$$

where f is the Fermi-Dirac distribution. In $(*)$ we notice no $\gamma\gamma$ or $\gamma^\dagger\gamma^\dagger$ terms in the Hamiltonian, so their expectation value is zero¹.

The expectation value $\langle a\hat{A} \rangle_\Phi$ of a scalar times an operator reads $\langle \Phi | a\hat{A} | \Phi \rangle_\Phi = a \langle \Phi | \hat{A} | \Phi \rangle_\Phi = a \langle \hat{A} \rangle_\Phi$. To certify this statement, we just take a look at the first quantization expression of this bracket. This result leads to the self-consistent equation:

$$\Delta_i = U_i \sum_{n \in \mathcal{N}_+} u_{ni\uparrow} v_{ni\downarrow}^* (1 - f(E_n)) + u_{ni\downarrow} v_{ni\uparrow}^* f(E_n) \quad (68)$$

We plan to solve this equation numerically, inserting some guess in the Hamiltonian, diagonalize it, update Δ_i and reinsert it into H. We should repeat this until we reach a fix point or the desired accuracy.

□ _____ □

¹This is like the expectation value of killing twice a fermion in a state. It is not possible, because we can not annihilate a state that has a possession number of zero. And in the same way due to the Pauli principle we can not have more than one particle in the same state, so $\langle \gamma^\dagger \gamma^\dagger \rangle = 0$. We are not finding these terms in the Hamiltonian. Here we removed the indices, in fact the diagonality takes also place on the indices, so that we end just with n . The Hamiltonian is diagonal in the quasiparticles' operators.

5.5.2 Currents

Using the charge conservation and the Heisenberg picture we are going to derive an expression for the current in the lattice. The system we are taking into account is two-dimensional. These derivations are based on the work of V. Risinggård and J. Linder [44].

The charge conservation reads

$$\partial_t \rho_i = -\nabla \mathbf{j}_i$$

and identifies the time variation of the charge density on the site i as the negative divergence of the current density. Now, performing some transformations, we bring this expression in a more useful form. The goal here is to integrate on both side over our two-dimensional surface Ω . For the charge density this yields to the charge at a site:

$$\int_{\Omega} \partial_t \rho_i d\mathbf{r} = \partial_t Q_i.$$

For the current density we can use the Gauss law to change the integration set:

$$\int_{\Omega} \nabla \mathbf{j}_i d\mathbf{r} = \int_{\partial\Omega} \mathbf{j}_i \mathbf{n} = \sum_n J_{i,n} a = \sum_n I_{i,n}$$

where $\partial\Omega$ is the boundary of Ω . The normal vector \mathbf{n} points in the 2D-plane, outward from the boundary. Assuming we have a square lattice, we can assign to each lattice site a square unit cell with side length a . The sum over n runs over all the sides.

Now introducing the Heisenberg picture with $\hbar = 1$ we get

$$\partial_t Q_i = i[H, Q_i].$$

Finlay we can introduce the second quantization in the charge:

$$Q_i = \sum_{\sigma} c_{i\sigma}^{\dagger} c_{i\sigma} = \sum_{\sigma} n_{i,\sigma}$$

which is quite trivial, summing over all the particle at a site leads the charge of the site. After putting all together, this yields

$$I_i^{+x} + I_i^{+y} + I_i^{-x} + I_i^{-y} = -i \left[H, \sum_{\sigma} n_{i,\sigma} \right] \quad (69)$$

This mean the last step to perform is to compute the commutator of the different terms of the Hamiltonian with the charge at a site i . We remind here, that our Hamiltonian contains a chemical potential, a hopping, a superconducting and an altermagnetic term.

The hopping term

We use a constant hopping amplitude $t_{ij} = t$.

$$\left[\sum_{\langle ij \rangle \sigma} c_{i\sigma}^{\dagger} c_{j\sigma}, \sum_{\sigma} n_{l\sigma} \right] = \sum_{\langle ij \rangle \sigma \sigma'} c_{i\sigma}^{\dagger} c_{j\sigma} n_{l\sigma'} - n_{l\sigma'} c_{i\sigma}^{\dagger} c_{j\sigma}$$

We can then introduce a useful trick that involves the commutator $[n_{\mu}, c_{\nu}] = -\delta_{\mu\nu} c_{\mu}$

$$\begin{aligned} c_{i\sigma}^{\dagger} c_{j\sigma} n_{i,\sigma'} &= c_{i\sigma}^{\dagger} \underbrace{(c_{j\sigma} n_{l\sigma'} - n_{l\sigma'} c_{j\sigma} + n_{l\sigma'} c_{j\sigma})}_{-[n_{l\sigma'}, c_{j\sigma}]} \\ &= c_{i\sigma}^{\dagger} (\delta_{\sigma'\sigma} \delta_{lj} c_{i\sigma'} + n_{l\sigma'} c_{j\sigma}). \end{aligned}$$

Following the same schema we derive the other part of the commutator. Here the expressions involves $[n_{\mu}, c_{\nu}^{\dagger}] = \delta_{\mu\nu} c_{\mu}^{\dagger}$:

$$\begin{aligned} n_{l\sigma'} c_{i\sigma}^{\dagger} c_{j\sigma} &= \underbrace{(n_{l\sigma'} c_{i\sigma}^{\dagger} - c_{i\sigma}^{\dagger} n_{l\sigma'})}_{[n_{l\sigma'}, c_{i\sigma}^{\dagger}]} + c_{i\sigma}^{\dagger} n_{l\sigma'} c_{j\sigma} \\ &= (\delta_{\sigma'\sigma} \delta_{li} c_{j\sigma'}^{\dagger} + c_{i\sigma}^{\dagger} n_{l\sigma'}) c_{j\sigma} \end{aligned}$$

After subtracting the second term from the first one we are left with

$$\begin{aligned} \left[\sum_{\langle ij \rangle \sigma} c_{i\sigma}^\dagger c_{j\sigma}, \sum_{\sigma} n_{i\sigma} \right] &= \sum_{\langle ij \rangle \sigma \sigma'} \delta_{\sigma' \sigma} \left(\delta_{lj} c_{i\sigma}^\dagger c_{j\sigma'} - \delta_{li} c_{i\sigma'}^\dagger c_{j\sigma} \right) \\ &= \frac{1}{2} \sum_{i \delta \sigma \sigma'} \delta_{\sigma' \sigma} \left(\delta_{l, i+\delta} c_{i\sigma}^\dagger c_{i+\delta, \sigma'} - \delta_{li} c_{i\sigma'}^\dagger c_{i+\delta, \sigma} \right) \end{aligned}$$

Because of the squared lattice we can summarize the neighbour set $\langle ij \rangle$ to $\{i + \delta_x, i - \delta_x, i + \delta_y, i - \delta_y\}$ involving δ_{axis} the displacement from the site to neighbour one along the given axis. This is abstracted in $i + \delta$. After summing up over the σ' and i , and writing explicitly everything we obtain

$$\begin{aligned} &= \frac{1}{2} \sum_{\sigma} (c_{l-\delta_x, \sigma}^\dagger c_{l, \sigma} - c_{l\sigma}^\dagger c_{l+\delta_x, \sigma}) + (c_{l+\delta_x, \sigma}^\dagger c_{l, \sigma} - c_{l\sigma}^\dagger c_{l-\delta_x, \sigma}) \\ &\quad + (c_{l-\delta_y, \sigma}^\dagger c_{l, \sigma} - c_{l\sigma}^\dagger c_{l+\delta_y, \sigma}) + (c_{l+\delta_y, \sigma}^\dagger c_{l, \sigma} - c_{l\sigma}^\dagger c_{l-\delta_y, \sigma}), \end{aligned} \quad (70)$$

where the one half factor avoids summing twice over the nearest neighbours. This proportional to the current at a site l . The current of one side of the square unit cell is represented by a pair of $c_{l\pm\delta_x, \sigma}^\dagger c_{l\sigma} - c_{l\sigma}^\dagger c_{l\pm\delta_x, \sigma}$ where the same displacement δ_x is involved. This will be an important consideration talking about the current in the altermagnet.

Chemical potential term

For the chemical potential term it is useful to introduce that the commutator between two number operator vanishes. Since the charge and the chemical potential operators involves only number operator, we find that this term doesn't take part to the current.

Superconducting term

The superconducting term has a peculiar behaviour. If one can solve the gap (self consistently), this term doesn't contribute to the current as we are going to see. We first form the commutator between the Hubbard term and the charge operator:

$$\left[\sum_i \left(\Delta_i c_{i\uparrow}^\dagger c_{i\downarrow}^\dagger + \Delta_i^* c_{i\uparrow} c_{i\downarrow} \right), \sum_{\sigma} n_{l, \sigma} \right]$$

again make the already introduced commutator appear, we obtain

$$\begin{aligned} &= \sum_{i\sigma} \delta_{il} \left(\Delta_i^\dagger (\delta_{\sigma\downarrow} + \delta_{\sigma\uparrow}) c_{i\downarrow} c_{i\uparrow} - \Delta_i (\delta_{\sigma\downarrow} + \delta_{\sigma\uparrow}) c_{i\uparrow}^\dagger c_{i\downarrow}^\dagger \right) \\ &= 2 \left(\Delta_i^\dagger c_{i\downarrow} c_{i\uparrow} - \Delta_i c_{i\uparrow}^\dagger c_{i\downarrow}^\dagger \right) \end{aligned}$$

This expression mixes creation and annihilation operators and makes it hard to recognize a current. One can view this term as a source [44], meaning we have a new term \mathcal{C}_i that appears in the equation

$$-\partial_t Q_i = \mathcal{C}_i + \sum_n I_{i,n}.$$

To know the contribution to the current we can investigate the rate of charge generation of this term. This is achieved by taking the quantum expectation and the thermal average of the system.

$$2 \left(\Delta_l^\dagger \langle c_{l\downarrow} c_{l\uparrow} \rangle - \Delta_l \langle c_{l\uparrow}^\dagger c_{l\downarrow}^\dagger \rangle \right) = \frac{2}{U_l} \left(-\Delta_l^\dagger \Delta_l + \Delta_l \Delta_l^\dagger \right)$$

This is achieved using the anticommutation relation of the fermionic operators Eq. 2 and Eq. 3. We have as well $\Delta_l^\dagger = U_i^* \langle (c_{l\uparrow} c_{l\downarrow})^\dagger \rangle = U_i \langle c_{l\downarrow}^\dagger c_{l\uparrow}^\dagger \rangle$. The dagger operator is assumed to be inserted into the expectation value using the linearity of the integral defining $\langle \cdot \rangle$.

Solving Δ self-consistently will lead to $\Delta \Delta^\dagger = \Delta^\dagger \Delta$, and therefore we find that the value vanishes.

Altermagnetic term

As we introduced it in a previous discussion, the altermagnetic term is more complicated than the last one treated and need more work. In essence, we describe an advanced hopping term, that changes regarding of the hopping axis. We can first bring the commutator where the matrix element $(\mathbf{m}_{ij} \cdot \boldsymbol{\sigma})_{\sigma\sigma'}$ is a scalar:

$$\begin{aligned} \left[\sum_{\langle ij \rangle \sigma \sigma'} (\mathbf{m}_{ij} \cdot \boldsymbol{\sigma})_{\sigma\sigma'} \cdot c_{i\sigma}^\dagger c_{j\sigma'}, \sum_{\tilde{\sigma}} n_{l,\tilde{\sigma}} \right] &= \sum_{\substack{\langle ij \rangle \\ \sigma \sigma' \tilde{\sigma}}} (\mathbf{m}_{ij} \cdot \boldsymbol{\sigma})_{\sigma\sigma'} \left(c_{i\sigma}^\dagger c_{j\sigma'} n_{l\tilde{\sigma}} - n_{l\tilde{\sigma}} c_{i\sigma}^\dagger c_{j\sigma'} \right) \\ &= \sum_{\substack{\langle ij \rangle \\ \sigma \sigma' \tilde{\sigma}}} (\mathbf{m}_{ij} \cdot \boldsymbol{\sigma})_{\sigma\sigma'} \delta_{\sigma\tilde{\sigma}} \left(\delta_{lj} c_{i\sigma}^\dagger c_{j\tilde{\sigma}} - \delta_{li} c_{i\tilde{\sigma}}^\dagger c_{j\sigma'} \right) \\ &= \frac{1}{2} \sum_{i\delta\sigma\sigma'} (\mathbf{m}_{i,i+\delta} \cdot \boldsymbol{\sigma})_{\sigma\sigma'} \left(\delta_{l,i+\delta} c_{i\sigma}^\dagger c_{i+\delta,\sigma} - \delta_{li} c_{i\sigma}^\dagger c_{i+\delta,\sigma'} \right) \end{aligned}$$

We use the same transformation we made earlier to introduce the commutator between n, c and n, c^\dagger . We sum over the $\tilde{\sigma}$ and i and introduce a new set made of $\boldsymbol{\delta}$, as we did before. The summation over the $\boldsymbol{\delta}$ results in the following cumbersome expression

$$\begin{aligned} &= \sum_{\sigma} \left[\sum_{\sigma'} (\mathbf{m}_{l,l+\delta_x} \cdot \boldsymbol{\sigma})_{\sigma\sigma'} \left(c_{l-\delta_x,\sigma}^\dagger c_{l\sigma} - c_{l\sigma}^\dagger c_{l+\delta_x,\sigma'} \right) \right. \\ &\quad + \sum_{\sigma'} (\mathbf{m}_{l,l-\delta_x} \cdot \boldsymbol{\sigma})_{\sigma\sigma'} \left(c_{l+\delta_x,\sigma}^\dagger c_{l\sigma} - c_{l\sigma}^\dagger c_{l-\delta_x,\sigma'} \right) \\ &\quad + \sum_{\sigma'} (\mathbf{m}_{l,l+\delta_y} \cdot \boldsymbol{\sigma})_{\sigma\sigma'} \left(c_{l-\delta_y,\sigma}^\dagger c_{l\sigma} - c_{l\sigma}^\dagger c_{l+\delta_y,\sigma'} \right) \\ &\quad \left. + \sum_{\sigma'} (\mathbf{m}_{l,l-\delta_y} \cdot \boldsymbol{\sigma})_{\sigma\sigma'} \left(c_{l+\delta_y,\sigma}^\dagger c_{l\sigma} - c_{l\sigma}^\dagger c_{l-\delta_y,\sigma'} \right) \right] \end{aligned} \quad (71)$$

When it will come to identify the current on each side of the unit cell, we will have to take into account the displacement δ that is involved in the $c_{l\pm\delta_x,\sigma}^\dagger c_{l\sigma} - c_{l\sigma}^\dagger c_{l\pm\delta_x,\sigma'}$. This has to be consistent with what we already did for the hopping term. The meaning is, that each current flowing through one side will be dependent on the spin hopping on both direction of the side's axis. It will become clear in the next section.

Side currents

Each unit cell were introduced as a square. We can from the last derived equation identify the contribution of the current on each side of the cell. We have a side on each axis direction $+x, +y, -x, -y$ as introduced in Eq. 69. Due to the symmetric properties of the current, we can abstract the notation for $r \in \{x, y\}$. Using Eq. 70 and Eq. 71 we can write the current on each side r as follows. We as well reintroduce the minus of every summand of the Hamiltonian (due to their attractive nature) we let aside for the commutator relations. Multiplied with the minus one from the Heisenberg picture, we obtain a positive expression. Further, taking $i = -1/i$ we get:

$$(I_i^{\pm r})_{hop} = -\frac{t}{2i} \sum_{\sigma} c_{i\pm\delta_r,\sigma}^\dagger c_{i\sigma} - c_{i\sigma}^\dagger c_{i\pm\delta_r,\sigma} \quad (72)$$

$$(I_i^{\pm r})_{AM} = -\frac{1}{2i} \sum_{\sigma\sigma'} c_{i\pm\delta_r,\sigma}^\dagger c_{i\sigma} (\mathbf{m}_{i,i\mp\delta_r} \cdot \boldsymbol{\sigma})_{\sigma\sigma'} - c_{i\sigma}^\dagger c_{i\pm\delta_r,\sigma'} (\mathbf{m}_{i,i\pm\delta_r} \cdot \boldsymbol{\sigma})_{\sigma\sigma'} \quad (73)$$

In this sense the hopping and altermagnetic term are very similar from nature. However, the altermagnetic term is scaled by the hopping amplitude t on each summand, which shows a spin-dependent behaviour.

We're not quite finished. The way we defined the matrix element, is to be isotropic on each axis. By doing so we can assume that $(\mathbf{m}_{i,i-\delta_r} \cdot \boldsymbol{\sigma})_{\sigma\sigma'} = (\mathbf{m}_{i,i+\delta_r} \cdot \boldsymbol{\sigma})_{\sigma\sigma'}$ so that:

$$(I_i^{\pm r})_{AM} = -\frac{1}{2i} \sum_{\sigma\sigma'} (\mathbf{m}_{i,i+\delta_r} \cdot \boldsymbol{\sigma})_{\sigma\sigma'} \left(c_{i\pm\delta_r,\sigma}^\dagger c_{i\sigma} - c_{i\sigma}^\dagger c_{i\pm\delta_r,\sigma'} \right). \quad (74)$$

Total currents

Until now, we are able to describe how the current flows through each faces of the unit cell. For this we can simply split the term we derived. From this we now aim to derive the current flows on each axis. This can easily be done assuming that the current flowing in the $-x$ direction subtracted from the current in the positive x direction forms the total current in e_x . From this we get for $r \in \{x, y\}$:

$$I_i^r = I_i^{+r} - I_i^{-r}.$$

The real current that we can measure can be obtained by taking the quantum expectation value and the thermal average of the currents. Further we also introduce the BdG-transformed operators with the eigenvalues at Eq. 65 and 66.

For the sake of readability we are going to stick with this r -notation. Due to the linearity of the commutator one can split the current in different terms. We first start with the derivation of the physical current that comes from the hopping term.

$$\langle I_i^r \rangle_{\text{hop}} = \frac{t}{2i} \left[\sum_{\sigma} \langle c_{i-\delta_r, \sigma}^{\dagger} c_{i\sigma} \rangle - \langle c_{i\sigma}^{\dagger} c_{i-\delta_r, \sigma} \rangle - \langle c_{i+\delta_r, \sigma}^{\dagger} c_{i\sigma} \rangle + \langle c_{i\sigma}^{\dagger} c_{i+\delta_r, \sigma} \rangle \right].$$

After introducing the BdG-transformed operators we obtain for the first term:

$$\begin{aligned} \langle c_{i-\delta_r, \sigma}^{\dagger} c_{i\sigma} \rangle &= \sum_{n, m \in \mathcal{N}_+} u_{n, i-\delta_r, \sigma}^* u_{ni\sigma} \underbrace{\langle \gamma_n^{\dagger} \gamma_m \rangle}_{\delta_{mn} f(E_n)} + u_{n, i-\delta_r, \sigma}^* v_{mi\sigma}^* \underbrace{\langle \gamma_n^{\dagger} \gamma_m^{\dagger} \rangle}_0 \\ &\quad + v_{n, i-\delta_r, \sigma} u_{mi\sigma} \underbrace{\langle \gamma_n \gamma_m \rangle}_0 + v_{n, i-\delta_r, \sigma} v_{mi\sigma}^* \underbrace{\langle \gamma_n \gamma_m^{\dagger} \rangle}_{\delta_{mn} (1-f(E_n))}. \end{aligned}$$

In the same way, we obtain for the other terms:

$$\begin{aligned} -\langle c_{i\sigma}^{\dagger} c_{i-\delta_r, \sigma} \rangle &= - \sum_{n \in \mathcal{N}_+} u_{ni\sigma}^* u_{n, i-\delta_r, \sigma} f(E_n) + v_{ni\sigma} v_{n, i-\delta_r, \sigma}^* (1 - f(E_n)), \\ -\langle c_{i+\delta_r, \sigma}^{\dagger} c_{i\sigma} \rangle &= - \sum_{n \in \mathcal{N}_+} u_{n, i+\delta_r, \sigma}^* u_{ni\sigma} f(E_n) + v_{n, i+\delta_r, \sigma} v_{ni\sigma}^* (1 - f(E_n)), \\ \langle c_{i\sigma}^{\dagger} c_{i+\delta_r, \sigma} \rangle &= \sum_{n \in \mathcal{N}_+} u_{ni\sigma}^* u_{n, i+\delta_r, \sigma} f(E_n) + v_{ni\sigma} v_{n, i+\delta_r, \sigma}^* (1 - f(E_n)). \end{aligned}$$

Here we can recognize a very useful relation that is going to simplify everything. We have $\langle c_{i\pm\delta_r, \sigma}^{\dagger} c_{i\sigma} \rangle = \langle c_{i\sigma}^{\dagger} c_{i\pm\delta_r, \sigma} \rangle^*$. We can then recall a useful relation that we can use in these expressions. Having z a complex we obtain $\mathcal{I}m(z) = \frac{1}{2i}(z - z^*)$. Further $\mathcal{I}m(z) + \mathcal{I}m(z') = \mathcal{I}m(z + z')$. The blue tones in the upper equations help to identify the z and z^* pairs. After summing up the terms we obtain the following expression for current of the hopping term along the axis r :

$$\begin{aligned} \langle I_i^r \rangle_{\text{hop}} &= t \cdot \mathcal{I}m \left[\sum_{\sigma} \sum_{n \in \mathcal{N}_+} f(E_n) u_{ni\sigma} (u_{n, i-\delta_r, \sigma}^* - u_{n, i+\delta_r, \sigma}^*) \right. \\ &\quad \left. + (1 - f(E_n)) v_{ni\sigma}^* (v_{n, i-\delta_r, \sigma} - v_{n, i+\delta_r, \sigma}) \right]. \end{aligned} \tag{75}$$

Inside the altermagnet we add the following term using the same derivation method. The matrix element $(\mathbf{m}_{i, i+\delta_r} \cdot \boldsymbol{\sigma})_{\sigma\sigma'}$ is a constant regarding the states-brackets. In this sense, the quantum expectation and thermal average leave this quantity unchanged. Finally, we obtain the exact same result than a t hopping but with a prefactor. This is consistent with the observation already made.

$$\langle I_i^r \rangle_{\text{AM}} = \frac{1}{2i} \sum_{\sigma\sigma'} (\mathbf{m}_{i, i+\delta_r} \cdot \boldsymbol{\sigma})_{\sigma\sigma'} \left[\langle c_{i-\delta_r, \sigma}^{\dagger} c_{i\sigma} \rangle - \langle c_{i\sigma}^{\dagger} c_{i-\delta_r, \sigma'} \rangle - \langle c_{i+\delta_r, \sigma}^{\dagger} c_{i\sigma} \rangle + \langle c_{i\sigma}^{\dagger} c_{i+\delta_r, \sigma'} \rangle \right]$$

which after using the same derivation method as before yields:

$$\begin{aligned}
\langle I_i^r \rangle_{\text{AM}} = \frac{1}{2i} & \left[\sum_{\sigma\sigma'} (\mathbf{m}_{i,i+\delta_r} \cdot \boldsymbol{\sigma})_{\sigma\sigma'} \right. \\
& \sum_{n \in \mathcal{N}_+} f(E_n) \left[u_{ni\sigma} (u_{n,i-\delta_r,\sigma}^* - u_{n,i+\delta_r,\sigma}^*) + u_{ni\sigma}^* (u_{n,i+\delta_r,\sigma'} - u_{n,i-\delta_r,\sigma'}) \right] \\
& \left. + (1 - f(E_n)) \left[v_{ni\sigma}^* (v_{n,i-\delta_r,\sigma} - v_{n,i+\delta_r,\sigma}) + v_{ni\sigma} (v_{n,i+\delta_r,\sigma'}^* - v_{n,i-\delta_r,\sigma'}^*) \right] \right]. \quad (76)
\end{aligned}$$

6 Simulations and results



In the last chapters we introduced the theoretical background of superconductivity and altermagnets. The goal of this thesis is to use numerical methods to solve self-consistently the superconductive gap. We remind here that the code is available publically on a GitHub repository at <https://github.com/Tamwyn001/Thesis>.

6.1 Methodology

We are going to simulate the s-wave superconductivity in a two-dimensional lattice, in a superconductor and a junction of a superconductor and an altermagnet. The orientation of the interface can play some role in the behaviour of the superconducting gap, which makes the study of a straight and diagonal interface a case of study of particular interest. Further we will illustrate how the phase gradient of the gap can induce a current in the superconductor. The shape of the d-wave gap parameter is also of interest. However, we missed the time to make a comprehensive study of it. The Josephon effect in a superconductor-altermagnet-superconductor (SC-AM-SC) trilayer is in the code as well but need to be reworked.

The repository contains the Matlab code (.m) used to generate the data in the form of (coordinate, value) files (.dat). Gnuplot scripts (.gp) allow us to produce some plots that we can then directly link to the Latex source code of this thesis. Finally, some PowerShell scripts (.ps1) automate the gnuplot-latex process.

The Matlab code contains two important files. The system.m file is a class that describes which material we are using for the lattice, the physical context like the temperature and the chemical potential as well as the use or not of periodic boundary conditions. It contains also the Hamiltonian of the system and keeps track of all lattice sites.

The LatticeSites.m describes the position of a lattice sites, stores its neighbours and monitor the lattice site specific physical quantities. For instance, these can be the superconducting gap or the current.

We introduced earlier the need of a self-consistent solution for the gap to correctly describe the Hamiltonian. This is achieved in the GapEquation.m file which is the main script we run. We start with a guess for Δ_i and introduce it in the Hamiltonian. This guess can depend on the material, or the site if we aim to introduce some phase shift at specific locations. We then derive a new site-dependent value using Eq. 68 for all site and reinsert it into the Hamiltonian. This requires to compute the eigenvectors and values of the Hamiltonian. This loop will be performed until the difference of each gap with its previous value reaches a variable threshold. We then have a proper Hamiltonian and can start to derivate some values of interest, like the current.

Matlab is a program that works well with matrices, so the choice was preferred during the prototyping. However, later in the process, the fact that Matlab works by values and not by reference made quite some complications. Instead of passing a reference to location a variable is stored at, we just copy it and pass it over. Here is an example: We have for each sites up to four neighbours. When computing the current divergence, we need the current of the neighbours. If we were to use reference method, then the lattice sites will be fixed defined in the memory, and we can read it from all the places. However since we work by values, we need to send the values in each copy of the site. So we have an array storing the lattice sites in the system, and another for each lattice point storing its neighbours. However, these sites *are the same entities*. Working by value means we need to set explicitly the value everywhere a site is stored. Working by reference would have just need to set the value where the site is stored in the memory, allowing all the references that points to this location being implicitly updated. In this sense a wiser choice would have been C++ with an appropriated diagonalization library.

The site coordinate is stored as (x, y) -tuple as well as an index i that iterates over y -row and then starts again at the beginning of the next row. This means that with different boundary

conditions we get the following shape for the system:

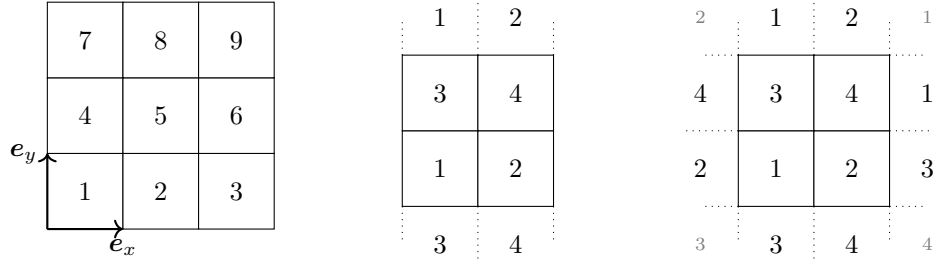


Figure 13: The sites indexing method as well as a representation of the different boundary conditions.

On the left, we have a 3×3 -system. The others are 2×2 with vertical periodic boundary conditions (PBC) and on the right with both vertical and horizontal PBC.

Mathematical definition of PBCs

We have a rectangular lattice of size $N_x \times N_y$. The quantities have to be the same on both side of the system along the axis having these PBC. Here we have vertical periodic boundary conditions. This means that the quantities have to be the same on the top and the bottom of the system. If we describe the system with a wavefunction $\Psi(x, y)$, we then have:

$$\Psi(x, y) = \Psi(x, y + N_y) \quad \forall x \in \llbracket N_x \rrbracket, \forall y \in \llbracket N_y \rrbracket \quad (77)$$

This leads to a finite number of possibilities for the Fourier transform of the wavefunction, as we are going to show in Sec. A.2.

We want to maximize the definition of the gap in the lattice. With the architecture we have (Intel i7 11th gen, 8 GB RAM), an upper bound of $40 \times 20 = 1200$ sites was achieved. Matlab being an interpreter, this could be optimized by using a compiled language. In the literature we find square lattices of 100×100 sites being used [45]. We compute with a convergence threshold of 1.0×10^{-3} .

Here we diagonalize $(-\check{H})$ in $H = E_0 + \frac{1}{2}\check{c}^\dagger(-\check{H})\check{c}$, use the positive eigenvalues and associated eigenvectors. Moreover, $\langle \gamma_n^\dagger \gamma_n \rangle = f(E_n)$. We already subtracted the chemical potential in E_n such that, with $k_B = 1$, we have $f(E) = \frac{1}{\exp(E/T)+1}$. The temperature is 0.001 K.

6.2 Results

We start with the simplest system, a superconductor involving some vertical periodic boundary conditions. We use an attractive potential of $U = -2$ eV for the on site superconductivity in the superconductor and zero everywhere else. The chemical potential is given in eV

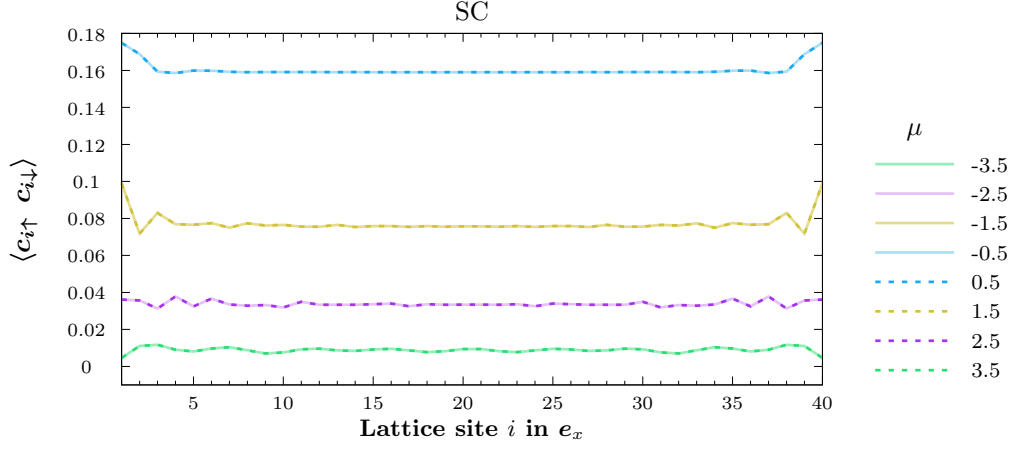


Figure 14: The expectation value of the c operators taking part into the gap as $\Delta_i = U_i \langle c_{i\uparrow} c_{i\downarrow} \rangle$. The vertical periodic boundary condition makes the results on each site on the same x -coordinate being the same. We can then form an average on each of these y -slices and plot the result.

The superconducting gap lies around $0.01 \cdot U$ and $0.16 \cdot U$ for the range of selected chemical potentials. Further we observe a clear symmetry in the Cooper pairs distribution around the level $\mu = 0$. The overlap of the Fermi surface with the s -wave seams to be the same for $\pm\mu$ (see Fig. 15). In fact if the accessible states are also found where the superconducting gap is defined, we expect the electrons to be more likely to bind into Cooper pairs.

Further we observe some oscillations on the left and right sides that are well-defined over three to four sites towards the bulk. On these locations the sites have only three neighbours, there are open boundaries, the rest is vacuum. One can see this lack of neighbours as impurities in the system. A first interpretation can be given by the Friedel oscillations [46]. The boundary disturbs the electron density and causes decreasing oscillations towards the bulk. The Cooper-pairs being made of electrons, these oscillations are reflected in the gap as well. Another contribution to the oscillations is the reflection of the quasiparticles. These oscillations may be caused by Andreev bound states [47], that may form because the quasiparticles are reflected at the boundary. These can interfere with the Cooper pairs and cause the oscillations in the spacial representation of the energy gap.

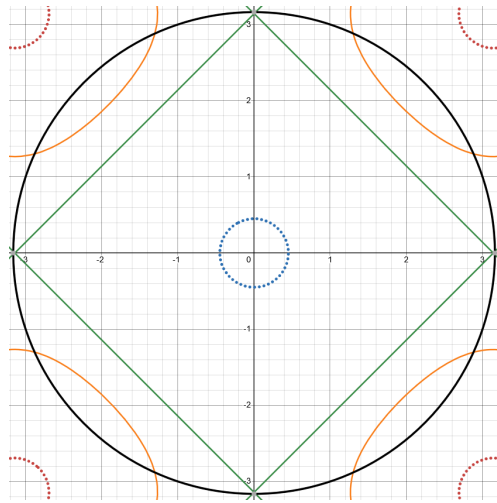


Figure 15: The first Brillouin zone with the Fermi surface for μ of -3.8 , 0 , 1.4 and 3.8 . The BCS gap is represented by the black circle. Its size is given such that we can see that at a $\mu > 0$ the states that can be found in the gap are less present until they vanish for a high μ . For low μ there is not many states accessible to fill the gap as well. The figure was made with Desmos.

In the simulation the size of the gap is such, that the Fermi surface covers the same area of the gap representation in reciprocal space for $\pm\mu$. A maximum around $\mu = 0$ is expected as the Fermi surface is the largest there.

From this we can consider a proximity system by adding a different material on the right side of the superconductor. The most simple one is a normal metal (N) that has a hopping t of 1 in every direction. Then we can replace it with an alternating hopping $t + m$ depending on a $\uparrow\uparrow$ interaction and a $t - m$ depending on a $\downarrow\downarrow$ interaction. If this hopping takes place in every direction, this describes a ferromagnetic material (FM). Making the sign of m alternating if we have a hopping along the x or the y axis describes an altermagnet (AM). Here we set $m = 0.5$ and study different results for the chemical potential $\mu < 0$ and compare the AM with the others. * represents a placeholder for the material a curve describes.

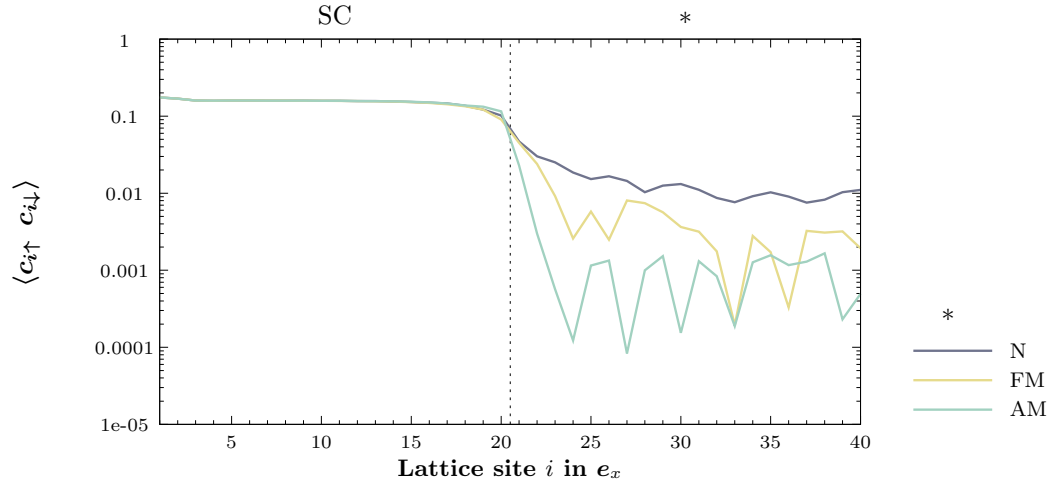


Figure 16: Evolution of the gap in the x direction for a junction of SC-N, SC-FM and SC-AM at $\mu = -0.5$. Hopping $m = 0.5$.

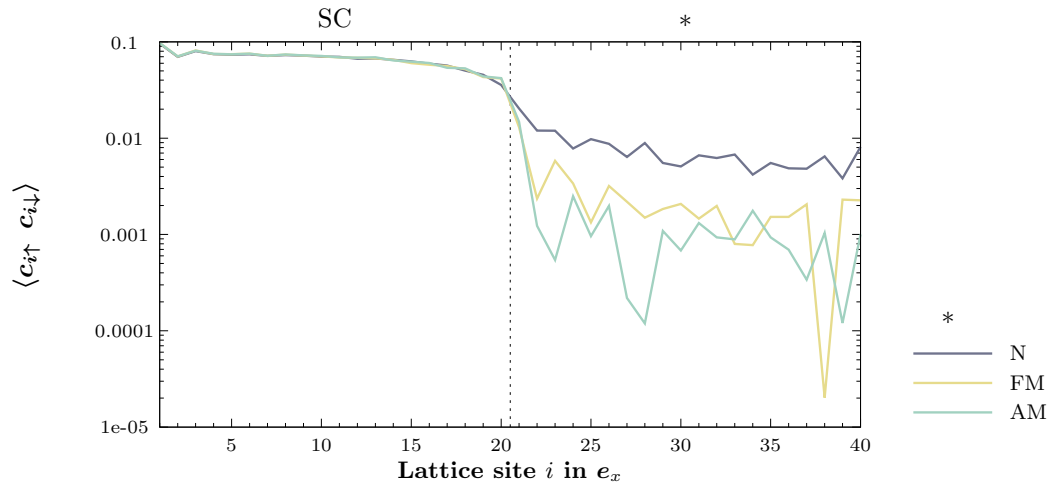


Figure 17: A junction of SC-N, SC-FM and SC-AM at $\mu = -1.5$, and a hopping $m = 0.5$.

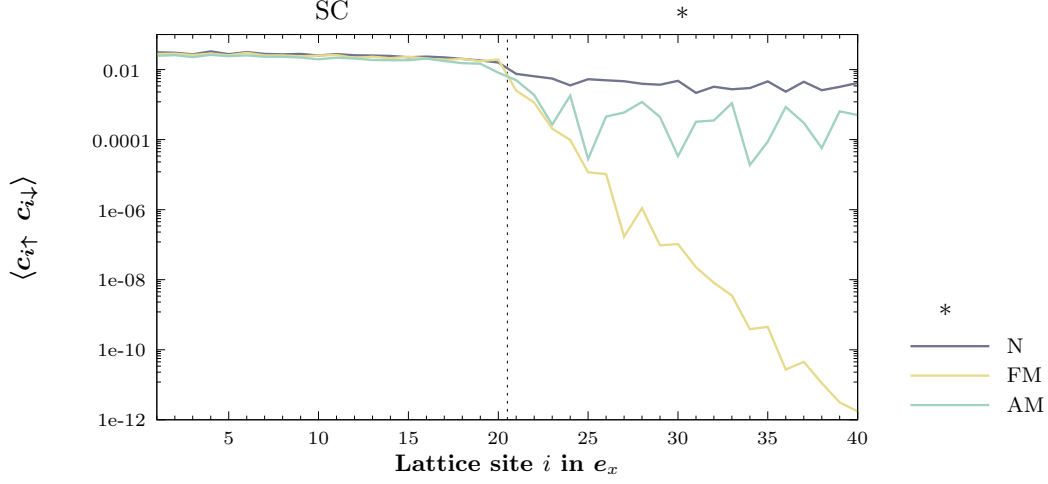


Figure 18: A junction of SC-N, SC-FM and SC-AM at $\mu = -2.5$, and a hopping $m = 0.5$.

We first take a look at the superconductor (SC). Inside it the gap is not be the same for $\mu = -0.5, -1.5$ and settles around $0.1 \cdot U$. Most likely the increase of the Fermi surface do not give an additional contribution to the gap. The gap is however one order of magnitude smaller for $\mu = -2.5$. Here the withdrawal of the Fermi surface is more relevant and the gap becomes smaller.

We have a clear decay of the gap after entering the normal metal (N). At this point, studies that were already made tend to have an exponential decay of the gap [45]. Having a logarithmic scale we would expect a more linear behaviour, but this is still a reasonable exponential decay. Another way to approach the line would be to increase the resolution of the lattice, as well as simulating a more squared one. This decay makes the expectation value results in a difference of an entire order of magnitude from one side to the other of the N. For the smallest μ we see that the decay is weaker, the gap lost half of its amplitude after crossing the N. Further we see that both the FM and the AM add some oscillations in the decay.

The ferromagnet follows closely the normal metal for $\mu = -0.5, -1.5$. It is interesting to note a clean exponential decay when having a chemical potential of -2.5 modulated by oscillations. We observe about the same number of oscillations and about of the same amplitude in these three cases. In the AM the initial decay is stronger in the sites near the interface than in the FM. Then the decay seems to follow the FM. We observe about the same number of oscillations in the FM and the AM. For $\mu = -0.5$ we observe a clean line in the first four sites of the AM. Then we have oscillations and the Cooper-pairs are more present than expected regarding the initial decay. The reason might be that the first oscillation combined with the initial decay make the line reach it's second-deepest point (around 10^{-4}) and therefore everything looks more flat.

In the AM the oscillation amplitude increases with a decreasing $|\mu|$. We observe nearly two orders of magnitude in their amplitude for $\mu = -0.5$ compared to one order of magnitude for $\mu = -2.5$. We tried to simulate these for a $\mu = -3.5$ but the algorithm converge to values that are numerically zero everywhere (10^{-16}). It looks like the Fermi-surface is too small and there is a lack of electrons to build the Cooper pairs.

These oscillations are more likely due to the fact that we have a spin-dependent hopping. In fact, we have the same behaviour for the AM and the FM, but not in the N. As a result of the spin-splitting Fermi surfaces the electrons in the Cooper pairs have different momenta. This phenomenon causes the superconductivity correlation in the FM to oscillate [48]. A similar behaviour happens inside the AM.

This dynamic influences the gap, and the different components of the gap interfere with each other, resulting periodically in especially low values. We see that the direction-dependence of the antiferromagnetic hopping causes a weaker gap and oscillations of bigger amplitudes. Traces of Friedel oscillations and quasiparticles' reflections are still visible, especially in the non-SC materials.

We now want to simulate the behaviour of the s -wave superconductivity on a diagonal

interface. We focus on three different values of $\mu < 0$. The diagonal is build by rotating the interface by 45° around the centre of the lattice. The upper-part, regarding the y -axis is the SC and the lower one the AM. We set $m = 0.5$.

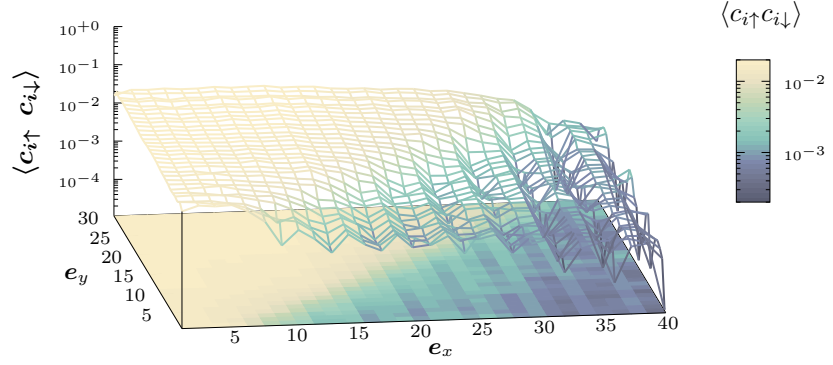


Figure 19: Diagonal interface of a SC and an AM at $\mu = -2.5$.

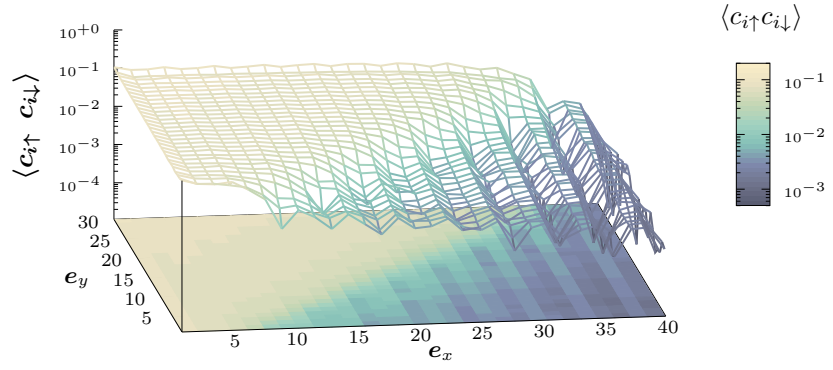


Figure 20: Diagonal interface of a SC and an AM at $\mu = -1.5$.

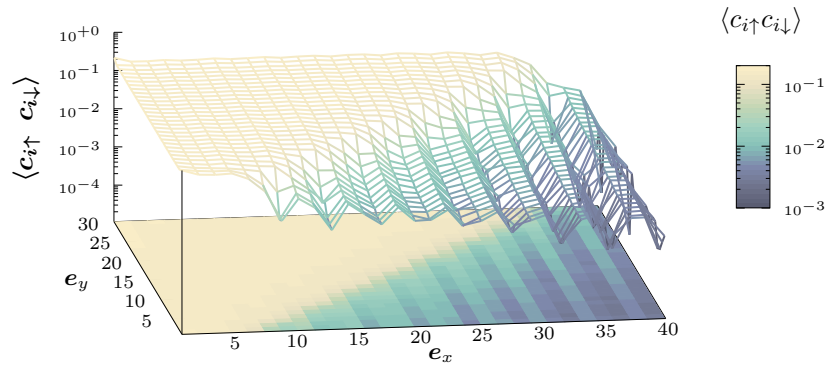


Figure 21: Diagonal interface of a SC and an AM at $\mu = -0.5$.

The superconductivity fills uniformly the superconductor. Consistent with the previous observations (Fig. 16, 17 and 18) its magnitude grows, while $|\mu|$ get closer to zero.

Once again the oscillating exponential decay is present. We count up to eight oscillations for the three cases of study, whose frequency is around three sites in all configurations. The oscillations take only place along the x axis but the exponential decay seems to point along the normal of the interface, making the $(40,0)$ region the less populated in Cooper pairs. The lower $|\mu|$, the less noise we observe in the plots. Similarly to the straight interface the decay is strong in the begging and then slows down when approaching the farthest regions from the interface.

If we try to find the line for a given y that has the same site length in the AM in the straight interface case, we can pick one the at $y = 15$. There we count the same number of oscillations in the AM than in the straight interface case. In fact at $y = 1$ we see that the AM was extended, and at $y = 30$ that the AM was shortened. This gives the room to more oscillations to happen in the first case, and less in the second one. The profile of the oscillations *along the x axis* is the same as in the straight interface case.

As before, this increase in Cooper pairs formation with decreasing $|\mu|$ is due to the shape of the Fermi surface. Considering only the SC, we see an increase of an order of magnitude between $\mu = -2.5$ and $\mu = -1.5$. On the other hand we only count a doubling of the Cooper pairs from $\mu = -1.5$ and $\mu = -0.5$. As before the majority of the newly accessible states provided by $\mu = -0.5$ are outside the s -wave range. This yields to a smaller increase in the number of Cooper pairs when compared to the first case.

We know that the Cooper pairs leak from the SC. It is reasonable to state that they can leak in every direction from a site on the interface. Due to interferences between them, we can expect to have a net diffusion along the normal of the interface. By doing so the leaking that we see should take place along the $(1, -1)$ axis: The leaking goes through the oscillations along the normal. This results in more spread oscillations than in the straight interface case for the same travel length.

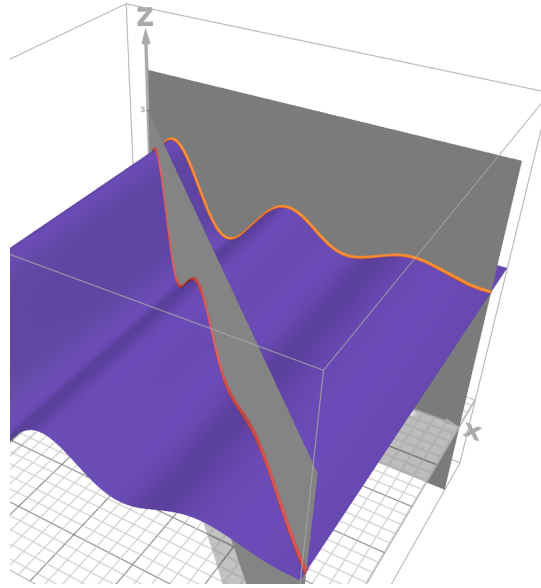


Figure 22: An arbitrary oscillating exponential decay in the x -direction. Going these oscillations along x or along the diagonal $(1, -1)$ axis results in different experienced oscillations for the same travel length. The plot was made with Desmos.

Towards simulating the Josephson junction we can represent the current in the superconductor. We know that the current is proportional to the phase gradient of the superconducting gap [49]. We can experimentally apply a voltage difference between the two sides of the superconductor to induce a phase gradient [49]. To simulate this we will hold the phase fixed on the sides maintaining a difference of 117° between the two sides. We start this gradient at two different angles $\varphi_0 = -2\pi/3$ and $\varphi_0 = \pi/3$ on the left side. To let the plot be more readable, we reduce the size of the system to 30×15 sites being used. We will study the current for

different chemical potentials.

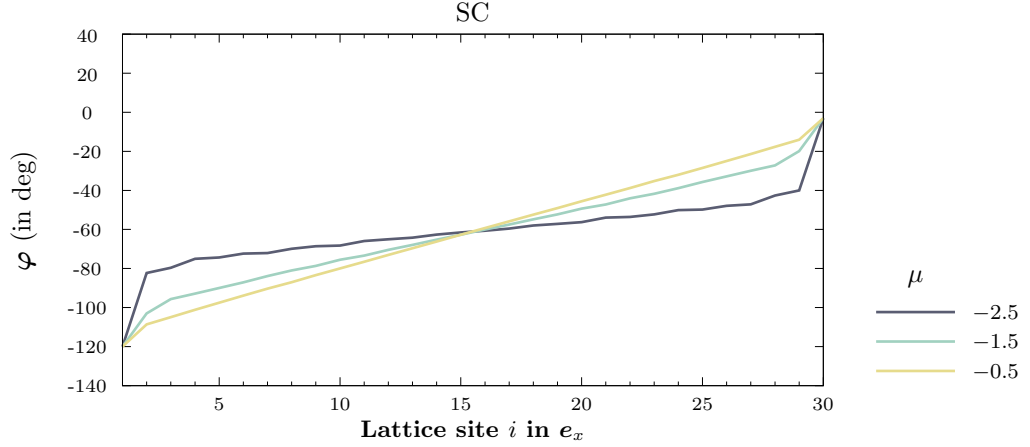


Figure 23: Progression of the complex phase of the gap in a 30 sites long SC for multiple chemical potentials. A phase on side $\varphi_0 = -2\pi/3$ and gradient of 117° .

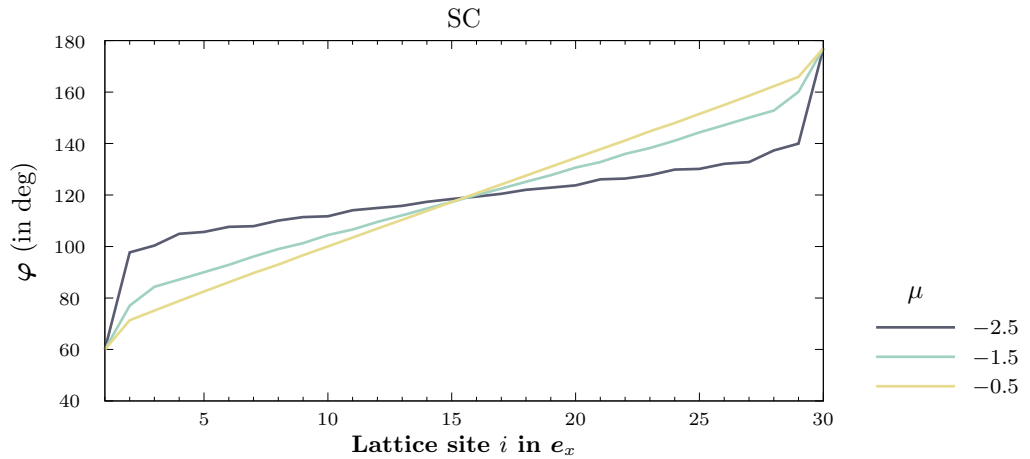


Figure 24: The complex phase of the gap in a 30 sites long SC. A phase on side $\varphi_0 = \pi/3$ and gradient of 117° .

We see that the profile of the curve is the same regardless the starting phase. The slope of the gradient increases with a falling $|\mu|$. Having the sides artificially fixed in the phase causes abrupt changes in the phase on the sides. However, when skipping the first three sites from the sides, we see that the self-consistent algorithm achieves a smooth transition.

The slope is related to the number of Cooper pairs present in the system. It looks like the pairs can not have a strong phase difference between each other. When we have more of these, they can arrange themselves to produce a strong slope in the gradient, while keeping a not to large difference between the neighbours. In this sense, fewer pairs means that the gradient will not be strong compared to a system with more pairs.

The algorithm makes the phase distribution centred around the mean value of the gradient. Then it draws the line with the respective slopes. This may yield to a strong change of the phase on the sides because we fixed the phase there, and the slope might not be sufficient to reach the values on the sides. We observe some noise in the phase gradient of the gap for $\mu = -2.5$. The small resolution of the system might make the algorithm converge to a less accurate result. At this chemical potential the electron filling is not very high as well. This results in less Cooper pairs and a less accurate phase gradient.

μ (in eV)	-2.5	-1.5	-0.5
Slope (in deg/site)	1.2726	2.6961	3.4564

Table 1: The slopes of the phase gradient for different chemical potentials.

We see that the difference in the slope between $\mu = -2.5$ and -1.5 is weaker than between $\mu = -1.5$ and -0.5 . As discussed earlier this is a proof that the extension of the Fermi surface does not bring a lot of additional states to contribute to the gap.

Now we can plot the spacial representation of the current in the superconductor with the different phase gradient produced above. We remember that we use vertical boundary conditions.

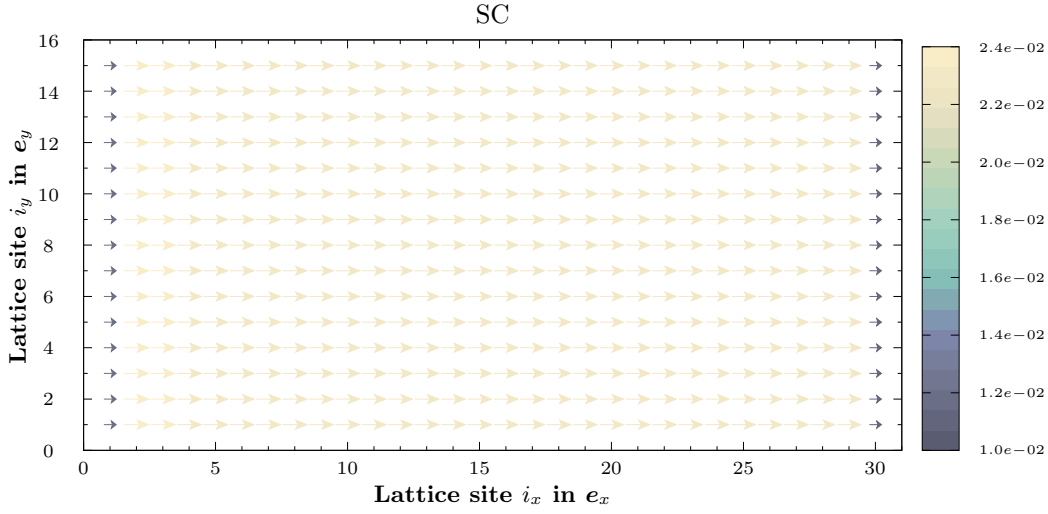


Figure 25: Current from a phase gradient of 117° at $\mu = -0.5$.

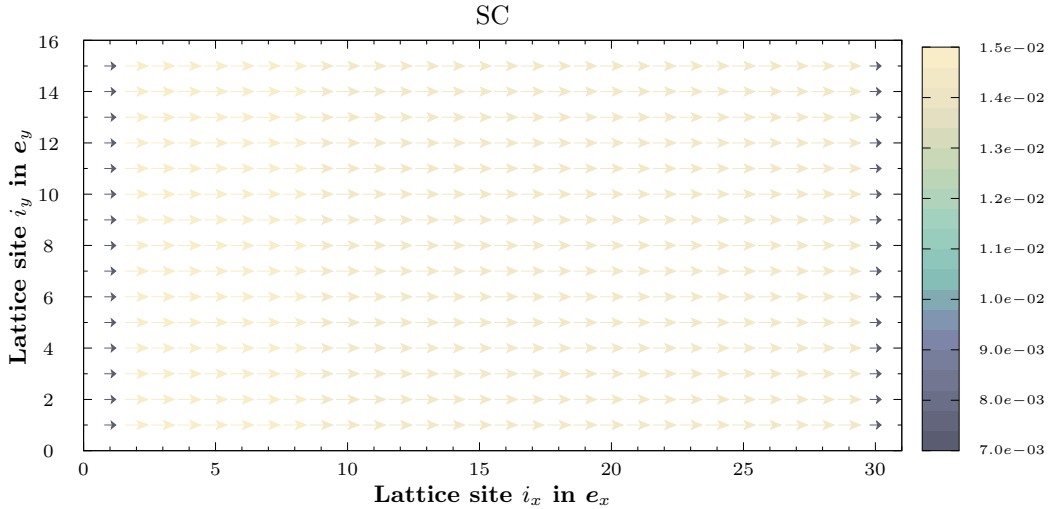


Figure 26: Current from a phase gradient of 117° at $\mu = -1.5$.

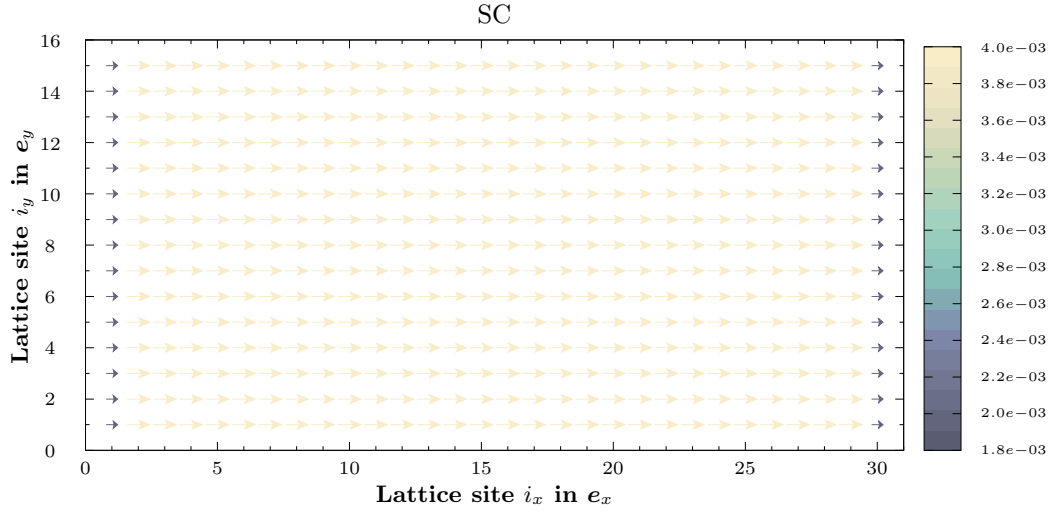


Figure 27: Current from a phase gradient of 117° at $\mu = -2.5$.

μ (in eV)	-2.5	-1.5	-0.5
Current (arb. unit)	0.004	0.015	0.023

Table 2: Average value of the current in the sites $i_x \in [2, 29]$ for different chemical potentials.

First, we observe a uniform current along the y direction. This is due to the vertical periodic boundary conditions. Because the values on the sides are much lower than the almost uniform ones in the middle, the plot looks bicolour. We see that the current is very much related to the slope of the gradient, as it should be. The abrupt changes described in Figs. 23 and 23 causes low values in the current on the sides of the system. The current in the middle is ten times stronger with a μ of -1.75 than with a μ of -2.75 . There are three orders of magnitude of difference between the current strength in $\mu = -1.75$ and -3.75 . The behaviour $I \propto \nabla\varphi$ [49] is nevertheless verified.

One last measurement to perform is the current continuity. No charges should be generated or lost. This of course doesn't apply on the sides where we artificially fix the phase. Taking a function f discretized on sites i we have $\partial_x f = (f_{i+1} - f_{i-1})/2a$, $\partial_y f = (f_{i+N_x} - f_{i-N_x})/2a$ with a the lattice spacing. We know that we normalized the lattice spacing to 1. Finally, we have $\nabla f = (\partial_x + \partial_y)f$ as the divergence of f .

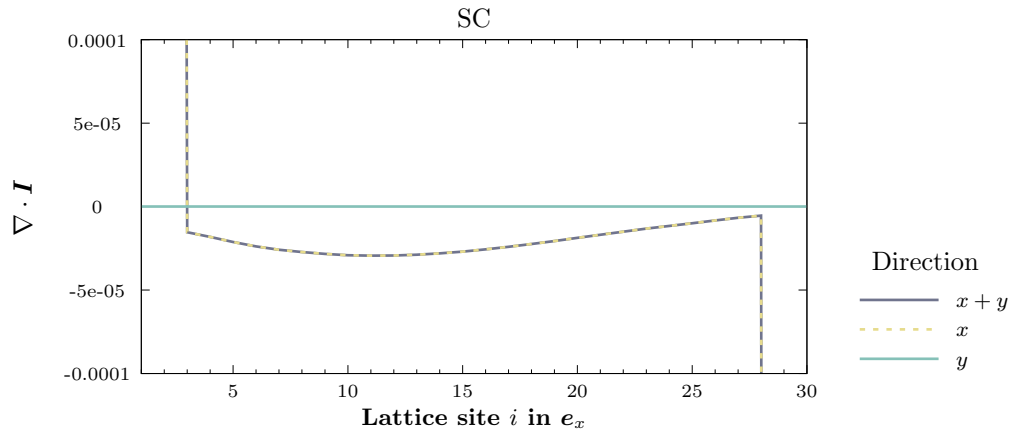


Figure 28: Continuity of the current from a phase gradient of 117° at $\mu = -0.5$. In both x and y direction as well as the total continuity.

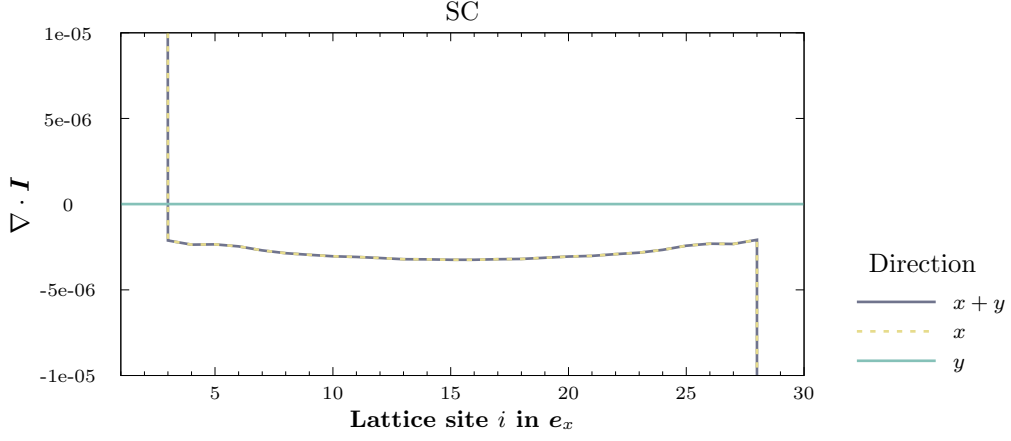


Figure 29: Continuity of the current from a phase gradient of 117° at $\mu = -1.5$. In both x and y direction as well as the total continuity.

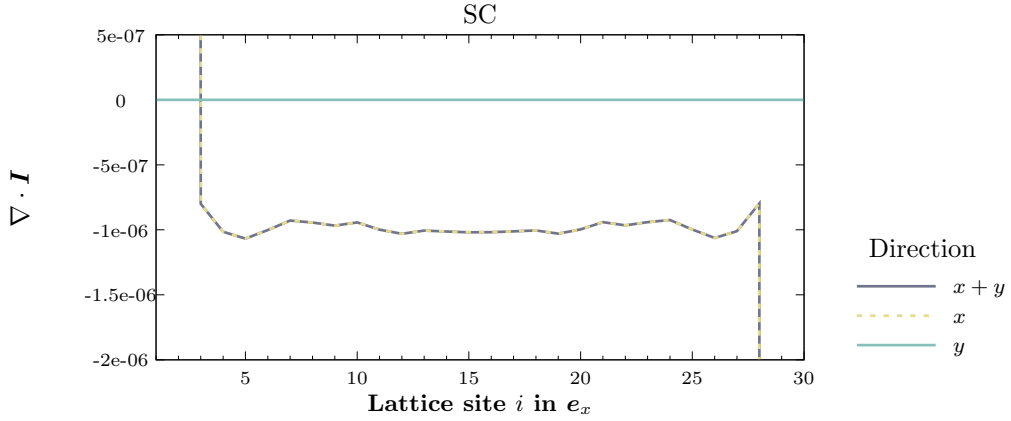


Figure 30: Continuity of the current from a phase gradient of 117° at $\mu = -2.5$. In both x and y direction as well as the total continuity.

We see that the total discontinuity is always three orders of magnitude smaller than the current itself. The current along the y -axis has no contribution to the total divergence. This is a result of the vertical periodic boundary conditions. The discontinuity is significantly smaller than the current, and we can assume that this one is conserved. Once again a smaller convergence threshold, as well as an increase in the lattice definition would make the discontinuity even smaller. We see that the x -component of the current is the one the less conserved. This fact is a direct result of the artificially fixed phased.

Far from the bulk, on the two first and last site, we observe cliff effects. This is due the abrupt changes in the phase we presented above. The first cliff is positive, and the second one is negative.: Considering the derivation we defined above, if the site $i + 1$ has a stronger current than the site i , then $\partial_x I > 0$. On the other hand for the last five sites we have $\partial_x I < 0$ due to $I_{i+1} < I_i$. Here the current difference involved displays two to three orders of magnitude. On the first and last site there is a discontinuity due to the missing neighbours. For the second and one before the last sites, there is a sudden change in the current between sites two and three, as well as between the last and the one before the last site.

6.3 Conclusion and outlook

We have seen that the BCS superconducting gap is influenced by the Fermi surface. The gap is the largest when the Fermi surface is the largest. The gap is also influenced by the presence

of interfaces. We observe oscillations in the gap near the open boundaries, which are due to the reflection of the quasiparticles with the sides.

Further we studied the leaking of the Cooper pairs in different materials. We observed an exponential decay in a normal metal. This decay is modulated by oscillations that are due to the spin-dependent hopping in both the ferro- and altermagnet. Due to the axis-dependence of the hopping, the oscillations are stronger in the altermagnet than in the ferromagnet. Adding a diagonal interface to the system, we observed the same exponential decay and oscillations. The oscillations are more spread when considering the leaking of the Cooper pairs along the normal of the interface. This is due to the interference of the leaking Cooper pairs.

Towards the modelling of a Josephon junction with an altermagnetic material, we achieved to represent the current in a superconductor. The current is proportional with the phase gradient of the superconducting gap, and its strength grows with the number of Cooper pairs. Moreover, the current verifies the charge conservation. More work needs to be done to represent the current in the altermagnet between two different superconductors.

d-wave superconductivity was already introduced as being of particular interest. This is a more complex system. As derived in the appendix A, the gap is now a neighbour dependent quantity and is not isotropic in the momentum space. The goal would have been to study the profile of the gap when the Cooper pairs enter along the nodal lines of the gap geometry. This would result in a clear difference when having a straight or diagonal interface. Some work has been done towards studying the proximity effect of a *d*-wave superconductor with the altermagnet. However, due to a lack of time, we only achieved to represent the *d*-wave in a superconductor.

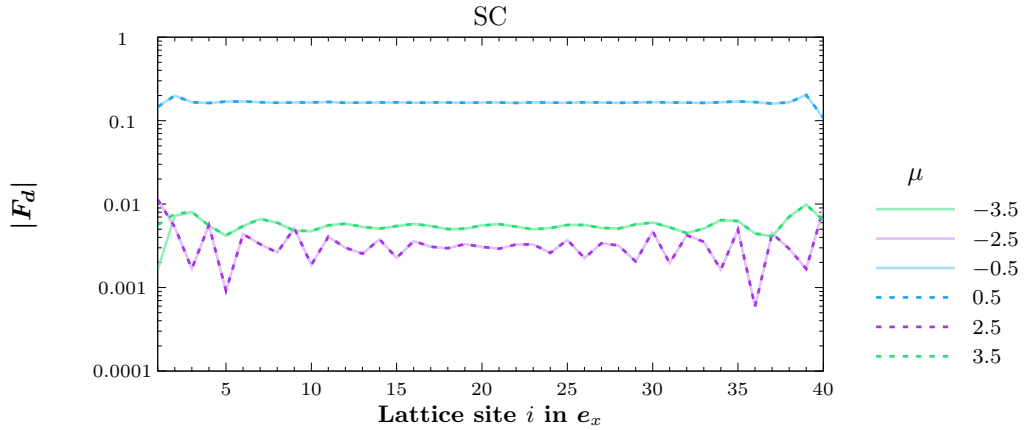


Figure 31: *d*-wave superconductive parameter F_d taking part into the gap $\Delta_{d,i} = V_i F_{d,i}$ for different chemical potential. This parameter is purely real

As we can see the amplitude of the *d*-wave gap is not the same as the conventional BCS gap. We still observe this symmetry around $|\mu|$ for the range of selected chemical potentials in the bulk. However, we have a decrease from ± 3.5 to ± 2.5 before growing towards ± 0.5 . The parameter is weaker for $\mu = \pm 2.5$ and ± 3.5 than the BCS gap but about the same value for ± 0.5 . We see that the Friedel oscillations as well as the presence of bound states still provoke oscillations on the sites near the vacuum.

We see as well that the gap is not symmetric around bulk along the x axis. This might be caused by the oscillations that have different amplitude and frequency for the different chemical potentials.

Appendices

A An unconventional superconductivity



A.1 Site dependent potential

In this section we are going to highlight how the neighbour-dependent potential can lead to a new kind of superconductivity. Among others, we are going to discuss the d -wave superconductivity which shares similarities with more exotic magnets, such as the altermagnet. Indeed, the spatial repartition of the phase of the gap shares a similar geometry with the spin polarization of the altermagnet.

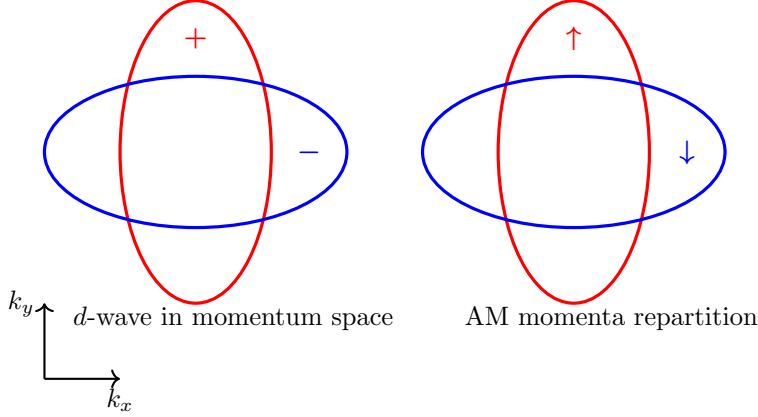


Figure 32: The positive and negative phase of the unconventional d -wave superconductive gap, as well as the spin splitting of the altermagnet in momentum space. The intersection of the lines are called nodes. A line from the centre to the node is called a nodal line. In a proximity system if the Cooper pairs enters the non-superconducting material along the nodal lines, we expect no preferred phase, as it could be if we enter from the left for example. Figure inspired by [17].

The derivations we are going to make are closely based on the work of A. H. Mjøs and J. Linder in [45].

The Hamiltonian being the ground stone of this discussion, we're going to begin with it. It differs slightly from the symmetric one we derived in Eq. 57. This extended version contains a neighbour-depending potential H_V that is going to produce the new superconductive Δ -part of the Hamiltonian. This potential is as well attractive such that $V > 0$, similar to the BCS theory.

$$H = -t \sum_{\langle ij \rangle \sigma} c_{i\sigma}^\dagger c_{j\sigma} - \mu \sum_{i\sigma} c_{i\sigma}^\dagger c_{i\sigma} - \frac{V}{2} \sum_{\langle ij \rangle \sigma} n_{i\sigma} n_{j\bar{\sigma}}. \quad (78)$$

Here the $\bar{\sigma}$ -notation means the opposite spin of σ . In other words the attraction finds only place between particles of opposite spin, mirroring the formation process of Cooper-pairs. We have a factor of one half to avoid counting twice the neighbours.

Trained eyes will recognize that H_V is not quadratic in the creation and annihilation operators which makes the Hamiltonian impossible to write in the BdG-formalism. For this reason we can use the so called Hartree-Fock mean field approximation $H_V \rightarrow H_V^{HF}$ defined as:

$$H_V^{HF} = -\frac{1}{2} \sum_{\langle ij \rangle \sigma} V_{ij} \left(F_{ij}^{\sigma\bar{\sigma}} c_{j\bar{\sigma}}^\dagger c_{i\sigma}^\dagger + \text{h.c.} + |F_{ij}^{\sigma\bar{\sigma}}|^2 \right), \quad (79)$$

involving the pairing amplitude $F_{ij}^{\sigma\bar{\sigma}} = \langle c_{i\sigma} c_{j\bar{\sigma}} \rangle$ that we already introduced. The V_{ij} are the neighbour-depending potential. The last term is a constant energy term, which we can discard during the diagonalization process. If one wanted to compute the free energy this must be included there. From this point simplifications can be made to reach out final Hamiltonian.

Using the fermionic property $[c_{i\sigma}^\dagger, c_{j\sigma}^\dagger]_+ = 0$ we have $c_{i\sigma}^\dagger c_{j\sigma}^\dagger = -c_{i\sigma}^\dagger c_{j\sigma}^\dagger$ which leads to $\langle c_{i\sigma}^\dagger c_{j\sigma}^\dagger \rangle = -\langle c_{i\sigma}^\dagger c_{j\sigma}^\dagger \rangle$. We can use this in the last step of the following simplification:

$$\begin{aligned} H_V^{HF} &= -\frac{1}{2} \sum_{\langle ij \rangle \sigma} V_{ij} \left(F_{ij}^{\sigma\bar{\sigma}} c_{j\bar{\sigma}}^\dagger c_{i\sigma}^\dagger + \text{h.c.} \right) \\ &= -\frac{1}{2} \sum_{\langle ij \rangle} V_{ij} \left(F_{ij}^{\uparrow\downarrow} c_{j\downarrow}^\dagger c_{i\uparrow}^\dagger + F_{ij}^{\downarrow\uparrow} c_{j\uparrow}^\dagger c_{i\downarrow}^\dagger + \text{h.c.} \right) \\ &= -\sum_{\langle ij \rangle} V_{ij} \left(F_{ij}^{\uparrow\downarrow} c_{j\downarrow}^\dagger c_{i\uparrow}^\dagger + \text{h.c.} \right) \end{aligned} \quad (80)$$

Using the relation $F_{ij}^{\uparrow\downarrow} = -F_{ij}^{\downarrow\uparrow}$ and the symmetry of the potential $V_{ij} = V_{ji}$ we can add the two terms up and remove the one half factor. We fix the spins in the pairing amplitude and define $F_{ij} = F_{ij}^{\uparrow\downarrow}$. The Hamiltonian is now ready to be diagonalized but first, we are going to discuss which advantages a Fourier transform of the Hamiltonian could bring us.

In a homogenous material we can consider a lattice and imagine some periodic boundary conditions in all directions. There is a translation invariance. In heterostructures however the material may vary, let's assume without loss of generality, in a direction. As we now, a periodic signal is a good candidate for a Fourier transform, which we can then express in a finite set of coefficient. This is very practical. However, the direction we want to transform on has to show a periodicity. For this reason homogenous two-dimensional lattice involves a Fourier transformation in two space dimensions while a heterostructure we transform only in the direction where the material is the same. For instance a multilayer material in the x -direction can be described by combining a real space description in the x -axis combined to a Fourier transformation in the y -direction. In this thesis we are going to focus ourselves on a multilayer material in the x -direction.

A.2 In the vertical periodic boundary setup

We assume we have a lattice of $N_x \times N_y$ sites. The description of the creation and annihilation operators with a step in the momentum space for the y -direction can be expressed as follows:

$$c_{xy\sigma} = \frac{1}{\sqrt{N_y}} \sum_{k_y} c_{xk_y\sigma} e^{ik_y y} \quad (81)$$

$$c_{xy\sigma}^\dagger = \frac{1}{\sqrt{N_y}} \sum_{k_y} c_{xk_y\sigma}^\dagger e^{-ik_y y} \quad (82)$$

How do we find an expression for k_y ? The periodicity (for example in the c operator) yields $c_{xy\sigma} = c_{x, y+N_x, \sigma}$ this means the following condition must be fulfilled:

$$\begin{aligned} c_{xy\sigma} = c_{x, y+N_x, \sigma} &\Leftrightarrow e^{ik_y y} = e^{ik_y (y+N_y)} \Leftrightarrow e^{ik_y N_y} = 1 \\ &\Leftrightarrow k_y = \frac{2\pi n}{N_y}. \end{aligned}$$

We know that the momentum index should cover the entire first Brillouin zone. This covers the momentum from $-\pi/a$ to π/a where a is the lattice constant. Further due to the $2\pi/a$ periodicity we have the same k_y at $-\pi/a$ and π/a . For this reason we need to map k_y in $[-\pi/a; \pi/a)$. This means we have $n \in [-N_y/2; N_y/2 - 1]$ including 0. For $n = 4$ we then have $k_y \in \{-\pi, -\pi/2, 0, \pi/2\}$.

For the readability we are going to use $k_y \rightarrow k$. Further to an index i can associate (x, y) and to j , (x', y') . We first want to transform the hopping term:

$$H_{\text{hop}} = - \sum_{\langle ij \rangle \sigma} t_{ij} \sum_{kk'} c_{xk\sigma}^\dagger c_{x'k'\sigma} e^{i(k'y' - ky)}$$

Here we can use the neighbour shift properties $y' = y + \delta_y$ where $\delta_y = \pm 1$. Doing so we have

$$e^{i(k'y' - ky)} = e^{i(k'(y + \delta_y) - ky)} = e^{i(k' - k)y} e^{ik'\delta_y}$$

No we need to express the neighbourhood sum. Precisely we have

$$\begin{aligned}
H_{\text{hop}} &= - \sum_{\langle ij \rangle \sigma} t_{ij} \sum_{kk'} c_{xk\sigma}^\dagger c_{x'k'\sigma} e^{i(k-k')y} e^{ik'\delta_y} \\
&= - \sum_{xy\sigma} \sum_{kk'} \left(\underbrace{t_{x,x+1} c_{xk\sigma}^\dagger c_{x+1k'\sigma} e^{ik'\cdot(0)}}_{+x \text{ hopping, no } \delta_y} + \underbrace{t_{x,x-1} c_{xk\sigma}^\dagger c_{x-1k'\sigma} e^{ik'\cdot(0)}}_{-x \text{ hopping, no } \delta_y} \right. \\
&\quad \left. + \underbrace{t_{x,y-1} c_{xk\sigma}^\dagger c_{xk'\sigma} e^{ik'\cdot(-1)}}_{\delta_y=-1} + \underbrace{t_{x,y+1} c_{xk\sigma}^\dagger c_{xk'\sigma} e^{ik'\cdot(1)}}_{\delta_y=1} \right) e^{i(k-k')y}
\end{aligned}$$

As we see the y direction is now expressed in the k -index, which is unique for each lattice y -slice. The information is then conserved. We know that system has different material on the x axis. This means $t_{x,y-1} = t_{x,x} = t_{x,y+1}$ because the material are isotropic in y . Every material has a different hopping term nevertheless. Besides, we can use the following relation $1/N_y \sum_y e^{i(k-k')y} = \delta_{kk'}$. Performing both expression leads after a summation over k' to

$$H_{\text{hop}} = - \sum_{xk\sigma} t_{x,x+1} c_{xk\sigma}^\dagger c_{x+1k\sigma} + t_{x,x-1} c_{xk\sigma}^\dagger c_{x-1k\sigma} + t_{x,x} c_{xk\sigma}^\dagger c_{xk\sigma} (e^{ik} + e^{-ik})$$

And now we can reintroduce an arbitrary second coordinate x' to describe the neighbours.

$$H_{\text{hop}} = - \sum_{xx'k\sigma} t_{x,x'} c_{xk\sigma}^\dagger c_{x'k\sigma} (\delta_{x+1,x'} + \delta_{x-1,x'} + \delta_{x,x'} 2 \cos(k)) \quad (83)$$

The chemical potential term is more easily given. In fact the number operator yields to use two operators $c^\dagger c$ at a same coordinate i .

$$H_\mu = -\mu \sum_{xk\sigma} c_{xk\sigma}^\dagger c_{xk\sigma} e^{i(k-k')y} = - \sum_{xx'k\sigma} \mu c_{xk\sigma}^\dagger c_{xk\sigma} \delta_{xx'} \quad (84)$$

We finally have for the terms involving $c_{xx'\sigma}^\dagger c_{xx'\sigma}$:

$$H_{\text{hop}} + H_\mu = \sum_{xx'k\sigma} \epsilon_{xx'k\sigma} c_{xk\sigma}^\dagger c_{x'k\sigma}$$

using

$$\epsilon_{xx'k\sigma} = -t_{xx'} (\delta_{x+1,x'} + \delta_{x-1,x'}) - (t_{xx'} 2 \cos(k) + \mu) \delta_{xx'}$$

Moving on to the potential term we have to introduce a new notation. The goal is to describe a displacement in a direction from a point. So assuming we follow the indexing introduced in Fig. 13: $i \pm \hat{x} = i \pm 1$ and $i \pm \hat{y} = i \pm N_x$. For the brevity we use $f(a) = V_{ia} F_{ia} c_{a\downarrow}^\dagger c_{i\uparrow}^\dagger$. Still assuming that $V_{ij} > 0$ and that the interaction is attractive, we have:

$$\begin{aligned}
H_V &= - \sum_{\langle ij \rangle} V_{ij} F_{ij} c_{i\downarrow}^\dagger c_{j\uparrow}^\dagger + \text{h.c.} \\
&= - \sum_i f(i-1) + f(i+1) + f(i+N_x) + f(i-N_x) + \text{h.c.}
\end{aligned}$$

We can now insert our Fourier transformation introduced in Eq. 82 and Eq. 81 to obtain

$$\begin{aligned}
H_V &= - \sum_{xy} \frac{1}{N_y} \sum_{kk'} \left(V_{x,x+1} F_x^{x+} c_{x+1,k,\downarrow}^\dagger c_{xk'\uparrow}^\dagger + V_{x,x-1} F_x^{x-} c_{x-1,k,\downarrow}^\dagger c_{xk'\uparrow}^\dagger \right. \\
&\quad \left. + V_{xx} (F_x^{y+} e^{-ik} - F_x^{y-} e^{ik}) c_{xk\downarrow}^\dagger c_{xk'\uparrow}^\dagger \right) e^{-i(k+k')y} + \text{h.c.}
\end{aligned}$$

Defining a more general form for the summand involving two sites i and j :

$$\begin{aligned}
F_{xx'k} &= V_{x,x'} (F_x^{x+} \delta_{x+1,x'} + F_x^{x-} \delta_{x-1,x'} \\
&\quad + (F_x^{y+} e^{-ik} - F_x^{y-} e^{ik}) \delta_{xx'}),
\end{aligned}$$

where we got $k' = -k$ from the sum over the y -direction. We can rewrite the expression of H_V as

$$H_V = - \sum_x \sum_{kk'} F_{xx'k} c_{xk\uparrow}^\dagger c_{x',-k,\downarrow}^\dagger + F_{xx'k}^* c_{x',-k,\downarrow} c_{xk\uparrow}.$$

Now using H_{hop} , H_μ and H_V we can write the full Hamiltonian as:

$$\begin{aligned} H &= \sum_{xx'k} \hat{c}_{xk}^\dagger H_{xx'k} \hat{c}_{x'k} \\ &= \sum_{xx'k} \begin{pmatrix} c_{xk\uparrow}^\dagger & c_{x,-k,\downarrow} \end{pmatrix} \begin{pmatrix} \epsilon_{xx'k\uparrow} & F_{xx'k} \\ F_{xx'k}^* & -\epsilon_{xx'k\downarrow} \end{pmatrix} \begin{pmatrix} c_{x'k\uparrow} \\ c_{x',-k,\downarrow}^\dagger \end{pmatrix}. \end{aligned} \quad (85)$$

This is a base we can start to work with. However, the altermagnetic matrix has a more complex spin structure and can be described with these \hat{c} . This requires additional work if we want to express the AM in a vertical periodic boundary setup.

The summation over all x, x' can be represented in a new matrix.

$$H = \sum_k \check{c}_k^\dagger H_k \check{c}_k$$

involving the $4N_x \times 4N_x$ matrix H_k and the $4N_x$ -dimensional vector \check{c}_k .

$$H_k = \begin{pmatrix} H_{11k} & \cdots & H_{1N_x k} \\ \vdots & \ddots & \\ H_{N_x 1k} & & H_{N_x N_x k} \end{pmatrix}$$

Please note that [45] uses the notation D_k for \check{c}_k , but we don't want to confuse the reader with the already defined eigenvalues diagonal matrix of Eq. 63. As before the y information is stored in the k -index, which is unique for each lattice y -slice. This said, we can diagonalize N_y times a $4N_x \times 4N_x$ matrix. Each H_k represents the interaction of a y -line with itself. The eigenvalues are the same for each y -slices and the physical quantities are going to be expressed with this summation over k and the eigenvalues, -vectors of each k (y -slice).

On the other hand the vector we use to carry the creation and annihilation operators is given as

$$\check{c}_k^\dagger = \begin{pmatrix} c_{1k\uparrow}^\dagger & c_{1,-k,\downarrow} & \cdots & c_{N_x k\uparrow}^\dagger & c_{N_x,-k,\downarrow} \end{pmatrix} \in \mathbb{H}^{2N_x}$$

A.2.1 BdG-transformation for a vertical Fourier transform

The eigenvalues' equation is similar to Eq. 61

$$H_k \mathfrak{X}_{nk} = E_{nk} \mathfrak{X}_{nk}. \quad (86)$$

The eigenvectors and -values are given as

$$\mathfrak{X}_{nk} = \begin{pmatrix} \mathfrak{x}_{n1k} \\ \vdots \\ \mathfrak{x}_{nN_x k} \end{pmatrix}, \quad \mathfrak{x}_{nk} = \begin{pmatrix} u_{n x k} \\ v_{n x k} \end{pmatrix}.$$

If we stick to the formalism we already derived in the earlier Sec. 5.4 we obtain similar eigenvectors where $u_{n x k}$ corresponds to $c_{xk\uparrow}$ and $v_{n x k}$ $c_{x,-k,\downarrow}$ (see Eq. 87). We are now going to transform the c operators. First we need to define $\mathfrak{X}_k = [\mathfrak{X}_{1k}, \dots, \mathfrak{X}_{2N_x k}] \in \mathbb{H}^{2N_x \times 2N_x}$ storing the number of lattice sites times the number of spins (2) in the first dimension, and the number of eigenvectors in the second dimension. Besides, we have $\mathfrak{g}_k = (\mathfrak{g}_{1k}, \dots, \mathfrak{g}_{2N_x k})^T \in \mathbb{H}^{2N_x}$ along with $D_k = \mathfrak{X}_k \mathfrak{g}_k$, delivering $\mathfrak{g}_k = \mathfrak{X}_k^\dagger D_k$ which is equivalent to:

$$\mathfrak{g}_{nk} = \sum_{x \in N_x} u_{n x k} c_{xk\uparrow} + v_{n x k} c_{x,-k,\downarrow}^\dagger. \quad (87)$$

Looking at $D_k = \mathfrak{X}_k \mathfrak{g}_k$ we can derive two very useful expressions:

$$c_{xk\uparrow} = \sum_{n \in [2N_x]} u_{n x k} \mathfrak{g}_{nk} \quad (88) \quad \begin{array}{c} \circ \\ \vdots \\ \circ \end{array} \quad c_{x,-k,\downarrow}^\dagger = \sum_{n \in [2N_x]} v_{n x k} \mathfrak{g}_{nk}. \quad (89)$$

These are the equivalent of Eqs. 65 and 66 for the Fourier transformed c -operators along the y -axis.

A.2.2 Pairing amplitudes

For the derivation of the pairing amplitudes along the x and y axis shares similarities. Therefore, we embed the axis into the variable $a \in \{\hat{x}, \hat{y}\}$. With $F_i^{\pm a}$ we mean $F_i^{\pm \hat{x}}$ or $F_i^{\pm \hat{y}}$ which are equivalent to $F_{i,i \pm x}$ and $F_{i,i \pm y}$. Doing so, we will use our BdG-transformation as we did earlier to be able to solve these parameters self-consistently using the eigenvectors and -values. We remember that the site i has the coordinate (x, y) and its neighbour j the coordinate (x', y') .

$$F_i^{\pm a} = \langle c_{i\uparrow} c_{i \pm a, \downarrow} \rangle = \frac{1}{N_y} \sum_{kk'} \langle c_{xk\uparrow} c_{x \pm \delta_x, k', \downarrow} \rangle e^{i(ky + k'y')} \\ \frac{1}{N_y} \sum_{kk'} \langle c_{xk\uparrow} c_{x \pm \delta_x, k', \downarrow} \rangle e^{i(k+k')y} e^{\pm i k' \delta_y}$$

using $y \pm \delta_y = y'$ and $x \pm \delta_x = x'$. Naturally we know that for $a = \hat{x}$ there is no hopping along the y -axis, such that $\delta_y = 0$ and in the same way for $a = \hat{y}$ we have $\delta_x = 0$. The expectation value is independent of the site vertical coordinate y . This means that we can achieve a site description by making the average of the value over a x -slice. In other words we can write:

$$F_i^{\pm a} = \frac{1}{N_y} \sum_{y \in \llbracket N_y \rrbracket} \frac{1}{N_y} \sum_{kk'} \langle c_{xk\uparrow} c_{x \pm \delta_x, k', \downarrow} \rangle e^{i(k+k')r_i} e^{\pm i k' \delta_y}$$

which after the summation over i yields, as we covered earlier, to $1/N_y \sum_y e^{i(k+k')y} = \delta_{k, -k'}$:

$$F_i^{\pm x} = \frac{1}{N_y} \sum_k \langle c_{xk\uparrow} c_{x \pm \delta_x, k, \downarrow} \rangle e^{\mp i k \delta_y}.$$

Now that we have simplified the Fourier transform we can incorporate the BdG-transformation. The process is very similar to Eq. 67 and after doing this, we obtain the following expression:

$$F_i^{\pm a} = \frac{1}{N_y} \sum_k \sum_{nn'} u_{n x k} v_{n', x \pm \delta_x, k}^* \langle \mathbf{g}_{nk} \mathbf{g}_{n'k}^\dagger \rangle e^{\mp i k \delta_y} \quad (90)$$

Recalling the a abstraction of the axis, we get:

$$F_i^{\pm x} = \frac{1}{N_y} \sum_{nk} u_{n x k} v_{n, x \pm \delta_x, k}^* (1 - f(E_{nk})) \quad (91)$$

$$F_i^{\pm y} = \frac{1}{N_y} \sum_{nk} u_{n x k} v_{n x k}^* (1 - f(E_{nk})) e^{\mp i k}, \quad (92)$$

where $x \pm \delta_x$ means $x \pm 1$.

A.2.3 In the open boundary setup

Here we need to reuse the equations of the Nambu-Spin formalism described in chapter 5. As we saw we need to first take care that the part of the Hamiltonian we want to introduce has to be hermitian. Moreover the eigenvectors need to respect the fermionic anticommutation properties. If we transform the Hartree-Fock Hamiltonian as it is in Eq. 80 we see that only the upper right quadrant of the matrix $H_{V,ij}^{HF}$ of $\tilde{c}_i^\dagger \cdot (H_V^{HF})_{ij} \cdot \tilde{c}_j$ is filled. We need to use the anticommutation relations to solve this. This delivers the following expression:

$$H_V^{HF} = - \sum_{\langle ij \rangle} V_{ij} \left(F_{ij}^{\uparrow\downarrow} c_{j\downarrow}^\dagger c_{i\uparrow}^\dagger + F_{ij}^{\uparrow\downarrow*} c_{i\uparrow}^\dagger c_{j\downarrow}^\dagger \right) \\ = - \sum_{\langle ij \rangle} V_{ij} \left(F_{ji}^{\uparrow\downarrow} c_{i\downarrow}^\dagger c_{j\uparrow}^\dagger + F_{ij}^{\uparrow\downarrow*} c_{i\uparrow}^\dagger c_{j\downarrow}^\dagger \right) \quad (93) \\ = - \frac{1}{2} \sum_{\langle ij \rangle} V_{ij} \left[F_{ij}^{\uparrow\downarrow} \left(c_{i\downarrow}^\dagger c_{j\uparrow}^\dagger - c_{i\uparrow}^\dagger c_{j\downarrow}^\dagger \right) + F_{ij}^{\uparrow\downarrow*} \left(c_{i\uparrow}^\dagger c_{j\downarrow}^\dagger - c_{i\downarrow}^\dagger c_{j\uparrow}^\dagger \right) \right]$$

which is achieved using Eq. 54, $V_{ij} = V_{ji}$, $F_{ij}^{\uparrow\downarrow} = -F_{ji}^{\downarrow\uparrow} = F_{ji}^{\uparrow\downarrow}$ using the anticommutation relation and a spin-echange. We then use $F_{ij}^{\uparrow\downarrow} = F_{ij}$ since all ambiguity has been removed.

Therefore, the matrix we obtain is given as

$$H_{V,ij}^{HF} = -\frac{1}{2} \begin{pmatrix} \mathcal{O} & & -F_{ij}^{\uparrow\downarrow} \\ & F_{ij}^{\uparrow\downarrow} & \\ -F_{ij}^{\uparrow\downarrow*} & F_{ij}^{\uparrow\downarrow*} & \mathcal{O} \end{pmatrix} = -\frac{1}{2} \begin{pmatrix} \mathcal{O} & -i\sigma_2 F_{ij} \\ i\sigma_2 F_{ij}^* & \mathcal{O} \end{pmatrix}, \quad (94)$$

and takes only place between two neighbouring sites i and j . For the accuracy one could multiply it with $(\delta_{i+1,j} + \delta_{i-1,j} + \delta_{i+N_x,j} + \delta_{i-N_x,j})$. This matrix can then be added to Eq. 59 replacing the on-site superconductive Δ -term by a neighbouring superconductive F -term.

Now that we have expressed the Hartree-Fock Hamiltonian in the correct manner, we can use our BdG-transformation to diagonalize the Hamiltonian and find a self-consistent solution for the F -parameters. Here we use the transformation between the creation and annihilation operators, and the eigenvectors, -values of the Hamiltonian given by Eqs. 65 and 66.

$$F_{ij} = \langle c_{i\uparrow} c_{j\downarrow} \rangle = \sum_{n \in \mathcal{N}_+} u_{ni\uparrow} v_{nj\downarrow}^* (1 - f(E_{nk})) + v_{ni\uparrow}^* u_{nj\downarrow} f(E_{nk}) \quad (95)$$

in a very similar way as Eq. 67.

A.3 Unconventional order parameters

In the more simple description of the superconductivity we outlied how the superconducting order parameter Δ depends on the pairing amplitude F . Because the potential was isotropic, we simply had $\Delta = U \langle c_{i\uparrow} c_{i\downarrow} \rangle$. Here however, the potential is anisotropic, and we obtain a linear combination of the pairing amplitudes in the different directions of the lattice. Achieving different combinations of the F s we obtain different superconducting states. Here is an exhaustive list.

$$\begin{aligned} \Delta_{s,i} &= V F_{s,i} = \frac{V}{4} \left(F_i^{x+(S)} + F_i^{x-(S)} + F_i^{y+(S)} + F_i^{y-(S)} \right) \\ \Delta_{d,i} &= V F_{d,i} = \frac{V}{4} \left(F_i^{x+(S)} + F_i^{x-(S)} - F_i^{y+(S)} - F_i^{y-(S)} \right) \\ \Delta_{p_x,i} &= V F_{p_x,i} = \frac{V}{2} \left(F_i^{x+(T)} - F_i^{x-(T)} \right) \\ \Delta_{p_y,i} &= V F_{p_y,i} = \frac{V}{2} \left(F_i^{y+(T)} - F_i^{y-(T)} \right) \end{aligned}$$

F_s , F_d , F_{p_x} and F_{p_y} are the pairing amplitudes for the s , d (also called $d_{x^2-y^2}$ because of its expression), p_x and p_y -wave superconductivity. The S and T are the singlet and triplet expressions of the pairing amplitudes. More precisely we define them as

$$F_{ij}^{(S)} = \frac{F_{ij} + F_{ji}}{2} \quad (96)$$

$$F_{ij}^{(T)} = \frac{F_{ij} - F_{ji}}{2} \quad (97)$$

Where we shorten the expression using $F_{ij}^{\uparrow\downarrow(S)} = F_{ij}^{(S)}$.

Symmetry discussion

We see that these parameters depends on the spin and the momentum. Therefore, it's a good idea to look at their respective behaviour under exchange of these variables. The discussion for the spin exchange is quite straight forward.

$$\begin{aligned} F_{ij}^{\uparrow\downarrow(S)} &= \frac{F_{ij}^{\uparrow\downarrow} + F_{ji}^{\uparrow\downarrow}}{2} = \frac{\langle c_{i\uparrow} c_{j\downarrow} \rangle + \langle c_{j\uparrow} c_{i\downarrow} \rangle}{2} \\ F_{ij}^{\uparrow\downarrow(T)} &= \frac{F_{ij}^{\uparrow\downarrow} - F_{ji}^{\uparrow\downarrow}}{2} = \frac{\langle c_{i\uparrow} c_{j\downarrow} \rangle - \langle c_{j\uparrow} c_{i\downarrow} \rangle}{2} \end{aligned}$$

using $\langle c_{i\uparrow}c_{j\downarrow} \rangle = -\langle c_{i\downarrow}c_{j\uparrow} \rangle$. Using the linearity of the expression we obtain

$$\begin{aligned} F_{ij}^{\uparrow\downarrow(S)} &= -F_{ij}^{\downarrow\uparrow(S)} \\ F_{ij}^{\uparrow\downarrow(T)} &= F_{ij}^{\downarrow\uparrow(T)}. \end{aligned}$$

This means that the singlet wave-pairing amplitude is antisymmetric under spin exchange and the triplet wave pairing is symmetric under spin exchange. Their names find place in the analogy of the wave function formalism.

For the momentum exchange we're going to take a look at the Fourier transformation of the pairing amplitudes. Using the transformation we made to reach Eq. 90 with any translation $x \rightarrow \mathbf{r}$, $r \in \{\mathbf{e}_x, \mathbf{e}_y\}$ we obtain

$$F_{i,i+\mathbf{r}} = \frac{1}{N} \sum_{\mathbf{k}} \langle c_{\mathbf{k}\uparrow}c_{-\mathbf{k},\downarrow} \rangle e^{-i\mathbf{k}\mathbf{r}}.$$

Changing the sign of the momentum we obtain $\frac{1}{N} \sum_{\mathbf{k}} \langle c_{-\mathbf{k},\uparrow}c_{\mathbf{k},\downarrow} \rangle e^{i\mathbf{k}\mathbf{r}} = F_{i,i-\mathbf{r}}$ because of the $\delta_{\mathbf{k},\mathbf{k}'}$ trick. For this reason $F_{i,i+\mathbf{r}} + F_{i,i-\mathbf{r}}$ is symmetric under momentum exchange while $F_{i,i+\mathbf{r}} - F_{i,i-\mathbf{r}}$ is antisymmetric.

Referring back to the order parameter definition we see that the s and d -wave are symmetric under momentum exchange, where the p_x and p_y -wave are antisymmetric in such exchange.

A.4 Implementation of the unconventional superconductivity

This is more complex to implement than the BCS superconductivity. We solved this without the periodic boundary conditions method. Here each site has to compute eight parameters, the four pairing amplitudes in the ij and ji direction. To do so we prepare a huge vector containing the eigenvectors' components u and v that all the parameters need and send this to each site. Further due to computation imprecisions, we may have $F_{ij}^{(S)} \neq F_{ji}^{(S)}$. However, the Hamiltonian should stay hermitian, so we impose $F_{ij}^{(S)} = F_{ji}^{(S)}$. Please compare the implementation of Eq. 94 in the Hamiltonian of the system to check that $H_{ij} = H_{ji}^*$ is actually verified. For the convergence criteria it is important to note the following: The individual F always change but the end result in F_d can converge, so we check $F_{d,i}$ on each step to see if it reaches a stable value.

7 Literature

- [1] Shannon K'doah Range. *GRAVITY PROBE B Examining Einstein's Spacetime with Gyroscopes*. 2004. URL: http://einstein.stanford.edu/content/education/GP-B_T-Guide4-2008.pdf.
- [2] RC JAKLEVIC et al. "QUANTUM INTERFERENCE EFFECTS IN JOSEPHSON TUNNELING". English. In: *Physical review letters* 12.7 (1964), pp. 159–160.
- [3] Takashi Nakamura et al. "Development of a superconducting bulk magnet for NMR and MRI". English. In: *Journal of magnetic resonance (1997)* 259 (2015), pp. 68–75.
- [4] Kenjiro Hashi et al. "Achievement of 1020 MHz NMR". English. In: *Journal of magnetic resonance (1997)* 256 (2015), pp. 30–33.
- [5] E. Sugiyama T. haishi M. Aoki. "Development of a 2.0 Tesla permanent magnetic circuit for NMR/MRI". In: *Proceedings of the 2005 Annual Meeting of ISMRM* (2005). URL: <https://cds.ismrm.org/protected/05MProceedings/PDFfiles/00869.pdf>.
- [6] Pascal Tixador. "Superconducting Magnetic Energy Storage: Status and Perspective". In: *IEEE/CSC & ESAS EUROPEAN SUPERCONDUCTIVITY NEWS FORUM, No. 3* (2008). URL: <https://cds.ismrm.org/protected/05MProceedings/PDFfiles/00869.pdf>.
- [7] A. Roque et al. "Superconductivity and their Applications". English. In: *RE&PQJ* 15.3 (2024). DOI: <https://doi.org/10.24084/repqj15.308>.
- [8] Shigehiro Nishijima et al. "Superconductivity and the environment: a Roadmap". English. In: *Superconductor science and technology* 26.11 (2013), pp. 113001–35.
- [9] J. G. Bednorz and K. A. Müller. "Possible highTc superconductivity in the Ba-La-Cu-O system". In: *Zeitschrift für Physik B Condensed Matter* 64.2 (June 1986), pp. 189–193. ISSN: 1431-584X. DOI: 10.1007/BF01303701. URL: <https://doi.org/10.1007/BF01303701>.
- [10] M. K. Wu et al. "Superconductivity at 93 K in a new mixed-phase Y-Ba-Cu-O compound system at ambient pressure". In: *Phys. Rev. Lett.* 58 (9 Mar. 1987), pp. 908–910. DOI: 10.1103/PhysRevLett.58.908. URL: <https://link.aps.org/doi/10.1103/PhysRevLett.58.908>.
- [11] Nicolas Doiron-Leyraud et al. "Quantum oscillations and the Fermi surface in an underdoped high-Tc superconductor". In: *Nature* 447.7144 (May 2007), pp. 565–568. ISSN: 1476-4687. DOI: 10.1038/nature05872. URL: <https://doi.org/10.1038/nature05872>.
- [12] Jian-Feng Ge et al. "Superconductivity above 100 K in single-layer FeSe films on doped SrTiO3". In: *Nature Materials* 14.3 (Mar. 2015), pp. 285–289. ISSN: 1476-4660. DOI: 10.1038/nmat4153. URL: <https://doi.org/10.1038/nmat4153>.
- [13] Mari Einaga et al. "Crystal structure of the superconducting phase of sulfur hydride". In: *Nature Physics* 12.9 (Sept. 2016), pp. 835–838. ISSN: 1745-2481. DOI: 10.1038/nphys3760. URL: <https://doi.org/10.1038/nphys3760>.
- [14] A. P. Drozdov et al. "Superconductivity at 250 K in lanthanum hydride under high pressures". In: *Nature* 569.7757 (May 2019), pp. 528–531. ISSN: 1476-4687. DOI: 10.1038/s41586-019-1201-8. URL: <http://dx.doi.org/10.1038/s41586-019-1201-8>.
- [15] Sukbae Lee, Ji-Hoon Kim, and Young-Wan Kwon. *The First Room-Temperature Ambient-Pressure Superconductor*. 2023. arXiv: 2307.12008 [cond-mat.supr-con]. URL: <https://arxiv.org/abs/2307.12008>.
- [16] W. Meissner and R. Ochsenfeld. "Ein neuer Effekt bei Eintritt der Supraleitfähigkeit". German. In: *Die Naturwissenschaften* 21.44 (1933), pp. 787–788.
- [17] Libor Šmejkal, Jairo Sinova, and Tomas Jungwirth. "Emerging Research Landscape of Altermagnetism". In: *Phys. Rev. X* 12 (4 Dec. 2022), p. 040501. DOI: 10.1103/PhysRevX.12.040501. URL: <https://link.aps.org/doi/10.1103/PhysRevX.12.040501>.
- [18] Johnof Folk. *Second quantization" (the occupation-number representation)*. 2014. URL: <https://johnof.folk.ntnu.no/second-quantization-2014.pdf>.

- [19] Kristian Fossheim and Asle Sudbø. John Wiley & Sons, Ltd, 2004. ISBN: 9780470020784. DOI: <https://doi.org/10.1002/0470020784>. eprint: <https://onlinelibrary.wiley.com/doi/pdf/10.1002/0470020784>. URL: <https://onlinelibrary.wiley.com/doi/abs/10.1002/0470020784>.
- [20] Cupcake Physics by Cyrus Vandrevalla. *The Fourier Transform of the Coulomb Potential*. 2014. URL: <https://cupcakephysics.com/electromagnetism/math%20methods/2014/10/04/the-fourier-transform-of-the-coulomb-potential.html>.
- [21] L. N. Cooper J. Bardeen and J. R. Schrieffer. “Theory of Superconductivity”. In: *Physical Review*, vol. 108, Issue 5, pp. 1175–1204 (1957). DOI: <https://doi.org/10.1103/PhysRev.108.1175>. URL: <https://journals.aps.org/pr/abstract/10.1103/PhysRev.108.1175>.
- [22] Prof. Dr. Matthias Fuchs and Philipp Baumgärtel. *Skript Vorlesung zur Statistischen Mechanik*. Last public available version 2010. 2023. URL: http://theorie.physik.uni-konstanz.de/lfsfuchs/lectures/statmech0910/Stat.Mech0910_Skript.pdf.
- [23] Louis Néel. “Propriétés magnétiques des ferrites ; ferrimagnétisme et antiferromagnétisme”. French. In: *Annales De Physique (Paris)* pp.137–198 (1936). DOI: <https://dx.doi.org/10.1051/anphys/194812030137>. URL: <https://hal.science/hal-02888371v1>.
- [24] Igor Mazin. *Altermagnetism Then and Now*. 2024. URL: <https://physics.aps.org/articles/v17/4>.
- [25] Libor Šmejkal, Jairo Sinova, and Tomas Jungwirth. “Beyond Conventional Ferromagnetism and Antiferromagnetism: A Phase with Nonrelativistic Spin and Crystal Rotation Symmetry”. In: *Phys. Rev. X* 12 (3 Sept. 2022), p. 031042. DOI: 10.1103/PhysRevX.12.031042. URL: <https://link.aps.org/doi/10.1103/PhysRevX.12.031042>.
- [26] Satoru Hayami, Yuki Yanagi, and Hiroaki Kusunose. “Momentum-Dependent Spin Splitting by Collinear Antiferromagnetic Ordering”. In: *Journal of the Physical Society of Japan* 88.12 (2019), p. 123702. DOI: 10.7566/JPSJ.88.123702. eprint: <https://doi.org/10.7566/JPSJ.88.123702>. URL: <https://doi.org/10.7566/JPSJ.88.123702>.
- [27] Alan Stonebraker. URL: <https://alanstonebraker.com/>.
- [28] Makoto Naka, Yukitoshi Motome, and Hitoshi Seo. “Perovskite as a spin current generator”. In: *Phys. Rev. B* 103 (12 Mar. 2021), p. 125114. DOI: 10.1103/PhysRevB.103.125114. URL: <https://link.aps.org/doi/10.1103/PhysRevB.103.125114>.
- [29] Sinova J. et al. Šmejkal L. MacDonald A.H. “Anomalous Hall antiferromagnets.” In: *Nature Reviews Materials (Nat Rev Mater)* 482–496 (2022). DOI: 10.1038/s41578-022-00430-3.
- [30] Libor Šmejkal et al. “Giant and Tunneling Magnetoresistance in Unconventional Collinear Antiferromagnets with Nonrelativistic Spin-Momentum Coupling”. In: *Phys. Rev. X* 12 (1 Feb. 2022), p. 011028. DOI: 10.1103/PhysRevX.12.011028. URL: <https://link.aps.org/doi/10.1103/PhysRevX.12.011028>.
- [31] Xin Chen et al. “Giant spin-splitting and tunable spin-momentum locked transport in room temperature collinear antiferromagnetic semimetallic CrO monolayer”. In: *Applied Physics Letters* 123.2 (July 2023). ISSN: 1077-3118. DOI: 10.1063/5.0147450. URL: <http://dx.doi.org/10.1063/5.0147450>.
- [32] Lin-Ding Yuan et al. “Prediction of low-Z collinear and noncollinear antiferromagnetic compounds having momentum-dependent spin splitting even without spin-orbit coupling”. In: *Phys. Rev. Mater.* 5 (1 Jan. 2021), p. 014409. DOI: 10.1103/PhysRevMaterials.5.014409. URL: <https://link.aps.org/doi/10.1103/PhysRevMaterials.5.014409>.
- [33] Makoto Naka, Yukitoshi Motome, and Hitoshi Seo. “Perovskite as a spin current generator”. In: *Phys. Rev. B* 103 (12 Mar. 2021), p. 125114. DOI: 10.1103/PhysRevB.103.125114. URL: <https://link.aps.org/doi/10.1103/PhysRevB.103.125114>.
- [34] Hiroaki Kusunose et al. Makoto Naka Satoru Hayami. “Spin current generation in organic antiferromagnets”. In: *Nat Commun* 10, 4305 (2019). DOI: 10.1038/s41467-019-12229-y.

- [35] E. J. O’Sullivan. “Magnetic Tunnel Junction-Based MRAM and Related Processing Issues”. In: *206th meeting of © The Electrochemical Society, Inc.* (2004). URL: https://www.researchgate.net/profile/Eugene-Osullivan/publication/238100771_Magnetic_Tunnel_Junction-Based_MRAM_and_Related_Processing_Issues/links/5925abc4aca27295a8eb2f7a/Magnetic-Tunnel-Junction-Based-MRAM-and-Related-Processing-Issues.pdf.
- [36] Manoj Kumar Yadav and Santosh Kumar Gupta. “FeAl/MgO/FeAl MTJ with enhanced TMR and low resistance area product for MRAM: A first principle study”. In: *Micro and Nanostructures* 165 (2022), p. 207192. ISSN: 2773-0123. DOI: <https://doi.org/10.1016/j.micrna.2022.207192>. URL: <https://www.sciencedirect.com/science/article/pii/S277301232200005X>.
- [37] Louis de Broglie. “Recherches sur la théorie des Quanta”. French. In: (1924). URL: <https://theses.hal.science/tel-00006807>.
- [38] Jabir Ali Ouassou, Arne Brataas, and Jacob Linder. “dc Josephson Effect in Altermagnets”. In: *Phys. Rev. Lett.* 131 (7 Aug. 2023), p. 076003. DOI: 10.1103/PhysRevLett.131.076003. URL: <https://link.aps.org/doi/10.1103/PhysRevLett.131.076003>.
- [39] Jabir Ali Ouassou. *Notes on lattice BdG formalism*. (unpublished). 2021.
- [40] Jabir Ali Ouassou, Takehito Yokoyama, and Jacob Linder. “RKKY interaction in triplet superconductors: Dzyaloshinskii-Moriya-type interaction mediated by spin-polarized Cooper pairs”. In: *Phys. Rev. B* 109 (17 May 2024), p. 174506. DOI: 10.1103/PhysRevB.109.174506. URL: <https://link.aps.org/doi/10.1103/PhysRevB.109.174506>.
- [41] Ivo Souza Nicola Marzari and David Vanderbilt. *An Introduction to Maximally-Localized Wannier Functions*. URL: <https://cfm.ehu.es/ivo/publications/marzari-psik03.pdf>.
- [42] Gregory H. Wannier. *The Structure of Electronic Excitation Levels in Insulating Crystals*. 1937. URL: <https://journals.aps.org/pr/abstract/10.1103/PhysRev.52.191>.
- [43] Terence Tao. URL: <https://terrytao.wordpress.com/2010/01/12/254a-notes-3a-eigenvalues-and-sums-of-hermitian-matrices/#more-3341> (visited on 01/19/2025).
- [44] Vetle Risinggård and Jacob Linder. “Direct and inverse superspin Hall effect in two-dimensional systems: Electrical detection of spin supercurrents”. In: *Phys. Rev. B* 99 (17 May 2019), p. 174505. DOI: 10.1103/PhysRevB.99.174505. URL: <https://link.aps.org/doi/10.1103/PhysRevB.99.174505>.
- [45] Andreas Halkjelsvik Mjøs and Jacob Linder. “Magnetism and Superconductivity in the Hubbard Model”. In: *NTNU Norwegian University of Science and Technology, Department of Physics* (2019).
- [46] Walter A. Harrison. *Solid state theory*. English. New York [u.a.]: McGraw-Hill, 1970.
- [47] G. A. Bobkov, I. V. Bobkova, and A. M. Bobkov. “Andreev bound states at nonmagnetic impurities in superconductor/antiferromagnet heterostructures”. In: *Physical Review B* 109.21 (June 2024). ISSN: 2469-9969. DOI: 10.1103/physrevb.109.214508. URL: <http://dx.doi.org/10.1103/PhysRevB.109.214508>.
- [48] M. J. M. de Jong and C. W. J. Beenakker. “Andreev Reflection in Ferromagnet-Superconductor Junctions”. In: *Phys. Rev. Lett.* 74 (9 Feb. 1995), pp. 1657–1660. DOI: 10.1103/PhysRevLett.74.1657. URL: <https://link.aps.org/doi/10.1103/PhysRevLett.74.1657>.
- [49] Terry P. Orlando. 2003. URL: <https://web.mit.edu/6.763/www/FT03/Lectures/Lecture11.pdf> (visited on 01/22/2025).

8 Administrative documents

ERKLÄRUNG:

Ich versichere hiermit, dass ich die anliegende Abschlussarbeit mit dem Thema:

Proximity effects in altermagnetic systems.

selbständig verfasst und keine anderen Hilfsmittel und Quellen als die angegebenen benutzt habe.

Falls ich textgenerierende KI-Tools als Hilfsmittel verwendet habe, ist mir bewusst, dass ich allein für die inhaltliche Richtigkeit von KI generierten Textpassagen und die Kennzeichnung von Formulierungen und Ideen anderer Personen gemäß den Grundsätzen der guten wissenschaftlichen Praxis verantwortlich bin. Die Stellen, die anderen von natürlichen Personen verfassten Werken (auch aus dem Internet und oder anderen elektronischen Text- und Datensammlungen entnommen) dem Wortlaut oder dem Sinn nach entnommen sind, habe ich in jedem einzelnen Fall durch Angabe der Quelle bzw. der Sekundärliteratur als Entlehnung kenntlich gemacht.

Ich habe zur Kenntnis genommen, dass die Prüfungs- oder Studienleistung bei Täuschung über die Eigenständigkeit oder durch Benutzung nicht zugelassener oder ggf. zugelassener aber nicht ausreichend angegebener Hilfsmittel als „nicht bestanden (5,0)“ bewertet wird und dass in besonders schwerwiegenden Täuschungsfällen der zuständige Prüfungsausschuss mich von der Wiederholungsprüfung ausschließen kann mit der Folge des endgültigen Verlustes des Prüfungsanspruchs.

Weiterhin versichere ich hiermit, dass die o.g. Arbeit noch nicht anderweitig als Abschlussarbeit einer Diplom-, Bachelor- bzw. Masterprüfung eingereicht wurde. Mir ist ferner bekannt, dass ich bis zum Abschluss des Prüfungsverfahrens die Materialien verfügbar zu halten habe, welche die eigenständige Abfassung der Arbeit belegen können.

Die Arbeit wird nach Abschluss des Prüfungsverfahrens der Bibliothek der Universität Konstanz übergeben und katalogisiert. Damit ist sie durch Einsicht und Ausleihe öffentlich zugänglich. Die erfassten beschreibenden Daten wie z.B. Autor, Titel usw. stehen öffentlich zur Verfügung und können durch Dritte (z.B. Suchmaschinenanbieter oder Datenbankbetreiber) weiterverwendet werden.

Als Urheber der anliegenden Arbeit stimme ich dem obigen Veröffentlichungsverfahren



zu



nicht zu.

Konstanz, den .27.01.2025.....



(Unterschrift)

Eingang Zentrales

Matrikel-Nr. 01/1176012

Vorname: Arto

Straße: Jacob-Burckhardt-Str. 35 G288

Tel.Nr.: +33 7 69 77 50 38

Proximity effects in alternating magnetic systems

Beginn der Bachelorarbeit: 1. September 2024

Verlängerungsantrag: 2 Monate, BA Arbeit wird extern angefertigt

Konstanz, den 08.06.2024

(Unterschrift Student)

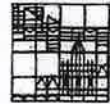
Prof. Dr. Wolfgang Belzig

Unterschrift

Unterschrift

Konstanz, den 12.06.2024

(Unterschrift Vorsitzender des StPA Physik)



Anmeldung externer Bachelorarbeiten

Persönliche Daten

Vorname und Name: Arto STEFFAN

Email Adresse: arto.steffan@uni-konstanz.de

Angaben zur Bachelorarbeit

Thema:

Proximity effects in altermagnetic systems.

Externer Betreuer (Ansprechpartner)/externe Betreuerin (Ansprechpartnerin):

Jacob Wüsthoff Linder

Lehrstuhl/AG/Abteilung: Department of Physics

Einrichtung/Firma: NTNU - Faculty of Natural Sciences

Ort: Trondheim

Land: Norwegen

Geplante Aufenthalt: von 1. September bis 3. Februar 2025

Finanzierungsquelle: Erasmus+

Gutachten

1. Gutachter/Gutachterin vom FB Physik-Universität Konstanz (Intern):

Wolfgang Belzig

2. Gutachter/Gutachterin

☐ extern

☐ intern

Konstanz, den 12.06.2024


Unterschrift Student/in

Unterschrift Vorsitzender/in StPA Physik